

Evaluation of the Sustainability of the Hydrothermal Processing of Select Organic Waste  
Feedstocks: Accounting for Water Quality and Nutrient Recovery Impacts

---

A Dissertation  
Presented to  
the faculty of the School of Engineering and Applied Science  
of the University of Virginia

---

In partial fulfillment of  
the requirements for the degree of  
Doctor of Philosophy

By

Sarah K. Bauer

August 2018

APPROVAL SHEET

This dissertation is submitted in partial fulfillment of  
the requirements for the degree of  
Doctor of Philosophy



Author

This dissertation has been read and approved by the examining committee:

Dr. Lisa Colosi Peterson  
Dissertation Director

Dr. James Smith  
Chairperson

Dr. Andres Clarens

Dr. Tony Singh

Dr. James Galloway

Accepted for the School of Engineering and Applied Science:



Craig H. Benson, Dean, School of Engineering and Applied Science

August 2018

## Abstract

In this dissertation, a combination of laboratory experiments, water chemistry modeling, and energy accounting techniques are used to evaluate the sustainability of the hydrothermal liquefaction (HTL) processing of select non-food, organic waste feedstocks, with emphasis on water quality impacts. Laboratory experiments include: (1) experimental characterization of the hydrothermal processing of select organic waste feedstocks, (2) evaluation of corresponding HTL products, specifically so-called aqueous co-product (ACP), and (3) assessment of ACP quality and suitability for discharge into receiving waters or a municipal wastewater treatment plant (WWTP). Water chemistry modeling includes an assessment of the treatability of ACP via the recovery of valuable, scarce nutrients (i.e., nitrogen [N] and phosphorus [P]) from the post-HTL ACP of select organic waste feedstocks as a means of both managing the ACP and producing valuable materials. Energy accounting includes adjusting the “energy return on investment” ( $EROI = E_{OUT}/E_{IN}$ ) of HTL systems to account for the production and management of ACP from the HTL processing of select organic waste feedstocks.

Experimental results of this research indicate that while the hydrothermal processing of select organic waste feedstocks generates liquid biofuel, HTL processing also produces substantial quantities of potent wastewater (i.e., ACP). The ACP arising from HTL processing contains very high concentrations of traditional wastewater pollutants (i.e., total nitrogen [TN], total phosphorus [TP], and dissolved organic carbon, measured as chemical oxygen demand [COD]), which has been largely overlooked by the current literature. The potency of the ACP renders it more noxious than relevant benchmark wastewaters, requiring management of the ACP prior to discharge into the receiving waters of a municipal WWTP. Adjustment of published energy ratio metrics to account for ACP management reveals that the energy

consumption required to remove TN, TP, and COD from the ACP to achieve typical permitted levels of WWTPs is on the same order of magnitude as that of liquefaction. The results of water quality modeling to assess the management of ACP via nutrient-based precipitation of valuable nutrients (i.e., N and P) from the ACP indicate that pH adjustment and the addition of magnesium ( $Mg^{2+}$ ) facilitate the theoretical precipitation of N and P as solid compounds (i.e., struvite and hydroxyapatite [HAP]) from the ACP. This is promising from an environmental perspective as precipitation-based nutrient recovery could enhance the appeal of waste HTL systems as a means of both valorizing waste materials into renewable energy and producing valuable nutrient-based materials. Additional work will comprise: (1) evaluating the impacts of various HTL processing conditions on the quantities and composition of HTL products, specifically ACP, (2) characterizing possible toxicity impacts of ACP, and (3) validating theoretical nutrient recovery yields from water chemistry modeling via laboratory experiments. The results from this work will offer insight into the water quality impacts of waste HTL systems, as well as mitigating the effects of ACP on water quality via novel ACP management and recovery of valuable, scarce nutrients.

## Acknowledgments

I would like to take this opportunity to acknowledge several individuals who have made a lasting impact on my doctoral studies in the Department of Civil and Environmental Engineering at the University of Virginia.

First and foremost, I would like to acknowledge my advisor, Dr. Lisa Colosi Peterson, without whom I would have never made it this far. Lisa, you are a trusted advisor, a talented scholar, and a dedicated professor. Thank you so much for always pushing me to achieve my best and for never giving up on me.

I would also like to acknowledge my advisory committee, Drs. James Smith, Andres Clarens, Tony Singh, and James Galloway. Thank you all for your continuous guidance and support.

I would like to thank the undergraduate research assistants who were instrumental to this research: Curtis Davis, Cameron McCarty, Catherine Reynolds, and Gabrielle Schleppebach. Thank you all for your constant enthusiasm for this research. You made the long hours of laboratory work enjoyable.

I would also like to thank Dr. Robert Davis and Mr. Jiahan Xie of the Department of Chemical Engineering at the University of Virginia for equipment access and technical support for this research.

To my parents: Mom and Dad, words cannot express how deeply grateful I am for your unwavering love, support, and encouragement to always reach for the stars.

To my family: It has been your constant love and support that has helped me achieve my best during graduate school.

To my friends and colleagues: It has been your friendship and company that has made my graduate school experience so memorable and enjoyable. Katie Nunnelley, Kassie Grimes, and Courtney Hill, I am forever grateful for your friendship. Thank you for being my roommates and helping me create a home in Virginia.

## List of Figures

<b>Figure 1-1.</b> Water (W) and land (L) use to produce 1 liter of ethanol (Le) or its equivalent as soy/algae biodiesel. Adapted from Dominguez-Faus et al. (2009), with algae data from Clarens et al. (2011). Water use equals the sum of irrigation + evapotranspiration (ET) for all feedstocks except algae. Algae is the only “second-generation” feedstock evaluated; it offers by far the lowest water footprint out of all feedstocks in this group.....	2
<b>Figure 1-2.</b> The interactions between the demand of water for energy production and the requirement of energy to supply and treat water, known as the Water-Energy Nexus. Adapted from Belesky et al. (2014).....	3
<b>Figure 1-3.</b> MSW generated in the U.S. and selected countries around the globe in 2009 (Giusti, 2009). In 2009, the U.S. generated more MSW than the other selected countries by an average of 130%.....	6
<b>Figure 1-4.</b> Schematic of the gasification process (NETL, 2009).....	9
<b>Figure 1-5.</b> Schematic of the pyrolysis process (Guedes et al., 2018).....	10
<b>Figure 1-6.</b> Schematic of the hydrothermal liquefaction process. Adapted from Tian et al. (2017).....	12
<b>Figure 2-1.</b> The overall framework of the dissertation, with interactions between two key research objectives.....	18
<b>Figure 3-1.</b> Parr Hast reactor setup, with (1) magnetic stirrer, (b) quartz liner, temperature sensor, pressure gauge, and gas inlet and outlet, and (c) electric furnace. Not shown is the control panel.....	24
<b>Figure 3-2.</b> HTL processing of dairy manure, including (a) raw waste feedstock slurry (TSS of 10%, m/m), (b) post-HTL waste feedstock, (c) post-HTL solid-phase biochar, and (d) post-HTL ACP (top layer) extracted from liquid-phase co-products via liquid-liquid phase extraction. Gaseous co-products were vented.....	25
<b>Figure 3-3.</b> Distribution of HTL products (i.e., biocrude, biochar, and ACP) for eight non-food, organic waste feedstocks. Biochar mass was measured directly. ACP and biocrude masses were	

computed from measured volumes using densities of 1.0 and 0.96 g/mL, respectively. Error bars correspond to  $\pm 1$  standard deviation (n = 3 replicates).....34

**Figure 3-4.** Percent distribution showing how feedstock (a) carbon and (b) nitrogen are distributed among the HTL product phases. These data are interpreted as follows, using annotated dairy manure carbon distribution as an example: 10 g dry weight of dairy manure solids comprising 40% carbon (m/m) is converted into HTL products. A% of the feedstock carbon is converted into biocrude and/or gas, B% is converted into ACP, and C% is converted into biochar; where  $A + B + C = 30 + 15 + 55 = 100\%$  of the 4 g initial feedstock carbon. Error bars correspond to  $\pm 1$  standard deviation (n = 3 replicates).....38

**Figure 4-1.** pH dependence of (a) orthophosphate (OP) and (b) ammonia, magnesium, and calcium speciation at 25°C. The speciation of ammonia between ionized ammonium ( $\text{NH}_4^+$ ) and free ammonia ( $\text{NH}_3$ ), as well as the orthophosphate species (i.e.,  $\text{H}_3\text{PO}_4$ ,  $\text{H}_2\text{PO}_4^-$ ,  $\text{HPO}_4^{2-}$ , and  $\text{PO}_4^{3-}$ ) is pH dependent.....62

## List of Tables

<b>Table 3-1.</b> Characterization and elemental analysis of as-received raw waste feedstocks prior to hydrothermal processing, as expressed using percent weight (wt %). Confidence intervals correspond to $\pm 1$ standard deviation (n = 3 replicates).....	31
<b>Table 3-2.</b> Characterization of ACP arising from the HTL conversion of eight non-food, organic waste feedstocks. Confidence intervals correspond to $\pm 1$ standard deviation (n = 3 replicates). Italicized font indicates pertinent wastewater benchmarks and post-HTL ACP laboratory results from relevant literature. NA = not reported.....	36
<b>Table 3-3.</b> Original and revised estimates of EROI for the HTL conversion of various feedstocks, as reported in previous literature. EROI values $>1$ are indicative of favorable energy yield, whereas EROI values $<1$ are indicative of unfavorable energy yields.....	42
<b>Table 4-1.</b> Summary of the life-cycle energy values of the various materials consumed and produced via the precipitation of nutrients from the post-HTL ACP of select organic waste feedstocks. Parameter values were taken from the ecoinvent database, as accessed using SimaPro v.3 and/or Clarens et al. (2010).....	57
<b>Table 4-2.</b> Characterization of pH and nutrient parameters of ACP produced from HTL processing of select waste feedstocks. Average values of pH, $\text{NH}_4^+$ , and $\text{PO}_4^{3-}$ from triplicate experiments are reported and used as inputs for Visual MINTEQ modeling. The summation of all orthophosphates (OP) is expressed as $\text{PO}_4^{3-}$ . Adapted from Bauer et al. (2018).....	60
<b>Table 4-3.</b> Additional characterization of post-HTL ACP to account for possible influences on the precipitation of nutrients (i.e., N and P). Average values are reported and used as inputs for Visual MINTEQ modeling. Blank values = under the detectable limit (0.5 mg/L).....	63
<b>Table 4-4.</b> Theoretical recovery of nutrients via the precipitation of solids from post-HTL dairy manure ACP at pH range of 4.4 to 14. NaOH is used to raise the alkalinity of the ACP; NaOH values are based on laboratory results. Columns 3-8 are based on results from the Visual MINTEQ model. $\text{MgCl}_2$ is added to facilitate the precipitation of nutrients as solids. Optimal pH for nutrient recovery from dairy manure ACP is 8.0. Initial $\text{PO}_4^{3-} = 1.27$ mM; Initial $\text{NH}_4^+ = 22.5$ mM.....	65

**Table 4-5.** Theoretical recovery of nutrients via the precipitation of solids from post-HTL pre-digested sludge ACP at pH range of 8.4 to 14. NaOH is used to raise the alkalinity of the ACP; NaOH values are based on laboratory results. Columns 3-8 are based on results from the Visual MINTEQ model. MgCl<sub>2</sub> is added to facilitate the precipitation of nutrients as solids. Optimal pH for nutrient recovery from pre-digested sludge ACP is 10.5. Initial PO<sub>4</sub><sup>3-</sup> = 3.6 mM; Initial NH<sub>4</sub><sup>+</sup> = 69.6 mM.....66

**Table 4-6.** Theoretical recovery of nutrients via the precipitation of solids from post-HTL digested sludge ACP at pH range of 8.6 to 14. NaOH is used to raise the alkalinity of the ACP; NaOH values are based on laboratory results. Columns 3-8 are based on results from the Visual MINTEQ model. MgCl<sub>2</sub> is added to facilitate the precipitation of nutrients as solids. Optimal pH for nutrient recovery from digested sludge ACP is 10.5. Initial PO<sub>4</sub><sup>3-</sup> = 0.99 mM; Initial NH<sub>4</sub><sup>+</sup> = 149.9 mM.....67

**Table 4-7.** Theoretical recovery of nutrients via the precipitation of solids from post-HTL brewing yeast ACP at pH range of 8.3 to 14. NaOH is used to raise the alkalinity of the ACP; NaOH values are based on laboratory results. Columns 3-8 are based on results from the Visual MINTEQ model. MgCl<sub>2</sub> is added to facilitate the precipitation of nutrients as solids. Optimal pH for nutrient recovery from brewing yeast ACP is 10.5. Initial PO<sub>4</sub><sup>3-</sup> = 24.3 mM; Initial NH<sub>4</sub><sup>+</sup> = 97.8 mM.....68

**Table 4-8.** Theoretical recovery of nutrients via the precipitation of solids from post-HTL spent grains ACP at pH range of 5.3 to 14. NaOH is used to raise the alkalinity of the ACP; NaOH values are based on laboratory results. Columns 3-8 are based on results from the Visual MINTEQ model. MgCl<sub>2</sub> is added to facilitate the precipitation of nutrients as solids. Optimal pH for nutrient recovery from spent grains ACP is 10.5. Initial PO<sub>4</sub><sup>3-</sup> = 11.4 mM; Initial NH<sub>4</sub><sup>+</sup> = 50.0 mM.....69

**Table 4-9.** Theoretical recovery of nutrients via the precipitation of solids from post-HTL dry hops ACP at pH range of 7.0 to 14. NaOH is used to raise the alkalinity of the ACP; NaOH values are based on laboratory results. Columns 3-8 are based on results from the Visual MINTEQ model. MgCl<sub>2</sub> is added to facilitate the precipitation of nutrients as solids. Optimal pH for nutrient recovery from dry hops ACP is 10.5. Initial PO<sub>4</sub><sup>3-</sup> = 9.3 mM; Initial NH<sub>4</sub><sup>+</sup> = 88.5 mM.....70

**Table 4-10.** Theoretical recovery of nutrients via the precipitation of solids from post-HTL white lees ACP at pH range of 6.4 to 14. NaOH is used to raise the alkalinity of the ACP; NaOH values are based on laboratory results. Columns 3-8 are based on results from the Visual MINTEQ model. MgCl<sub>2</sub> is added to facilitate the precipitation of nutrients as solids. Optimal pH for nutrient recovery from white lees ACP is 9.0. Initial PO<sub>4</sub><sup>3-</sup> = 1.1 mM; Initial NH<sub>4</sub><sup>+</sup> = 2.2 mM.....71

**Table 4-11.** Theoretical recovery of nutrients via the precipitation of solids from post-HTL red lees ACP at pH range of 8.8 to 14. NaOH is used to raise the alkalinity of the ACP; NaOH values are based on laboratory results. Columns 3-8 are based on results from the Visual MINTEQ model. MgCl<sub>2</sub> is added to facilitate the precipitation of nutrients as solids. Optimal pH for nutrient recovery from red lees ACP is 10.5. Initial PO<sub>4</sub><sup>3-</sup> = 22.2 mM; Initial NH<sub>4</sub><sup>+</sup> = 79.6 mM.....72

**Table 4-12.** Optimum theoretical recovery of N and P via precipitation of solids from post-HTL ACP at optimal pH values of select waste feedstocks based on Visual MINTEQ model outputs.....75

**Table 4-13.** Estimates of EROI to account for the management of the ACP arising from the HTL processing of select waste feedstocks via nutrient-based precipitation. EROI values >1 are indicative of favorable energy yield, whereas EROI values <1 are indicative of unfavorable energy yields.....77

## Definition of Acronyms and Chemical Formulas

ACP	aqueous co-product
BOD	biological oxygen demand
COD	chemical oxygen demand
DCM	dichloromethane
ECR	energy consumption ratio
$E_{IN}$	energy consumption (i.e., “energy in”)
$E_{OUT}$	energy production (i.e., “energy out”)
EROI	energy return on investment
HAP	hydroxyapatite
HTL	hydrothermal liquefaction
LCA	life-cycle assessment
MAP	monoammonium phosphate
MSW	municipal solid waste
$NH_3$	ammonia
$NH_4^+$	ammonium
OP	orthophosphates
$PO_4^{3-}$	reactive phosphate
TN	total nitrogen
TOC	total organic carbon
TP	total phosphorus
TSP	triple superphosphate
TSS	total suspended solids
VS	volatile solids
WWTP	wastewater treatment plant

## Related Publications and Presentations

- **Bauer, S.**, F. Cheng, C. Davis, C. McCarty, G. Schleppenbach, and L. Colosi (2018) “Evaluating the Impacts of ACP Management via Nutrient Recovery on the Energy Performance of Hydrothermal Liquefaction”, *In Preparation*.
- **Bauer, S.**, C. Reynolds, S. Peng, and L. Colosi (2018) “Evaluating the Water Quality Impacts of Hydrothermal Liquefaction: Assessment of Carbon, Nitrogen, and Energy Recovery Impacts”, *Bioresource Technology Reports*, **2**, 115-120.  
doi.org/10.1016/j.biteb.2018.04.010.
- McCarty, C. G. Schleppenbach, and C. Davis (2018) “Evaluating the Sustainability of Energy Production from Winery Waste in Central Virginia”, *The Oculus: The Virginia Journal of Undergraduate Research*, **16**, 48-63, *Mentored Research Project*.
- **Bauer, S.** and L. Colosi (2018) “Evaluation of the Hydrothermal Processing of Select Waste Feedstocks into Biocrude with Assessment of Water Quantity and Quality Impacts”, Featured Presenter, Poster Presentation at the GEM-ASEE Doctoral Engineering Research Showcase, Washington, D.C., January 2018.
- **Bauer, S.** and L. Colosi (2016) “Evaluating the Water Footprint of Hydrothermal Liquefaction Conversion of Waste Feedstocks to Biofuel”, Finalist, Poster Presentation at the Society of Women Engineers’ WE16 National Conference, Philadelphia, PA, October 2016.
- **Bauer, S.** (2016) “Evaluating the Environmental Impacts of Renewable Energy Technologies with Regards to the Water-Energy Nexus”, Featured Presenter, Oral Presentation at the UVa Civil and Environmental Engineering Department Seminar Series, Charlottesville, VA, September 2016.

## Table of Contents

<b>Abstract</b> .....	i
<b>Acknowledgements</b> .....	iii
<b>List of Figures</b> .....	iv
<b>List of Tables</b> .....	vi
<b>Definition of Acronyms and Chemical Formulas</b> .....	ix
<b>Related Publications and Presentations</b> .....	x
<b>1.0 Introduction</b> .....	1
<b>1.1 The Water-Energy Nexus</b> .....	1
<b>1.2 Waste Management and Materials Scarcity Concerns</b> .....	4
<b>1.3 Thermochemical Processing for Alternative Energy Production</b> .....	8
<b>1.4 Conclusions</b> .....	13
<b>1.5 References</b> .....	13
<b>2.0 Research Objectives</b> .....	17
<b>3.0 Objective 1: Evaluating the Water Quality Impacts of Hydrothermal Liquefaction with Assessment of Carbon, Nitrogen, and Energy Recovery Impacts</b> .....	19
<b>3.1 Introduction</b> .....	19
<b>3.2 Materials and Methods</b> .....	22
3.2.1 Raw Feedstock Collection and Characterization.....	22
3.2.2 HTL Conversion and Characterization of Resulting Products.....	23
3.2.3 Energy Ratio Metrics.....	26
3.2.3.1 ACP Management Assumptions.....	26
3.2.3.2 Energy Ratio Formulas and Parameterization.....	29
<b>3.3 Results and Discussion</b> .....	30

3.3.1 Characterization of Raw Feedstocks.....	30
3.3.2 Characterization of HTL Products.....	33
3.3.2.1 Carbon Distribution among HTL Products.....	37
3.3.2.2 Nitrogen Distribution among HTL Products.....	40
3.3.2.3 Energy Recovery Impacts.....	41
<b>3.4 Conclusions.....</b>	<b>44</b>
<b>3.5 References.....</b>	<b>44</b>
<b>4.0 Objective 2: Evaluating the Impacts of ACP Management via Nutrient Recovery on the Energy Performance of Hydrothermal Liquefaction.....</b>	<b>49</b>
<b>4.1 Introduction.....</b>	<b>49</b>
<b>4.2 Materials and Methods.....</b>	<b>53</b>
4.2.1 HTL Conversion and Characterization of ACP.....	53
4.2.2 Recovery of Nutrients from ACP.....	55
4.2.3 Energy Ratio Formulas and Parameterization.....	56
<b>4.3 Results and Discussion.....</b>	<b>59</b>
4.3.1 Characterization of ACP.....	59
4.3.2 Considerations for the Recovery of Nutrients from ACP.....	60
4.3.3 Recovery of Nitrogen and Phosphorus from ACP via Precipitation of Solids.....	63
4.3.4 Energy Recovery Impacts.....	76
<b>4.4 Conclusions.....</b>	<b>78</b>
<b>4.5 References.....</b>	<b>79</b>
<b>5.0 Conclusions and Future Work.....</b>	<b>84</b>
<b>5.1 References.....</b>	<b>86</b>

## **1.0 Introduction**

Rapidly increasing global energy demand due to continued increase in the world's population, compounded by concern about the dwindling supply of fossil fuels, energy security, and climate change, is creating unprecedented challenges for our society. The bulk of energy used across the globe comes from a finite supply of fossil fuels. In the U.S., energy demand is so high that the population must rely on foreign sources for approximately 30% of its energy needs (EIA, 2012). Existing transportation infrastructure in the U.S., and elsewhere, is especially reliant on domestic and foreign petroleum-derived liquid fuels; therefore, it is of critical economic importance to develop domestically-sourced alternatives to fossil fuels that are compatible with current transportation infrastructure. Biofuels have been gaining traction as a renewable, theoretically carbon-neutral, and seemingly environmentally preferable alternative to traditional fossil fuels. These attributes make biofuels appealing from the perspective of environmental sustainability. Accordingly, the *Energy Independence and Security Act of 2007* (EISA) mandated production of 16 billion gallons of biofuels per year from cellulosic crops by 2022, virtually guaranteeing that there will be a large increase in the production of U.S. biofuels in the coming years in order to meet the growing demand for energy (Dominguez-Faus et al., 2009).

### **1.1 The Water-Energy Nexus**

Due to growing global populations and a dwindling supply of fossil fuels, the development of biofuels that are renewable and theoretically carbon-neutral has become increasingly attractive worldwide. First-generation biofuels, produced from food crops, however, adversely impact the global food supply and consume substantial quantities of water (e.g., 500-4,000 liters of water per liter of fuel [Figure 1-1]) (Dominguez-Faus et al., 2009).

Therefore, increasing demand for domestic biofuels could significantly exacerbate existing water quantity and quality difficulties in the U.S. via increased demand for irrigation of feedstock crops, increased water pollution from agricultural drainage, and increased generation of fuel processing wastewaters. Algae, which is the only “second-generation” feedstock (i.e., non-food feedstock) evaluated in Figure 1-1, offers a lower water footprint than the other feedstocks evaluated. Therefore, feedstocks that offer lower water footprints need to be evaluated.

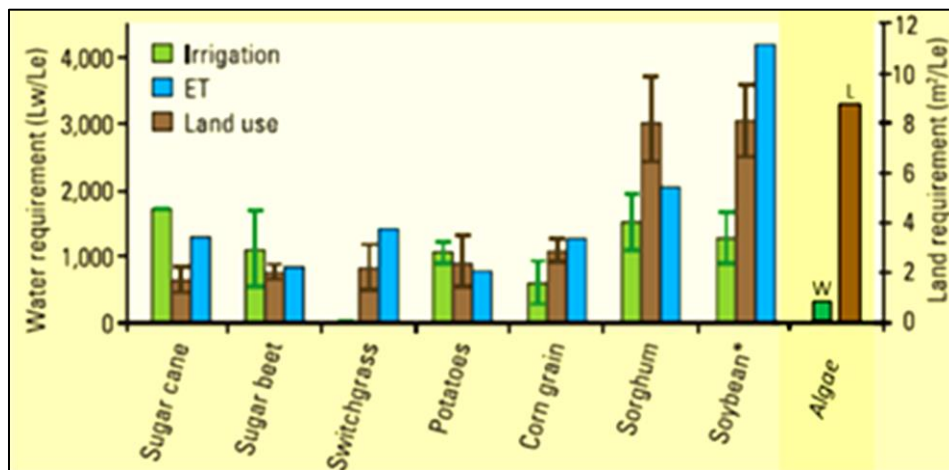


**Figure 1-1.** Water (W) and land (L) use to produce 1 liter of ethanol (Le) or its equivalent as soy/algae biodiesel. Adapted from Dominguez-Faus et al. (2009), with algae data from Clarens et al. (2011). Water use equals the sum of irrigation + evapotranspiration (ET) for all feedstocks except algae. Algae is the only “second-generation” feedstock evaluated; it offers by far the lowest water footprint out of all feedstocks in this group.

Historically, water and energy have been developed and managed independently of each other. Today, however, this presumption is being challenged, as water and energy are becoming tightly intertwined within our society and worldwide. Water and energy underpin economic and social development, as water is used in almost every stage of energy production and electricity generation, while energy is used to withdraw, treat, and distribute water for countless needs

(Miller, 2012; Gresham, 2016). This intricate connection between water and energy is known as the Water-Energy Nexus (Figure 1-2).

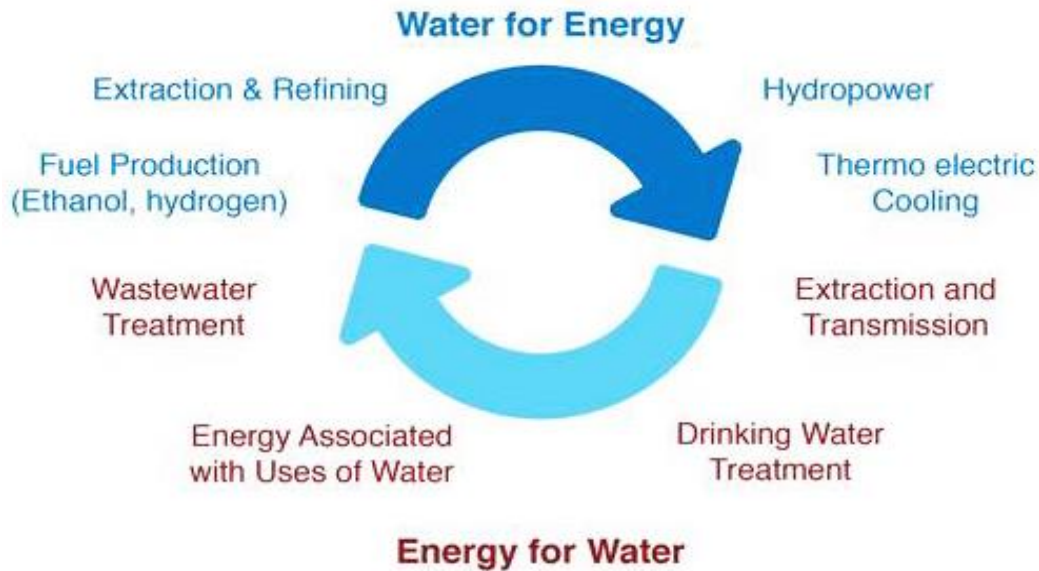


**Figure 1-2.** The interactions between the demand of water for energy production and the requirement of energy to supply and treat water, known as the Water-Energy Nexus. Adapted from Belesky et al. (2014).

In order to meet the energy demands of our growing population, increased consumption of water, adverse impacts on the quality of our water supply, and dwindling natural resources are of growing concern. Increased generation of biofuels leads to an increase in land and fertilizer use, which in turn increases the quantity of nutrients, such as nitrogen (N) and phosphorus (P), in our waterways, diminishing our natural resources and greatly impacting the N and P cycles. High concentrations of N and P in our waterways lead to the creation of large algae blooms, known as eutrophication (Reddy et al., 2018; Altieri and Gedan, 2015). Increased usage of N through fertilizer application and eutrophication leads to high levels of nitrous oxide ( $N_2O$ ) in our atmosphere, which is a very potent greenhouse gas, as well as high levels of nitrate ( $NO_3^-$ ) in our waterways (Montzka et al., 2011; Reddy et al., 2018). The increase in N usage as fertilizer

also has obvious adverse effects on human health, including pulmonary disease from air particles and tropospheric ozone, and cancer from elevated  $\text{NO}_3^-$  levels in our drinking water supply (Galloway et al., 2008).

Anthropogenic and land-use changes are also having huge implications on the carbon (C) cycle. The industrial burning of fossil fuels has led to large increases in the concentration of carbon dioxide ( $\text{CO}_2$ ) in the atmosphere and oceans (Le Quéré et al., 2017). Therefore, as the global energy demand increases, renewable energy technologies need to consider the C cycle (Le Quéré et al., 2017; Armstrong et al., 2014). Common land-based renewable energies can alter local C cycles due to small changes in temperature, precipitation, evapotranspiration, and the balance of direct and diffuse radiation (Armstrong et al., 2014). These direct effects can also cause indirect effects on soil microbial systems, altering the C cycling as well (Armstrong et al., 2014).

Increasing energy demand, dwindling supplies of natural resources, and more recently climate change, are bringing into focus the links between water and energy in unprecedented ways. Predictions show that our population's energy demand will increase by 30% by 2040 (compared to that of 2010); while water shortages are occurring more frequently across the globe (Miller, 2012). The Clean Water America Alliance (2009) suggests that due to the relationship between water and energy, the availability of water will drive the development of domestically-sourced biofuels in the 21<sup>st</sup> century, and vice versa.

## **1.2 Waste Management and Materials Scarcity Concerns**

In recent years, research into developing so-called second-generation biofuels has expanded, due to the fact that second-generation biofuels have a lessened environmental impact

on land and water usage compared to first-generation biofuels. Second-generation biofuels are produced from non-food, ligno-cellulosic feedstocks, such as municipal solid waste (MSW), wastewater treatment plant (WWTP) biosolids, animal manure, agricultural waste, and food and beverage waste, all of which are abundant in the U.S. and worldwide (Dominguez-Faus et al., 2009). Such non-food, waste materials offer lower water footprints than purposefully grown first-generation feedstocks (Figure 1-1) (Dominguez-Faus et al., 2009). Waste management is a significant concern worldwide that is worsening with increasing population and rates of urbanization. In particular, in 2012, MSW generation was approximately 1.3 billion tons per year, globally. By 2025, global MSW generation is expected to increase to approximately 2.2 billion tons per year. As a nation, the U.S. generates more waste than any other nation in the world, with the U.S. alone producing 254.1 million tons of MSW per year, which equates to 2 kg per person per day (Figure 1-3) (Rajaeifar et al., 2017). This waste is primarily in the form of MSW, agricultural and animal wastes, and industrial wastes. These materials have traditionally been viewed as an environmental liability. In recent years, however, with the growth in the production of second-generation biofuels, there is increasing interest in researching ways of converting such waste materials into usable energy products.

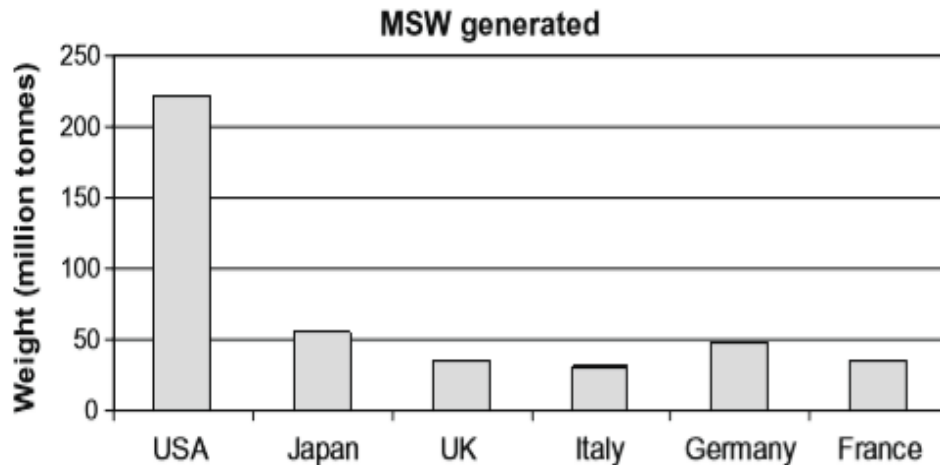


**Figure 1-3.** MSW generated in the U.S. and selected countries around the globe in 2009 (Giusti, 2009). In 2009, the U.S. generated more MSW than the other selected countries by an average of 130%.

In conjunction with the increased generation of waste (e.g., municipal, industrial, and agricultural) throughout the globe over the past few decades, there has also been a rise in the consumption of natural resources. Valuable natural resources are being depleted due to growing energy and agricultural demands, as well as stricter environmental standards on recycled nutrients (Gilbert, 2009). There is mounting concern for the future of our natural resources, specifically the availability of N and P, which are important components for plant and agricultural growth. N and P are both necessary to sustain the increase in populations worldwide, and many nations are already suffering from a lack of fertilizer availability (Larsen et al., 2007). Therefore, in the coming years, the major challenges of nutrient availability will be how to maximize nutrient benefits where necessary and minimize unwanted consequences. For example, nutrient deficiency in soils increases erosion rates, which causes an abundance of nutrients in bodies of water, leading to eutrophication (Larsen et al., 2007). However, excess

nutrients in soils can also lead to eutrophication, as well as increased production of atmospheric particulate matter (Galloway et al., 2008).

Increased use of fossil fuels, growing demand for N use in agriculture production, and N inefficiency are triggering the N cycle to change. These changes are being seen through the loss of N to the air, water, and land, leading to both environmental and human health impacts, such as increased groundwater pollution, ambient ammonia (NH<sub>3</sub>) and particle emissions, and N deposition (Galloway et al., 2008). Unlike N, P is a non-renewable resource. A study by the U.S. Geological Survey (USGS), along with several other studies, estimates that around 62 billion tons of phosphate remain in the ground worldwide, which would last for approximately 70-125 more years if demand for fertilizer continues to grow as expected (Gilbert, 2009). Despite the quickly diminishing reserves of P, many industries are continuing to use rock phosphate as opposed to recovered phosphate, because it is cheaper; however, the less expensive cost of rock phosphate does not take into account the environmental externalities associated with mining phosphate (Molinos-Senante et al., 2010). With the finite supply of phosphate quickly dwindling, recovery and recycling are the only possibilities for continued P use, and the most significant source of recovered phosphate is waste products (Gilbert, 2009).

With current concerns about shortages of the supplies of natural resources and fossil fuels, waste management, and climate change, research is turning to developing and optimizing processes that produce renewable energy sources in order to help alleviate these concerns and lead our society to a more sustainable future. In particular, interest in thermochemical processes (e.g., gasification, pyrolysis, and liquefaction) is growing (Yao et al., 2018). As organic waste continues to be produced in abundance and a growing nuisance to manage in the U.S. and across the globe, thermochemical processes have the potential to utilize waste biomass and potentially

help reduce our society's dependence on fossil fuels (Kumar and Samadder, 2017; Yao et al., 2018).

### **1.3 Thermochemical Processing for Alternative Energy Production**

Three of the most commonly researched thermochemical processes are gasification, pyrolysis, and liquefaction. Such thermochemical conversion processes are appealing for alternative energy production from organic wastes, because they make use of the entire feedstock without intensive pre-treatment steps (Elliott et al., 2014; Toor et al., 2011). Gasification is a general process where heat and pressure are used to convert a biomass into a combustible fuel with less oxygen provided than required for stoichiometric combustion (Figure 1-4).

Gasification occurs in a gasifier where gaseous reactions convert carbonaceous materials into combustible gas, known as synthesis gas (or syngas), as well as liquid fuel. Different types of gasifiers include: the counter-current fixed bed or “up draft” gasifier, co-current fixed bed or “down draft” gasifier, fluidized bed reactor, and entrained flow gasifier, with fluidized bed gasifiers being the most common gasifier used for medium- to large-scale waste biomass (Kouhia, 2011, Sansaniwal et al., 2017).

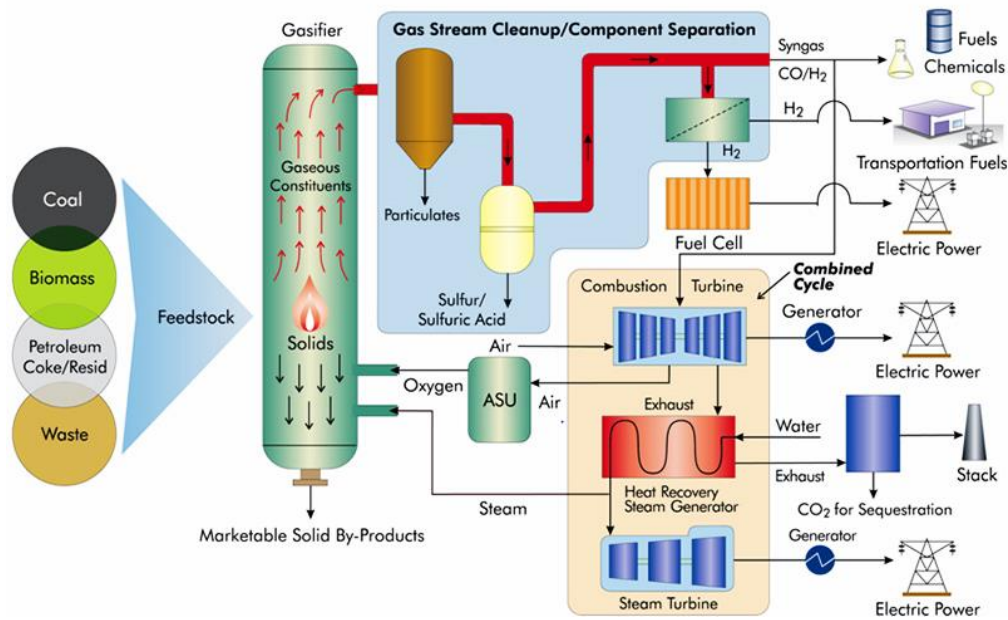


**Figure 1-4.** Schematic of the gasification process (NETL, 2009).

Syngas primarily consists of hydrogen, carbon monoxide, CO<sub>2</sub>, methane, and N (Kumar and Samadder, 2017; Sansaniwal et al., 2017). It can be combusted to produce energy or feedstocks for chemical and liquid fuel (Kumar and Samadder, 2017). Various applications for the liquid fuel generated via gasification include: gas engines and turbines, direct heating applications, and fuel cells (Sansaniwal et al., 2017). Although gasification does not form dioxins, furans, or large amounts of N or sulfur oxides due to the low levels of oxygen present, there are still substances, such as solid particulate matter, alkali metals, NH<sub>3</sub>, sulfur, and hydrochloric acid, that need to be removed through conditioning before producing high-quality biofuel (Sansaniwal et al., 2017). Gasification has been traditionally used in the coal industry but is starting to be applied to the processing of waste biomasses. The process of gasification has potential as it has been shown to produce less CO<sub>2</sub> than traditional incinerators, which is an advantage when it comes to energy recovery and environmental sustainability (Kumar and Samadder, 2017).

Pyrolysis is more favorable than incineration in terms of environmental favorability. Pyrolysis is the processing of heating a biomass (to between 400-800°C) without the presence of oxygen (Figure 1-5). Pyrolysis produces gas, bio-oil, and biochar. Although there are few commercial-scale pyrolysis processing facilities around the world, it is known that this process is efficient in treating specific waste streams. According to Lombardi et al. (2015), one of the current uses of pyrolysis is recycling tires to recover bio-oil, wire, carbon black, and gas. The quantity and quality of bio-oil yield via pyrolysis primarily depends upon heating rate, processing temperature, and residence time (Lombardi et al., 2015). Composition and particle size of the waste feedstock is also important, as the quality of bio-oil increases with processing waste feedstocks that are similar in composition and particle size (Kumar and Samadder, 2017). Both gasification and pyrolysis achieve lower environmental emissions and higher energy recovery efficiency than incineration. From a waste standpoint, these processes are also preferable, as they reduce the volume of waste up to 95% (Kumar and Samadder, 2017).

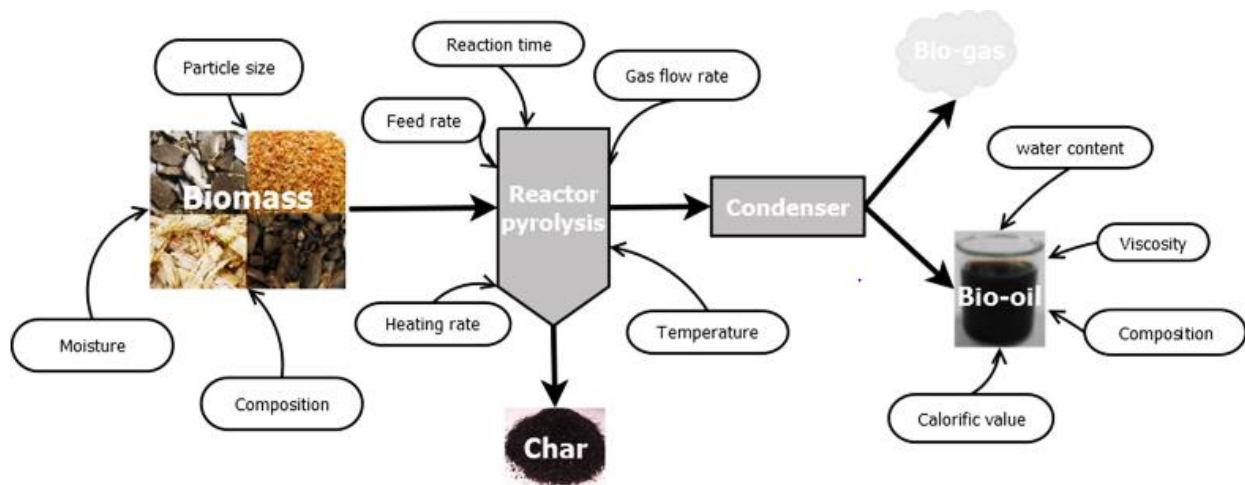


**Figure 1-5.** Schematic of the pyrolysis process (Guedes et al., 2018).

Hydrothermal liquefaction (HTL) is a process by which high heat and pressure are used to accelerate the natural humification process, whereby wet organic materials, initially comprised primarily of C, hydrogen, oxygen, N, and P, as a mixture of carbohydrates, proteins, and lipids, are transformed into long-chain, alkane hydrocarbons (i.e., biocrude) (Figure 1-6) (Elliot et al., 2014). During this process, water acts as an aggressive solvent for hydrophobic biomass constituents, which causes most of the cellular components, such as lipids, proteins, and saccharides, to be utilized, increasing energy efficiency compared to other thermochemical conversion processes. The ability of HTL conversion to utilize wet biomasses is an advantage, as this reduces the energy consumption required to dry the feedstock. The use of a wet biomass in HTL also uses a lower operating temperature and produces a higher energy efficiency and lower biochar yield compared to pyrolysis, making HTL a desirable platform for biofuel production (Gollakota et al., 2018).

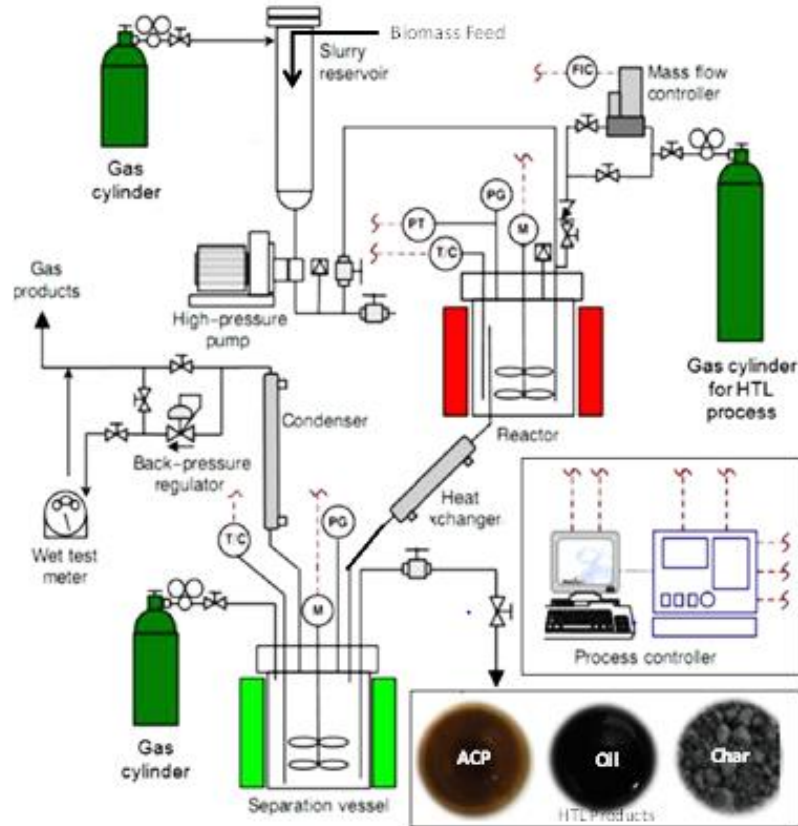


**Figure 1-6.** Schematic of the hydrothermal liquefaction process. Adapted from Tian et al. (2017).

HTL is of growing interest as a platform for energy production from wet biomasses. Specifically, HTL has recently been gaining interest as a platform for converting wet, organic waste biomasses into biocrude, a second-generation biofuel. HTL provides a pathway for converting waste biomass into a liquid biocrude that is immediately compatible with existing petroleum refining and distribution infrastructure (Toor et al., 2011). In addition to liquid biocrude, HTL produces gas, biochar, and aqueous co-product (ACP) (Toor et al., 2011). Various technologies exist to convert gaseous and solid biochar products into usable energy or materials. Thus far, there are not many uses for the ACP, which constitutes an appreciable fraction of total HTL products (where processing 1 ton of algae via HTL yields as much as 1,140

gallons of ACP) (Jena et al., 2011; Elliott et al., 2014). Thus, the production of ACP could prove to be problematic for our already dwindling water supply. Previous studies that have researched the production of ACP have primarily evaluated the reuse of ACP as a growth medium for algae cultivation (Biller et al., 2012; Jena et al., 2011). Further research into the effects of the production and management of ACP via HTL on our water supply is of interest for the sustainability of HTL systems.

#### **1.4 Conclusions**

To summarize, with increasing population and energy demand and compounding concerns about water quality, waste management, and dwindling supplies of natural resources, our society will continue to face unprecedented challenges in the coming decades. Thus, it is imperative to design technologies that mitigate burdens on our already strained energy, water, resources, and food supplies. The production of renewable energy via the thermochemical processing of waste materials could be a promising alternative to the use of fossil fuels, while lessening the burden of several of these pressing challenges. Energy accounting tools (e.g., life-cycle assessment [LCA]) provide a framework for decision-making as a quantitative means of evaluating the life-cycle energy and environmental performance of a system. Therefore, it is of importance to evaluate the impacts that the thermochemical processing of waste materials can have on water, nutrients, and waste before implementation at commercial scale.

#### **1.5 References**

- Altieri, A. H. and Gedan, K. B. (2015). Climate change and dead zones. *Global Change Biology*, 21 (4), 1395-1406.
- Armstrong, A., Waldron, S., Whitaker, J. and Ostle, N. J. (2014). Wind farm and solar park effects on plant-soil carbon cycling: uncertain impacts of changes in ground-level microclimate. *Global Change Biology*, 20 (6), 1699-1706.

- Belesky, P., Lehana, S., Power, L., Shepard, B., Cribb, J., Keogh, M., Bell, R. and Falvey, J. (2014). *Food and Water Security: Our Global Challenge Landmark Study*. Future Directions International Research Institute Pty Ltd, ISBN: 978-0-9757634-9-0.
- Clarens, A. F., Nassau, H., Resurreccion, E. P., White, M. A. and Colosi, L. M. (2011). Environmental impacts of algae-derived biodiesel and bioelectricity for transportation. *Environ. Sci. Technol.*, 45 (17), 7554-7560.
- Clean Water America Alliance (2009). A Call to Action: The Need for an Integrated National Water Policy. *Clean Water America Alliance*. Washington.
- Dominguez-Faus, R., Powers, S. E., Burken, J. G. and Alvarez, P. J. (2009). The Water Footprint of Biofuels: A Drink or Drive Issue? *Environmental Science & Technology*, 43 (9), 3005–3010.
- Elliott, D. C., Biller, P., Ross, A. B., Schmidt, A. J. and Jones, S. B. (2014). Hydrothermal liquefaction of biomass: Developments from batch to continuous process. *Bioresource Technology*, 178, 147–156.
- Energy Information Association (EIA). (2012). *Annual Energy Review: 2011* (DOE/EIA-0384). Washington D.C: Government Printing Office. Retrieved from <[www.eia.gov/totalenergy/data/annual/pdf/aer.pdf](http://www.eia.gov/totalenergy/data/annual/pdf/aer.pdf)>.
- Galloway, J. N., Townsend, A. R., Erisman, J. W., Bekunda, M., Cai, Z. C., Freney, J. R., Martinelli, L. A., Seitzinger, S. P. and Sutton, M. A. (2008). Transformation of the Nitrogen Cycle: Recent Trends, Questions, and Potential Solutions, *Science*, 320 (5878), 889-892.
- Gilbert, N. (2009). The Disappearing Nutrient. *Nature*, 461, 716–718.
- Giusti, L. (2009). A review of waste management practices and their impact on human health. *Waste Management*, 29, 2227–2239.
- Gollakota, A. R. K., Kishore, N. and Gu, S. (2018). A review on hydrothermal liquefaction of biomass. *Renewable and Sustainable Energy Reviews*, 81, 1378–1392.
- Gresham, R. M. (2016). The Water-Energy Nexus. *Tribology and Lubrication Technology*, 72 (7), 20-22.
- Guedes, R. E., Luna, A. S. and Torres, A. R. (2018). Operating parameters for bio-oil production in biomass pyrolysis: A review. *Journal of Analytical and Applied Pyrolysis*, 129, 134–149.

- Jena, U., Vaidyanathan, N., Chinnasamy, S. and Das, K. C. (2011). Evaluation of microalgae cultivation using recovered aqueous co-product from thermochemical liquefaction of algal biomass. *Bioresource Technology*, 102 (3), 3380–7.
- Kouhia, M. (2011). Biomass Gasification. *Aalto University School of Engineering*, 48. Retrieved from <[https://users.aalto.fi/~mkouhia/pub/2011-04-11\\_biomass-gasification.pdf](https://users.aalto.fi/~mkouhia/pub/2011-04-11_biomass-gasification.pdf)>.
- Kumar, A. and Samadder, S. R. (2017). A review on technological options of waste to energy for effective management of municipal solid waste. *Waste Management*, 69, 407–422.
- Larsen, T. A., Maurer, M., Udert, K. M. and Lienert, J. (2007). Nutrient cycles and resource management: implications for the choice of wastewater treatment technology. *Water Science & Technology*, 56 (5), 229–237.
- Le Quéré, C., Andrew, R. M., Friedlingstein, P., Sitch, S., Pongratz, J., Manning, A. C., Korsbakken, J. I., Peters, G. P., Canadell, J. G. and Jackson, R. B. (2018). Global Carbon Budget 2017. *Earth System Science Data*, 10, 405–448.
- Lombardi, L., Carnevale, E. and Corti, A. (2015). A review of technologies and performances of thermal treatment systems for energy recovery from waste. *Waste Management*, 37, 26–44.
- Miller, P. (2012). The energy water nexus. *Hydrocarbon Processing*, 91 (11), 33.
- Molinos-Senante, M., Hernandez-Sancho, F., Sala-Garrido, R. and Garrido-Baserba, M. (2010). Economic Feasibility Study for Phosphorus Recovery Processes. *Ambio.*, 40 (4), 408–416.
- Montzka, S. A., Dlugokencky, E. J. and Butler, J. H. (2011). Non-CO<sub>2</sub> greenhouse gases and climate change. *Nature*, 476 (7358), 43–50.
- National Energy Technology Laboratory (NETL). (2009). Gasifier: Gasification Introduction. *U.S. Department of Energy*. Retrieved from <[www.netl.doe.gov/research/coal/energy-systems/gasification/gasifipedia/intro-to-gasification](http://www.netl.doe.gov/research/coal/energy-systems/gasification/gasifipedia/intro-to-gasification)>.
- Rajaeifar, M. A., Ghanavati, H., Dashti, B. B., Heijngs, R., Aghbashlo, M. and Tabatabaei, M. (2017). Electricity generation and GHG emission reduction potentials through different municipal solid waste management technologies: A comparative review. *Renewable and Sustainable Energy Reviews*, 79, 414–439.
- Reddy, V. R., Cunha, D. G. F. and Kurian, M. (2018). A Water-Energy-Food Nexus Perspective on the Challenge of Eutrophication. *Water*, 10 (2), 101.

- Sansaniwal, S. K., Rosen, M. A. and Tyagi, S. K. (2017). Global challenges in the sustainable development of biomass gasification: An overview. *Renewable and Sustainable Energy Reviews*, 80, 23–43.
- Tian, C., Liu, Z., Zhang, Y., Li, B., Cao, W., Lu, H. and Zhang, T. (2014). Hydrothermal liquefaction of harvested high-ash low-lipid algal biomass from Dianchi Lake: Effects of operational parameters and relations of products. *Bioresource Technology*, 184, 336–343.
- Toor, S. S., Rosendahl, L. and Rudolf, A. (2011). Hydrothermal liquefaction of biomass: A review of subcritical water technologies. *Energy*, 36 (5), 2328–2342.
- Yao, Z., You, S., Ge, T. and Wang, C.-H. (2018). Biomass gasification for syngas and biochar co production: Energy application and economic evaluation. *Applied Energy*, 209, 43–55.

## 2.0 Research Objectives

The overall goal of this research is to evaluate the sustainability of the hydrothermal liquefaction (HTL) processing of select non-food, organic waste feedstocks, with emphasis on assessing the water quality impacts of waste HTL systems. The first step towards achieving this goal is to use experimental laboratory approaches to process select organic waste feedstocks via HTL and quantify the resulting product phases, specifically the production of so-called aqueous co-product, or ACP (i.e., “wastewater”). The second step is to characterize the ACP for relevant wastewater constituents in order to assess the water quality impacts arising from the production of ACP via hydrothermal processing. Energy accounting techniques are used to evaluate the energy performance of the proposed waste-to-energy system, specifically the energy consumption of ACP management. Water chemistry modeling techniques are also used to evaluate the management of ACP via nutrient-based precipitation of valuable, scarce nutrients from the ACP as a means of offsetting the energy cost of ACP management, as well as producing valuable nutrient-based materials.

Specifically, this dissertation consists of the two following objectives:

- Objective 1.* Evaluating the Water Quality Impacts of Hydrothermal Liquefaction with Assessment of Carbon, Nitrogen, and Energy Recovery Impacts
- Objective 2.* Evaluating the Impacts of ACP Management via Nutrient Recovery on the Energy Performance of Hydrothermal Liquefaction

Each objective is the topic of one dissertation chapter (Chapters 3 and 4), as noted above.

Overall conclusions from this work, as well as future research goals are presented in Chapter 5.

Figure 2-1 expresses how the individual chapters fit together within the overall framework of the

dissertation research, contributing to a comprehensive assessment of the water quality impacts of the hydrothermal processing of select non-food, organic waste feedstocks.

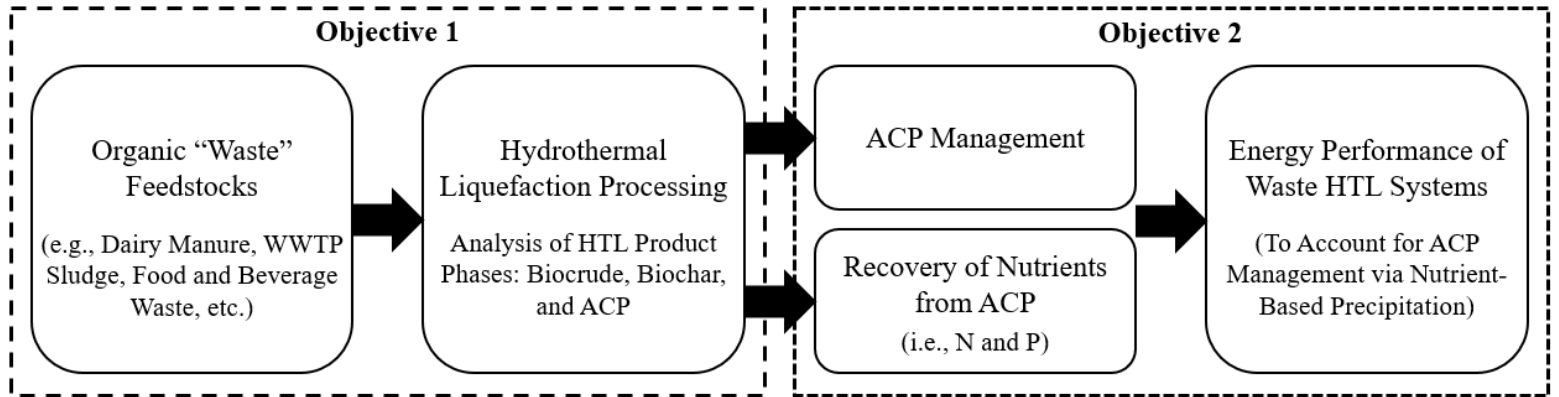


**Figure 2-1.** The overall framework of the dissertation, with interactions between two key research objectives.

### **3.0 Objective 1: Evaluating the Water Quality Impacts of Hydrothermal Liquefaction with Assessment of Carbon, Nitrogen, and Energy Recovery Impacts**

This chapter summarizes dissertation content pertaining to Objective 1. In this objective, experimental laboratory approaches are used to evaluate the feasibility of energy production from several non-food, organic waste feedstocks via hydrothermal liquefaction (HTL), with full characterization of water quantity and quality impacts, which has been largely overlooked in previous work. Although the commercialization of fuel production via HTL processing of waste feedstocks will ultimately hinge on the favorability of biocrude yield, it is valuable to anticipate possible water quantity and quality impacts so that the system can be designed to minimize and/or mitigate them. Therefore, this objective has two aims: (1) to characterize the quantity and quality of so-called aqueous co-product (ACP) arising from the HTL conversion of non-food, organic waste feedstocks and (2) to revise existing estimates of HTL energy ratio metrics (i.e., “energy consumption ratio” [ECR] or “energy return on investment” [EROI]) to account for the management of post-HTL ACP. This research will provide insight into the feasibility of waste-to-energy systems, with emphasis on the production of ACP via HTL processing. The material in this chapter was adapted from Bauer et al., (2018), which has been published in *Bioresource Technology Reports*.

#### **3.1 Introduction**

Next-generation biofuels produced from non-food feedstocks are of growing interest to help meet our increasing demand for energy without exacerbating competition with global land and food supply. It is especially of interest to leverage organic materials that would otherwise constitute “wastes” as feedstocks for energy production, including: municipal solid waste (MSW), wastewater treatment plant (WWTP) biosolids, animal manure, food and beverage

waste, and agricultural residue (Dominguez-Faus et al., 2009). It has been demonstrated that many of these waste materials are suitable for conversion into liquid fuels via the thermochemical transformation process known as HTL (Elliott, et al., 2014; Toor et al., 2011). HTL is a means of converting organic feedstocks into liquid biocrude, which is compatible with existing petroleum refining and distribution infrastructure (Toor et al., 2011). Previously published literature has investigated HTL processing of several non-food feedstocks, including biosolids and microalgae from WWTPs, dairy manure, and poultry litter (Huang et al., 2013; Pham et al., 2013; Theegala and Midgett, 2012; Vardon et al., 2011). Few studies have also used HTL to process organic waste materials, most notably residues from commercial food and beverage production; e.g., spent coffee grounds (Caetano et al., 2014; Yang et al., 2016), apple and grape pomace (i.e., pulp produced during pressing to release juices) (Corbin et al., 2015; Gama et al., 2015), and various organic slurries from beer brewing and wine making (Sturm et al., 2012; Subagyono et al., 2015).

HTL and other thermochemical conversion processes (e.g., gasification and pyrolysis) are appealing for alternative energy production from organic wastes, because they make use of the entire feedstock without intensive pre-treatment steps (Bhutto et al., 2016; Elliott et al., 2014; Toor et al., 2011). HTL is of particular relevance for wet biomasses (i.e., up to 90% water content), because the feedstock can be processed without significant pre-drying (Elliott et al., 2014); however, because the feedstocks are so wet, HTL is known to produce substantial quantities of ACP from small quantities of solids during HTL reactions (Jena et al., 2011; Elliott et al., 2014). This can be problematic, as ACP may contain very high concentrations of dissolved carbon (C), nitrogen (N), and phosphorus (P), and may be unsuitable for direct discharge into receiving waters or municipal WWTPs (Jena et al., 2011; Elliott et al., 2014).

Despite this, existing studies have generally ignored or understated the potential adverse water impacts of HTL.

Previous studies have primarily focused on optimizing feedstock characteristics and/or reaction conditions (e.g., catalyst, temperature, heating rate, residence time, etc.) to maximize biocrude quantity and quality (Akhtar and Amin, 2011; Zhang et al., 2009; Toor et al., 2011). A key conclusion from the previous body of work is that biocrude yield generally increases with increasing temperature up to 300-315°C; however, reaction hold time mediates a mixed effect on biocrude yield based on temperature. Increased yields are observed with longer hold times at lower temperatures, whereas decreased yields are observed with longer hold times at higher temperatures (Zhong and Wei, 2004; Xu and Etcheverry, 2008; Valdez et al., 2012; Zhang et al., 2009). Several studies have also evaluated the energy performance of HTL using various energy ratio metrics: e.g., ECR, in which the numerator corresponds to energy consumption for liquefaction ( $E_{IN}$ ), and the denominator corresponds to energy production ( $E_{OUT}$ ) via creation of biocrude (Sawayama et al., 1999; Vardon et al., 2012); or EROI, in which the numerator corresponds to  $E_{OUT}$ , and the denominator corresponds to  $E_{IN}$  (Connelly et al., 2015).

Several of the HTL studies that do address ACP characterization pertain to liquefaction of various pure microalgae and mixed-culture WWTP algae (Biller et al., 2012; Jena et al., 2011; Gai et al., 2015; Chen et al. 2014). These such studies evaluated the capacity of HTL to convert various algae feedstocks into energy-rich biocrude, while also concentrating feedstock nutrients (most notably N and P) into ACP for the desire to reuse the ACP as growth medium for algae cultivation (Biller et al., 2012; Gai et al., 2015; Garcia-Alba et al., 2012; Huang et al., 2013; Jena et al., 2011; Pham et al., 2013). Fewer studies have characterized ACP quantity and quality arising from non-algae feedstocks. Maddi et al. (2017) evaluated the HTL conversion of eight

organic waste feedstocks (i.e., three industrial food production residues, three WWTP residues, and two biomasses grown on other waste streams), with a goal of quantifying and characterizing organic C in the ACP. This study found that 20-55% of the initial feedstock C partitions into the ACP during HTL processing. In contrast, Ekpo et al. (2016) focused on N and P behaviors during thermal hydrolysis (at 120 or 170°C) and hydrothermal carbonization (at 200 or 250°C) of swine manure. This study evaluated conversion at multiple pH values, with or without various catalysts. Ekpo et al. (2016) concluded that thermochemical processing is more effective at concentrating N into ACP compared to P.

From limited data, it is presumed that ACP may be unsuitable for direct discharge into receiving waters without substantial dilution and/or application of conventional wastewater treatments (e.g., anaerobic digestion) or novel ACP management approaches (Tao et al., 2016; Tommaso et al., 2015; Vardon et al., 2011). Thus, this research aims to evaluate the possible water impacts arising from the creation of potent wastewaters via the HTL processing of select non-food, organic waste feedstocks through the characterization of ACP quantity and quality and revising the existing estimation of HTL EROI to account for ACP management.

## **3.2 Materials and Methods**

### **3.2.1 Raw Feedstock Collection and Characterization**

Eight non-food, organic waste feedstocks were selected for experimental evaluation based on bulk characteristics (e.g., water content and organic load) and logistical considerations (e.g., quantities produced per year, cost, availability of competing management strategies, etc.). These feedstocks include: (1) pre-digested WWTP sludge, (2) digested WWTP sludge, (3) dairy manure, and five residues from beer and wine production, i.e. (4) brewery yeast, (5) spent grains,

and (6) dry hops from craft beer production, and (7) white lees and (8) red lees from wine production. All feedstocks were collected from within central Virginia. Pre- and post-digested sludge samples were collected from a 15-million gallon per day (MGD) wastewater treatment facility; dairy manure was collected from a small, 150-head family-owned farm; brewing wastes (i.e., brewing yeast, spent grains, and dry hops) were collected from a craft production facility producing 27,000 barrels per year; and winery wastes (i.e., white and red lees) were collected from a small winery producing 8,000 cases per year. All samples were collected, immediately characterized, and stored at 4°C prior to HTL processing.

Feedstock characterization protocols were adapted from Huang et al. (2013) and Pham et al. (2013). All feedstocks were thoroughly homogenized via blending and analyzed for total suspended solids (TSS), volatile solids (VS), and ash content according to APHA Standard Methods (APHA, 2013). Elemental C and N contents were measured using a Thermo Scientific Flash 2000 NC Soil Analyzer. Pre- and post-digested WWTP sludge samples were dewatered via sedimentation and light centrifuging followed by decanting of the bulk supernatant. Prior to HTL processing, all feedstocks were adjusted to a solids content of 10% (m/m) via addition of deionized (DI) water, resulting in a paste-like consistency (Jena et al., 2011).

### **3.2.2 HTL Conversion and Characterization of Resulting Products**

HTL conversion experiments were performed in triplicate using a procedure adapted from Garcia Alba et al. (2012) and Pham et al. (2013). In brief, 100 g of wet feedstock paste (90% water content, m/m) was added to a 300-mL Parr Hast reactor with quartz liner, external heater, and asbestos insulation (Figure 3-1). The reactor was sealed with a PTFE flat-gasket, purged three times with pure nitrogen gas (N<sub>2</sub>), pressurized to 100 psi to prevent boiling, and continuously stirred at 300 rpm. The reactor was heated at ~8-10°C/min until the target

temperature of  $300 \pm 5^\circ\text{C}$  was reached. This temperature was maintained for a 30-min residence time. Temperature and residence time values were selected based on published studies utilizing “conventional” HTL feedstocks, with emphasis on characterizing ACP properties arising from “typical” HTL conditions (Akhtar and Amin, 2011; Huang et al., 2013; Pham et al., 2013; Vardon et al., 2011; Garcia Alba et al., 2012).

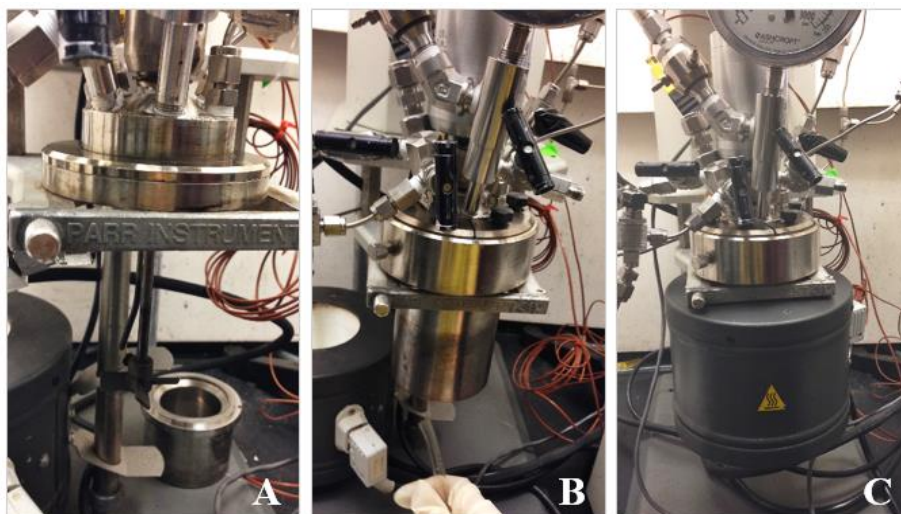


**Figure 3-1.** Parr Hast reactor setup, with (1) magnetic stirrer, (b) quartz liner, temperature sensor, pressure gauge, and gas inlet and outlet, and (c) electric furnace. Not shown is the control panel.

HTL produces a mixture of products, including bio-oil (or liquid biocrude), biochar, gas, and ACP (Toor et al., 2011) (Figure 3-2). After each reaction, the reactor was cooled and gaseous co-products were vented. The biochar was separated from the liquid phase via filtration, oven-dried at  $105^\circ\text{C}$ , and weighed. The liquid biocrude was separated from the ACP via extraction into dichloromethane (DCM), as previously described by Xu and Savage (2014), by which 1-2x vol/vol DCM was added to HTL liquids, and the mixture was decanted and centrifuged to facilitate phase separation. The ACP was manually drawn off, such that the liquid

biocrude was operationally defined based on solubility in DCM. The solvent was then evaporated using a gentle stream of N<sub>2</sub> gas for a 24-hr period. Final quantities of ACP and biocrude were measured and recorded.

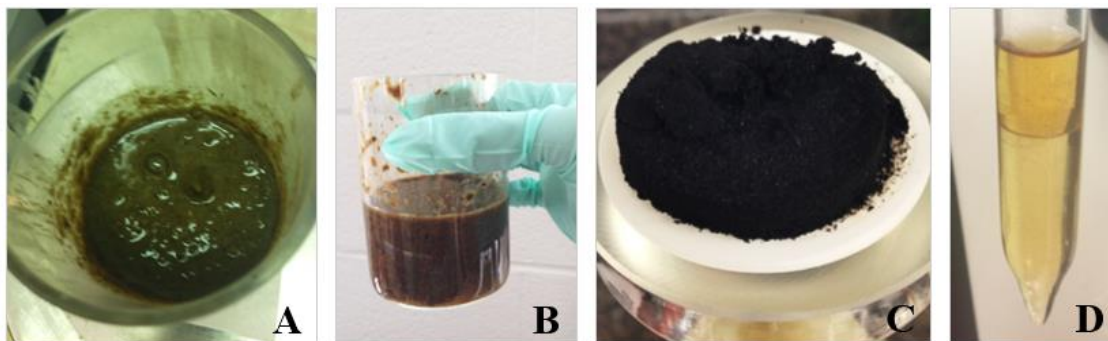


**Figure 3-2.** HTL processing of dairy manure, including (a) raw waste feedstock slurry (TSS of 10%, m/m), (b) post-HTL waste feedstock, (c) post-HTL solid-phase biochar, and (d) post-HTL ACP (top layer) extracted from liquid-phase co-products via liquid-liquid phase extraction. Gaseous co-products were vented.

The resulting ACP was filtered using a 0.22-um pore-size filter to remove particulates, and characterized using procedures from Jena et al. (2011) and Pham et al. (2013). Each ACP was characterized based on traditional wastewater parameters, including: pH, dissolved organic content (as measured using chemical oxygen demand [COD]), total nitrogen (TN), ammonium (NH<sub>4</sub>-N), total phosphorus (TP), and orthophosphate (PO<sub>4</sub>-P). These parameters were measured using APHA Standard Methods or commercial HACH kits (APHA, 2013). Total organic carbon (TOC) content of the ACP was computed from measured COD concentrations based on the empirical formula given by Equation 3-1.

$$COD = 3.00 \times TOC - 49.2$$

*Equation 3-1*

Here, TOC and COD are in units of mg/L (Dubber and Gray, 2010). Because all of the initial feedstocks comprised biomass in DI water, it was assumed that inorganic C was approximately zero. ACP quality was further assessed by comparison to the standard water quality parameter levels of several benchmark wastewaters from literature (Tchobanoglous et al., 2003; Rajeshwari et al., 2000; Jena et al., 2011; Biller et al., 2012; Tommaso et al., 2015).

### **3.2.3 Energy Ratio Metrics**

Energy ratio metrics were collected from several existing literature studies. ECR values were obtained from Sawayama et al. (1999) and Vardon et al. (2012); EROI values were obtained from Connelly et al. (2015). These studies provided sufficient detail to facilitate adjustment of the energy consumption term ( $E_{IN}$ ) to calculate adjusted EROI values that account for the management of ACP produced via HTL processing. This analysis assumed that all ACP is discharged to a municipal WWTP, where it is diluted into the influent at the head of the plant. There were several assumptions made to determine the energy consumption for ACP management, including: ACP volume and COD, TN, and TP removal. These assumptions are discussed in the following section.

#### *3.2.3.1 ACP Management Assumptions*

In order to determine ACP volume, for Connelly et al. (2015), it was assumed that the water content in the initial feedstock algae (75%, m/m) was converted directly to ACP (Liu et al., 2012). The amount of algae biomass feedstock (in kg) corresponding to the selected calculations basis (1 MJ as upgraded fuel) in Connelly et al. (2015) was computed based on the energy content and biocrude yield parameters from the supplemental information document for this study. The estimated mass of ACP produced per the 1-MJ calculations basis was converted to

ACP volume assuming an ACP density of 1 g/mL. For Vardon et al. (2012), it was also assumed that the water content in the initial feedstock (80%, m/m) was converted directly to ACP. In this study, the water weight of the raw feedstock was 200 g. The ACP mass was converted to ACP volume also assuming an ACP density of 1 g/mL. Sawayama et al. (1999) did not report water contents for their evaluated feedstocks. Therefore, it was assumed that feedstock water content was 90% (m/m), for consistency with the experiments performed in this dissertation. As with the other studies, it was assumed that feedstock water content was converted directly to ACP, and the resulting ACP mass was converted to ACP volume using an ACP density of 1 g/mL.

COD is removed via biological oxidation (i.e., activated sludge treatment). In order to account for the energy consumption required for COD removal from the ACP, an average COD concentration was assumed based on experimental results and converted to biological oxygen demand (BOD) concentration using the empirical formula given by Equation 3-2.

$$BOD = 0.589 \times COD - 11.3 \quad \text{Equation 3-2}$$

Here, BOD and COD are in units of mg/L (Dubber and Gray, 2010). BOD and COD are both widely used surrogates for oxidizable organic C content in wastewaters; however, BOD better accounts for the fraction of organic C that will be readily degraded (i.e., “removed”) during conventional biological treatment. After COD was converted into BOD, the resulting concentration was multiplied by the volume of ACP to compute the BOD mass (in kg) to be oxidized during treatment. Estimates of energy demand for BOD removal were collected from relevant literature, resulting in an average value of 8.7 MJ/kg BOD (Bodik and Kubaska, 2013; Guzman and McFarland, 2015). This value was multiplied by the mass of BOD in ACP to compute the energy consumption required for BOD (i.e., COD) removal. With respect to the

permitted effluent levels for BOD versus COD in a typical WWTP, most regulations are written on a BOD basis, and 30 mg/L is the minimum standard for BOD effluent in the U.S.

(Tchobanoglous et al., 2003). Applying Equation 3-2 to this value, it can be assumed that effluent COD concentrations must be less than roughly 50 mg/L.

TN is removed via nitrification (i.e., conversion of ammonia [ $\text{NH}_3$ ] and organic N into nitrate [ $\text{NO}_3^-$ ]), followed by denitrification (i.e., conversion of  $\text{NO}_3^-$  into  $\text{N}_2$  gas) (Tchobanoglous et al., 2003). Oxygen is consumed during biological nitrification, but this consumption was previously accounted for in the estimated energy consumption for COD removal. Denitrification requires methanol as co-substrate. In order to determine the energy consumption required for TN removal from the ACP, an average TN concentration was assumed based on experimental results. This concentration was multiplied by ACP volume to compute the TN mass (in kg) to be denitrified during treatment and was then multiplied by methanol demand (3.4 kg methanol/kg N) and the energy intensity of methanol production (38 MJ/kg methanol) to compute energy consumption for TN removal (Clarens et al., 2010).

TP is removed via precipitation using ferrous sulfate ( $\text{FeSO}_4$ ). In order to calculate the energy consumption required to remove TP from the ACP, an average TP concentration was assumed based on experimental results and multiplied by ACP volume to compute the TP mass (in kg) to be removed during treatment. This value was then multiplied by  $\text{FeSO}_4$  demand (1.8 kg  $\text{FeSO}_4$ /kg P) and the energy intensity of  $\text{FeSO}_4$  production (1.95 MJ/kg) to compute energy consumption for TP removal (Clarens et al., 2010).

### 3.2.3.2 Energy Ratio Formulas and Parameterization

Two different energy ratio metrics were used in the original papers: EROI (i.e.,  $E_{OUT}/E_{IN}$ ) and ECR (i.e.,  $E_{IN}/E_{OUT}$ ), where  $E_{IN}$  is equal to the energy “input” (i.e., consumption), and  $E_{OUT}$  is equal to the energy “output” (i.e., production). EROI and ECR are inverses of one other, such that higher values of EROI are indicative of better energy performance, and lower values of ECR are indicative of better energy performance. For both metrics, 1 is the “breakeven” energy point. Connelly et al. (2015) originally computed EROI, whereas Sawayama et al. (1999) and Vardon et al. (2012) originally computed ECR. In order to facilitate comparison across studies, all revised energy ratio metrics were converted to EROI format.

In the original papers,  $E_{OUT}$  was parameterized based on the quantity and energy density of the biocrude/bio-oil product. Connelly et al. (2015) normalized all energy quantities to an assumed energy output of 1 MJ, so the  $E_{OUT}$  value was nominally 1 MJ. Sawayama et al. (1999) computed energy output based on assumed production of 1 kg bio-oil and reported LHV (lower heating value) for the produced oils.  $E_{OUT}$  was given by 1 kg bio-oil  $\times$  bio-oil LHV (in MJ/kg). Vardon et al. (2012) reported bio-oil yields from HTL processing of 50 g dry weight feedstock and 200 g water and reported HHV (higher heating value) for the produced bio-oils and accounted for the efficiency of combustion energy ( $R_C = 0.7$ ).  $E_{OUT}$  was given by the product of bio-oil yield (in kg)  $\times$  bio-oil HHV (in MJ/kg)  $\times$   $R_C$ .

Sawayama et al. (1999) and Vardon et al. (2012) parameterized  $E_{IN}$  using very similar approaches. The estimates of  $E_{IN}$  from these studies accounted only for the energy consumption to heat the HTL feedstocks. The general formulation for this calculation is given by Equation 3-3, where:  $C_{PF}$  and  $C_{PW}$  are specific weights of the dry feedstock and water, respectively, and  $\Delta T$  is temperature change. Vardon et al. (2012) also accounted for the efficiency of heat recovery

( $R_H = 0.7$ ). Sawayama et al. (1999) and Vardon et al. (2012) both provide adequate detail to replicate  $E_{IN}$  calculations using this approach.

$$E_{IN} = (\text{Feedstock Dry Mass} \times C_{PF} + \text{Feedstock Water Mass} \times C_{PW}) \times \Delta T \quad \text{Equation 3-3}$$

Connelly et al. (2015) conducted a life-cycle assessment (LCA) for the HTL-based production of algae-derived liquid transportation fuels. Accordingly,  $E_{IN}$  accounted for all phases on the algae supply chain, not just the liquefaction process itself. The calculations in Connelly et al. (2015) were scaled to an assumed energy output of 1 MJ.  $E_{IN}$  was computed by taking the sum of the “energy use” from the supplemental information document of this study.

None of the original papers accounted for ACP management as a contributor to  $E_{IN}$ . Therefore, it was necessary to adjust the  $E_{IN}$  values to account for the energy consumption for the removal of COD, TN, and TP. For all studies, energy consumption required for ACP treatment was normalized to the same basis as the original calculations (e.g., 1 MJ or 1 kg) and then linearly added to the originally reported  $E_{IN}$  value. Revised EROI values were then computed using original  $E_{OUT}$  and revised  $E_{IN}$  values.

### **3.3 Results and Discussion**

#### **3.3.1 Characterization of Raw Feedstocks**

Because previous HTL research has focused almost exclusively on optimizing biocrude yield, the goal of this study was to analyze the quantity and quality of the ACP arising from the HTL processing of several non-food, organic waste feedstocks and assess what treatment(s), if any, would be required for the management of ACP. It was hypothesized that feedstock properties could affect ACP quality; therefore, it was of interest to evaluate various parameters for each selected feedstock. Table 3-1 summarizes pertinent pre-HTL processing characteristics

for the eight as-received waste feedstocks included in this study, including: TSS, VS, ash content, water content, and percent N and C contents. From this data, there is wide variability in feedstock composition. This is potentially valuable for understanding how different feedstock qualities give rise to different quantities and qualities of HTL products, such as biocrude and ACP. Three important observations arising from this data pertain to water content, C content, and nutrient/ash content.

**Table 3-1.** Characterization and elemental analysis of as-received raw waste feedstocks prior to hydrothermal processing, as expressed using percent weight (wt %). Confidence intervals correspond to  $\pm 1$  standard deviation ( $n = 3$  replicates).

<b>Waste Feedstock</b>	<b>TSS (wt %)</b>	<b>VS (wt %)</b>	<b>Ash (wt %)</b>	<b>Water Content (wt %)</b>	<b>N (wt %)</b>	<b>C (wt %)</b>
Dairy Manure	15.2 $\pm$ 0.8	88.6 $\pm$ 1.6	13.0 $\pm$ 3.1	84.7 $\pm$ 0.8	1.8 $\pm$ 0.1	39.8 $\pm$ 0.7
Pre-Digested Sludge	10.5 $\pm$ 0.5	28.8 $\pm$ 0.8	55.7 $\pm$ 0.9	89.5 $\pm$ 0.5	4.1 $\pm$ 0.3	35.2 $\pm$ 0.6
Digested Sludge	8.5 $\pm$ 1.5	81.9 $\pm$ 0.7	32.3 $\pm$ 2.2	91.5 $\pm$ 1.5	4.4 $\pm$ 0.6	24.0 $\pm$ 2.1
Brewing Yeast	16.8 $\pm$ 0.2	92.9 $\pm$ 0.2	7.1 $\pm$ 0.2	83.2 $\pm$ 0.2	5.3 $\pm$ 0.4	44.3 $\pm$ 0.3
Spent Grains	22.1 $\pm$ 0.8	96.0 $\pm$ 1.9	4.0 $\pm$ 1.9	77.9 $\pm$ 0.8	4.6 $\pm$ 0.5	51.7 $\pm$ 1.1
Dry Hops	12.3 $\pm$ 0.2	93.6 $\pm$ 0.9	6.4 $\pm$ 0.9	87.7 $\pm$ 0.2	3.6 $\pm$ 0.2	47.9 $\pm$ 1.1
White Lees	26.2 $\pm$ 0.3	82.0 $\pm$ 4.1	18.0 $\pm$ 4.1	73.8 $\pm$ 0.3	0.38 $\pm$ 0.06	41.1 $\pm$ 0.9
Red Lees	11.3 $\pm$ 0.9	64.2 $\pm$ 1.5	35.8 $\pm$ 1.5	88.7 $\pm$ 0.9	4.1 $\pm$ 0.3	42.8 $\pm$ 0.9

Regarding water content, TSS was measured on as-received and/or bulk-dewatered (in the case of the pre- and post-digested WWTP sludge samples) feedstocks to assess what adjustments were required to achieve an optimal moisture content of 90% (m/m) (Jena et al., 2011). All selected feedstocks exhibited water contents over a somewhat narrow range of 74-92%. Four feedstocks required little to no water addition: pre-digested sludge, digested sludge, dry hops from beer brewing, and red lees from wine making. It is also significant that none of the feedstocks required significant drying or dewatering beyond passive sedimentation and bulk decanting, given that drying is very energy-consuming at large scale.

Feedstock composition, most notably C content, is also critically important to the overall energy favorability of HTL. Under ideal conditions, feedstock C is completely transformed into liquid biocrude and isolated from all other feedstock constituents (e.g., oxygen, hydrogen, N, P, etc.), maximizing the quantity and quality of the biocrude produced (Bhutto et al., 2016; Toor et al., 2011; Chen et al., 2014). Thus, high values of feedstock C are preferable for HTL (Vardon et al., 2011; Huang et al., 2013; Pham et al., 2013). The feedstocks analyzed in this study exhibit moderate variability in C content over a range of 24-52%. These values are comparable to microalgae (30-50% C) reported in existing literature (Jena et al., 2011; Biller et al., 2012; Gai et al., 2015).

Nutrient and ash content are also important considerations related to HTL feedstock composition. Under optimal HTL conditions, nutrients will partition to the ACP, which is itself a “waste” (i.e., “wastewater”). Higher concentrations of N, P, and other salts in the feedstocks give rise to correspondingly higher concentrations in the ACP, thereby increasing its noxiousness and rendering it potentially unsuitable for direct discharge to receiving waters or municipal WWTPs. From Table 3-1, there is also moderate variability in N content (2-5%), with white lees as an obvious outlier. However, there is dramatic variability in ash content: i.e., low ash content (4-7%) for the brewing residues; medium ash content (13-18%) for the dairy manure and white lees; and high ash content (30-55%) for the WWTP sludges and red lees. It is desirable for HTL feedstocks to have minimal ash content, as inert materials constituting ash cannot be converted into fuel, but still consume energy for heating during HTL conversion. As hypothesized, it is of possible interest to examine how these and other feedstock attributes affect HTL product distribution, most notably ACP quantity and quality.

### 3.3.2 Characterization of HTL Products

HTL processing reactions were conducted to analyze the conversion of each of the selected organic waste feedstocks. Figure 3-3 presents the quantities of products (i.e., biocrude, biochar, and ACP) arising from the HTL conversion of 100 g wet weight of each waste feedstock. From this data, all feedstocks produce similar quantities of biochar (2.1-4.0 g per 100 g feedstock) and comparable volumes of liquid products (roughly 80-96 mL per 100 g feedstock). Of the liquid products, biocrude constitutes ~5-20 mL (6-22%), and ACP constitutes ~65-90 mL (74-92%). For all feedstocks, the volume of ACP produced is much greater than the volume of biocrude, with ratios (ACP:biocrude) spanning 3-15x. Thus, significant quantities of ACP are produced during HTL conversion of the selected waste feedstocks. This has not been overtly evident from existing HTL literature. Considering only product quantity, and temporarily leaving aside quality, pre- and post-digestion WWTP sludge and the white lees feedstocks deliver the best ratios of biocrude to ACP. This is an unexpected grouping, based on Table 3-1, since these three feedstocks do not exhibit any obvious similarities in feedstock characteristics, relative to the other feedstocks.

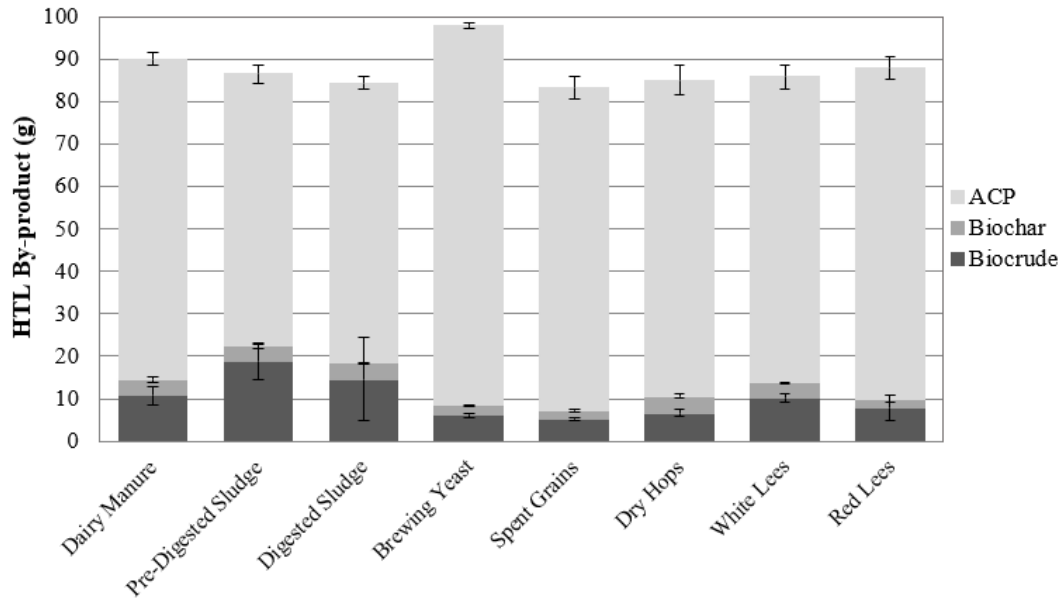


**Figure 3-3.** Distribution of HTL products (i.e., biocrude, biochar, and ACP) for eight non-food, organic waste feedstocks. Biochar mass was measured directly. ACP and biocrude masses were computed from measured volumes using densities of 1.0 and 0.96 g/mL, respectively. Error bars correspond to  $\pm 1$  standard deviation ( $n = 3$  replicates).

It should be noted that some biocrude masses in Figure 3-3 are higher than expected, based on the initial feedstock loading (10 g dry solids for all feedstocks). Also, some ACP masses are lower than expected based on the initial feedstock loading (90 g water for all feedstocks). Taken together, these observations suggest that there was incomplete phase separation during the DCM extraction; i.e., some ACP was drawn off with the biocrude, thereby artificially increasing apparent biocrude yields and artificially decreasing apparent ACP yields. Previous research has drawn attention to variability in product yields arising from operational definition based on solubility in a selected solvent (Xu and Savage, 2014). Additionally, it was observed that a small amount of steam was visible when the HTL reactor was vented. The loss of water vapor could also have contributed to lower than expected ACP yields. Unfortunately, the gaseous products were not measured, because this study focuses primarily on ACP. It is,

therefore, presumed that gases account for the difference between total measured product masses (i.e., biochar + biocrude + ACP) and initial mass loading (100 g for each feedstock). Referring again to Figure 3-3 and taking into account the higher and lower than expected yields of biocrude and ACP, respectively, it can be surmised that the aforementioned ratios of ACP to biocrude are possible underestimates for this parameter. This observation has not been overtly emphasized in previous studies. Also, the creation of appreciable biochar indicates that the selected HTL conditions are not optimal for all evaluated feedstocks. Future work should elucidate the impacts of HTL processing conditions on product yields and composition, with special emphasis on ACP production.

Finally, comparison of Table 3-1 and Figure 3-3 reveals that there is no obvious relationship between feedstock properties and HTL product-phase distribution. Although there is fair variability in feedstock properties (Table 3-1), the measured attributes are not obviously correlated with product distribution. Rather, all waste feedstocks produce roughly the same amount of biocrude relative to ACP and biochar. This has ramifications for commercialization of HTL, insofar as it suggests that there is no need to process individual feedstocks separately from one other. Rather, since all feedstocks give roughly similar products, it is acceptable to aggregate all available feedstocks and process them together for convenience.

Turning to ACP quality, Table 3-2 presents characterization data for each ACP arising from the HTL processing of the selected waste feedstocks, with emphasis on wastewater-relevant parameters and constituents. These data are presented alongside water quality benchmarks to communicate the potency of ACP relative to more familiar wastewaters, such as raw (i.e., influent) domestic wastewater, industrial wastewaters (e.g., slaughterhouse, dairy, distillery, and paper manufacturing wastewaters), and landfill leachate (Biller et al., 2012; Tommaso et al.,

2015; Tchobanoglous et al., 2003; Rajeshwari et al., 2000; Christensen et al., 2001; Oman and Junestedt, 2008). A key conclusion from Table 3-2 is that ACP is more noxious than several well-known industrial wastewaters (e.g., raw industrial wastewater and landfill leachate). ACP exhibits widely variable pH and contains very large quantities of COD, TN, and TP. Thus, it is evident that ACP will require significant dilution and/or treatment before it can be safely discharged into the receiving waters of a municipal WWTP. This is noteworthy, because ACP management could become cost-prohibitive at commercial scale.

**Table 3-2.** Characterization of ACP arising from the HTL conversion of eight non-food, organic waste feedstocks. Confidence intervals correspond to  $\pm 1$  standard deviation ( $n = 3$  replicates). Italicized font indicates pertinent wastewater benchmarks and post-HTL ACP laboratory results from relevant literature. NA = not reported.

Feedstock	pH	COD (mg/L)	TN (mg/L)	NH <sub>4</sub> -N (mg/L)	TP (mg/L)	PO <sub>4</sub> -P (mg/L)
Dairy Manure	4.4 $\pm$ 0.2	29,200 $\pm$ 200	1,050 $\pm$ 70	315 $\pm$ 220	477 $\pm$ 40	39.3 $\pm$ 9.0
Pre-Digested Sludge	8.4 $\pm$ 0.4	32,275 $\pm$ 1,500	3,250 $\pm$ 200	975 $\pm$ 160	800 $\pm$ 60	112 $\pm$ 22
Digested Sludge	8.6 $\pm$ 0.9	20,800 $\pm$ 3,950	2,180 $\pm$ 460	2,100 $\pm$ 125	220 $\pm$ 140	31 $\pm$ 11
Brewing Yeast	8.3 $\pm$ 0.1	65,750 $\pm$ 4,735	2,450 $\pm$ 315	1,370 $\pm$ 190	2,195 $\pm$ 95	753 $\pm$ 4.0
Spent Grains	5.3 $\pm$ 0.8	31,500 $\pm$ 1,000	2,050 $\pm$ 600	700 $\pm$ 170	1,038 $\pm$ 60	352 $\pm$ 2.0
Dry Hops	7.0 $\pm$ 0.6	103,500 $\pm$ 3,160	2,500 $\pm$ 50	1,240 $\pm$ 60	2,425 $\pm$ 60	287 $\pm$ 12
White Lees	6.4 $\pm$ 0.3	16,115 $\pm$ 610	96 $\pm$ 20	31 $\pm$ 2.8	45 $\pm$ 18	53 $\pm$ 6.7
Red Lees	8.8 $\pm$ 0.3	234,200 $\pm$ 6,600	1,890 $\pm$ 220	1,115 $\pm$ 160	3,632 $\pm$ 180	687 $\pm$ 80
<i>Algae ACP<sup>a</sup></i>	8.4-9.2	28,000-43,000	2,900-8,100	2,900-6,300	40-1,100	40-280
<i>Raw Domestic WW<sup>b</sup></i>	6.0-9.0	250-800	20-70	12-50	4-12	2-6
<i>Raw Industrial WW<sup>c</sup></i>	5.0-8.0	5,200-11,400	NA	19-74	7-28	NA
<i>Landfill Leachate<sup>d</sup></i>	6.4-8.5	250-1,300	54-865	4-740	0.1-4.0	0.03-3.5

<sup>a</sup>Based on literature averages for various algae (e.g. *Chlorella*, *Scenedesmus*, *Spirulina*, etc.) (Jena et al., 2011; Biller et al., 2012; Garcia Alba et al., 2012; Tommaso et al., 2015).

<sup>b</sup>Based on raw domestic influent from municipal WWTPs (Tchobanoglous et al., 2003).

<sup>c</sup>Based on literature averages for several industrial wastewaters (e.g. slaughterhouse, dairy manufacturing, and paper manufacturing wastewaters) (Rajeshwari et al., 2000).

<sup>d</sup>Based on literature averages from municipal landfill sites (Christensen et al., 2001; Oman and Junestedt, 2008).

Other important observations arising from Table 3-2 pertain to pH and the distribution of selected feedstock constituents among HTL product phases. Regarding pH, there is dramatic variability among the measured values, ranging from relatively acidic (4.4 for dairy manure and 5.3 for spent grains) to slightly basic ( $\geq 8$  for brewing yeast, pre- and post-digested sludge, and red lees). Only two feedstocks produced ACP with pH in the circumneutral range (6-8). As such, most of the ACP will likely require pH adjustment prior to discharge into the receiving waters of a municipal WWTP. The distributions of C and other feedstock constituents among HTL product phases are discussed in the following sections.

#### *3.3.2.1 Carbon Distribution among HTL Products*

The principal goal of HTL processing is to maximize conversion of feedstock C into biocrude. It is also desirable to isolate feedstock C from N, oxygen, and other elements, in order to optimize biocrude quality (Akhtar and Amin, 2011; Toor et al., 2011). Therefore, it is of interest to evaluate the distribution of C, as well as other feedstock components, amongst the various HTL product phases. This analysis is also germane to anticipating possible water quality impacts due to the production of ACP, because polar constituents could accumulate in the ACP. Figure 3-4a summarizes the distribution of feedstock C among the various HTL product phases for each of the eight selected waste feedstocks.

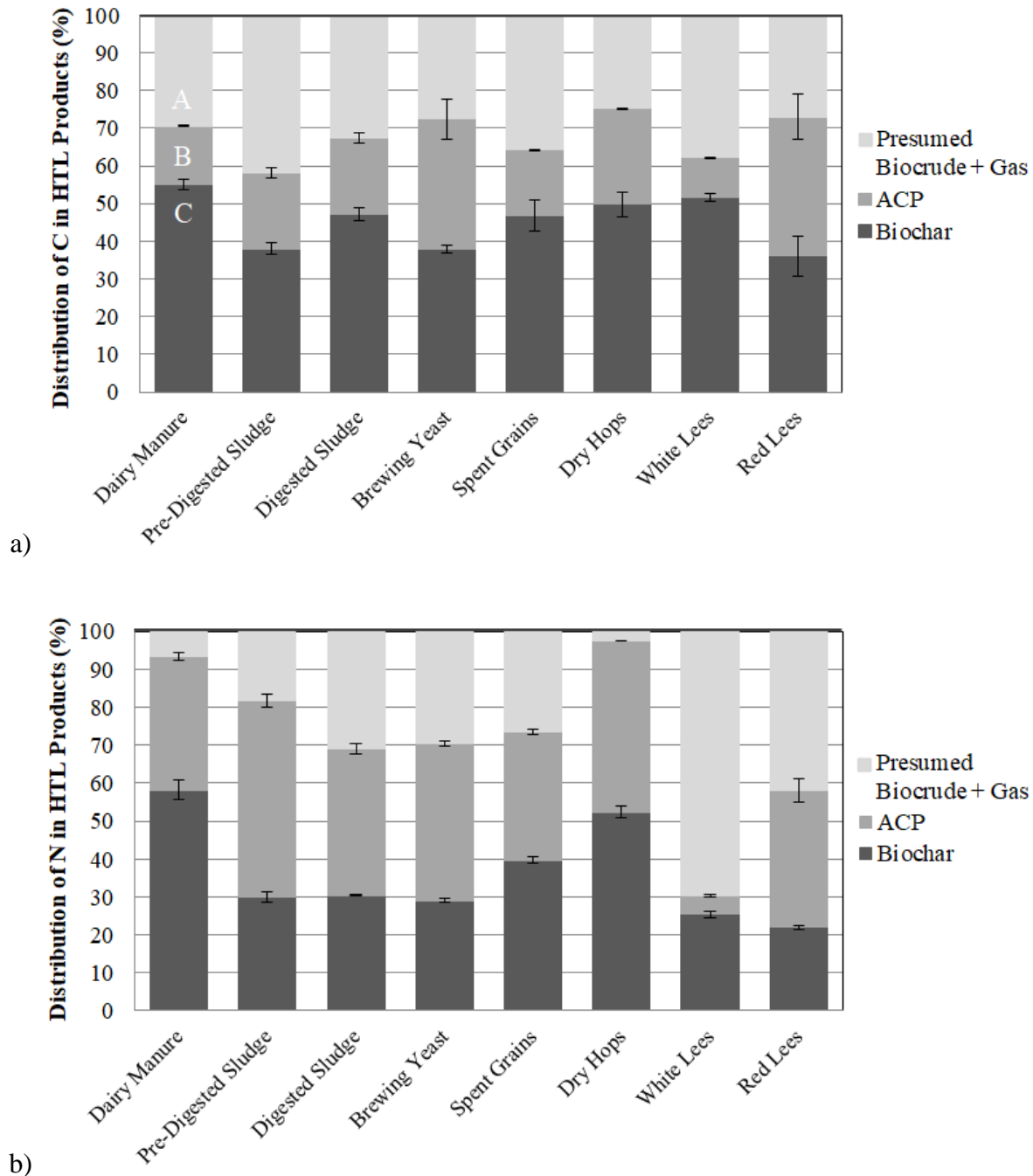


**Figure 3-4.** Percent distribution showing how feedstock (a) carbon and (b) nitrogen are distributed among the HTL product phases. These data are interpreted as follows, using annotated dairy manure carbon distribution as an example: 10 g dry weight of dairy manure solids comprising 40% carbon (m/m) is converted into HTL products. A% of the feedstock carbon is converted into biocrude and/or gas, B% is converted into ACP, and C% is converted into biochar; where  $A + B + C = 30 + 15 + 55 = 100\%$  of the 4 g initial feedstock carbon. Error bars correspond to  $\pm 1$  standard deviation ( $n = 3$  replicates).

From Figure 3-4a, roughly 25-30% of initial feedstock C is converted into biocrude during HTL. This is consistent with Maddi et al. (2017), who observed 20-55% of feedstock C partitioning into biocrude for various organic waste feedstocks. Biochar and ACP account for approximately 45% and 23% of initial feedstock C, respectively, and it is assumed that the remainder (~5-10%) is transformed into unmeasured gaseous products. It is somewhat surprising that the biochar accounts for such a significant fraction of initial feedstock C, given the very small quantities of solids that are produced (2.1-4.0 g per 100 g feedstock) (Figure 3-3). This disparity is explained by very high C contents in the biochar (38-76%, m/m). Although it is less desirable for C to transform into biochar versus biocrude, there are potential commercial applications for biochars with appreciable organic contents; e.g., as slow-release agricultural fertilizer or as feedstock for additional thermochemical processing (Biller et al., 2012; Jena et al., 2015).

It is undesirable for feedstock C to transform into ACP for several reasons. First, the presence of dissolved organic C in ACP reduces biocrude yield, thereby contributing to reduced energy recovery (Maddi et al., 2017). Second, organic C is a regulated wastewater pollutant (Tchobanoglous et al., 2003). Table 3-2 reveals high dissolved organic content in all ACP samples, with the average COD concentration in the ACPs nearly 67,000 mg/L, which is much higher than the COD levels seen in most industrial wastewaters. COD is used as an easily measurable, widely used surrogate for oxidizable organic C in wastewaters. Treatment facilities and other discharging entities are frequently subject to COD permit levels on the order of 50 mg/L (Tchobanoglous et al., 2003). Thus, ACP will likely require treatment to remove organic C content. Finally, it was hypothesized that there may be relationships between feedstock attributes and the quantities and/or C concentrations of corresponding HTL products. However,

there is no clearly discernable trend in the distribution of C among HTL product phases as a function of measured feedstock characteristics.

### *3.3.2.2 Nitrogen Distribution among HTL Products*

It is also of interest to evaluate the distribution of non-C feedstock constituents among HTL products. As previously mentioned, it is desirable to separate C from other elements (i.e., N, oxygen, P, etc.) in order to enhance biocrude quality (Elliott et al., 2014; Ekpo et al., 2016). Figure 3-4b summarizes the distribution of feedstock N among HTL product phases for each of the eight evaluated waste feedstocks. Unlike the case for C, there is no clear ranking of preference for N distribution. In particular, there is no clear “best” or “worst” option for N distribution among HTL products. It is undesirable to have appreciable N content in the biocrude since N heteroatoms increase the downstream processing that is required to produce a drop-in fuel and can contribute to the formation of greenhouse gases (e.g., nitrous oxides [NO<sub>x</sub>]) during fuel combustion (Chen et al., 2014; Ross et al., 2010). It is similarly undesirable to transform feedstock N into gaseous HTL products (e.g., NH<sub>3</sub> or NO<sub>x</sub>), because these gases adversely affect air quality and the global climate. From this data, it is evident that the biocrude and gas phases together account for roughly 30% of initial feedstock N. The remaining feedstock N partitions into the biochar and ACP. The biochar accounts for approximately 36% (on average) of initial feedstock N. The biochar contains appreciable N (1-7%, m/m), as well as C (as referenced above), which could make it suitable for use as agricultural fertilizer or a soil amendment (Elliott et al., 2014; Jena et al., 2015; Bhutto et al., 2016). The remaining feedstock N (roughly 36%) is present in the ACP.

From Table 3-2, ACP contains (on average) approximately 1,900 mg/L TN. This concentration is appreciably higher than in most industrial wastewaters and landfill leachate.

ACP also contains much higher TP (1,350 mg/L) than the selected benchmark wastewaters. As was previously mentioned, this contributes to the unsuitability of ACP for direct discharge into the receiving waters of a municipal WWTP, such that it is seemingly undesirable to have appreciable TN and TP in the ACP. Like COD, TN and TP are regulated wastewater pollutants, such that permitted discharging facilities are required to achieve low concentrations (e.g., 15-35 mg/L TN and 4-10 mg/L TP) in their effluents (Clarens et al., 2010). Thus, the ACP will likely require treatment to remove TN and TP down to acceptable levels. This is noteworthy given the high energy intensity and economic cost associated with nutrient removal during municipal wastewater treatment. Finally, as with C, there were no discernible trends in the distribution of N among HTL products as a function of measured feedstock characteristics.

### *3.3.2.3 Energy Recovery Impacts*

Existing literature does not address what impacts ACP management could have on the overall energy recovery of HTL systems. To address this knowledge gap, previously published estimates of energy ratio metrics were revised to include anticipated energy consumption for ACP treatment. Revised estimates of EROI ( $E_{OUT}/E_{IN}$ ) are presented in Table 3-3. For this metric, values greater than 1 are increasingly favorable. As seen in Table 3-3, accounting for ACP treatment does mediate moderate reductions in EROI. Energy consumption for ACP treatment (i.e., to remove COD, TN, and TP) is of the same order of magnitude as the energy consumption required for liquefaction. On average, anticipated ACP treatment accounts for almost 30% of the revised  $E_{IN}$  estimate.

**Table 3-3.** Original and revised estimates of EROI for the HTL conversion of various feedstocks, as reported in previous literature. EROI values >1 are indicative of favorable energy yield, whereas EROI values <1 are indicative of unfavorable energy yields.

Author/ Year	Feedstock/ Scenario	Original E <sub>IN</sub>	Revised E <sub>IN</sub>	Original EROI <sup>a</sup>	Revised EROI <sup>b</sup>
Connelly et al., 2015	Algae, “CO <sub>2</sub> from ethanol”	0.76 MJ/MJ biocrude	0.91 MJ/MJ biocrude	1.3	1.1
	Algae, “CO <sub>2</sub> from natural wells”	0.83 MJ/MJ biocrude	0.99 MJ/MJ biocrude	1.2	<b>1.0</b>
Sawayama et al., 1999	<i>B. braunii</i> (algae)	7 MJ/kg bio-oil	12 MJ/kg bio-oil	6.7	3.7
	<i>D. tertiolecta</i> (algae)	12 MJ/kg bio-oil	17 MJ/kg bio-oil	2.9	2.0
	Japanese oak	13 MJ/kg bio-oil	18 MJ/kg bio-oil	1.8	1.3
	Japanese larch bark	29 MJ/kg bio-oil	35 MJ/kg bio-oil	0.9	0.8
	Sewage sludge	11 MJ/kg bio-oil	16 MJ/kg bio-oil	2.9	2.0
	Barley silage	15 MJ/kg bio-oil	20 MJ/kg bio-oil	2.3	1.7
	Kitchen garbage	51 MJ/kg bio-oil	57 MJ/kg bio-oil	0.7	0.6
Vardon et al., 2012	<i>Scenedesmus</i> (algae), 80% moisture	173 kJ/50 g dw <sup>c</sup>	297 kJ/50 g dw <sup>c</sup>	2.3	1.3
	Defatted <i>Scenedesmus</i> , 80% moisture	173 kJ/50 g dw <sup>c</sup>	297 kJ/50 g dw <sup>c</sup>	1.8	1.1
	<i>Spirulina</i> (algae), 80% moisture	173 kJ/50 g dw <sup>c</sup>	297 kJ/50 g dw <sup>c</sup>	1.6	<b>0.9</b>

The results shown in Table 3-3 correspond to average ACP concentrations for COD, TN, and TP from Table 3-2. Energy consumption for ACP treatment increases with increasing concentrations of each pollutant; however, it could be advantageous to have very high TN and TP concentrations in ACP if the nutrients could be efficiently recovered in a useable form. The growing scarcity of N and P to support agriculture and other industries has spurred research interest in fertilizer recovery from highly potent wastewaters (e.g., landfill leachate, human urine, animal wastes, etc.) (Gruber and Galloway, 2008; Yetilmmezsoy et al., 2017; Kataki et al., 2016; Di Iaconi et al., 2010; Ekpo et al., 2016). Because ACP is so highly concentrated, it may be desirable to recover N (i.e., as ammonium [NH<sub>4</sub><sup>+</sup>]) and P (i.e., as orthophosphate [PO<sub>4</sub><sup>3-</sup>]) before discharging the ACP to a municipal WWTP. This could improve the EROI in two ways:

1) by reducing energy consumption for TN and TP removal and 2) by potentially creating a valuable substitute for fertilizer; e.g., struvite ( $\text{NH}_4\text{MgPO}_4 \times 6\text{H}_2\text{O}$ ) or hydroxyapatite (HAP,  $\text{Ca}_5[\text{PO}_4]_3[\text{OH}]$ ) (Yetilmezsoy and Sapci-Zengin, 2009; Kataki et al., 2016; Yetilmezsoy et al., 2017; Tsuji and Fujii, 2014; Teymouri et al., 2018). From Table 3-2,  $\text{NH}_4^+$  accounts for nearly 50% (on average) of ACP TN, and  $\text{PO}_4^{3-}$  accounts for nearly 26% (on average) of ACP TP. Thus, for the relatively small volumes of highly concentrated wastewater produced as ACP, it may be more cost-effective and less resource-consuming to recover N and/or P from ACP in the form of fertilizer, rather than diluting the concentrated nutrients into a larger volume of WWTP influent and removing these nutrients at very low concentrations.

Future work should evaluate the realistic practicality of nutrient recovery via precipitation from ACP, taking into account the following factors: specific ACP compositions arising from different HTL conditions, rather than the average values and uniform HTL conditions used in this study; detailed ACP chemistry considerations (e.g., recovery yields as a function of pH, competing side-reactions, etc.); and logistical considerations (e.g., feedstock availability, life-cycle energy footprints for the various reactants and products, etc.). Future research should also characterize possible toxicity impacts of the ACPs evaluated in this study, as means of assessing the suitability of ACP for subsequent conventional treatment, such as anaerobic digestion (to produce methane-derived bioelectricity) (Tommaso et al., 2015) or reuse as algae growth medium (Pham et al., 2013). This information will be valuable for assessing the extent to which HTL is an effective platform for producing not only alternative energy from waste, but also generating valuable nutrient-based materials.

### 3.4 Conclusions

HTL produces appreciable quantities of ACP, which contains high concentrations of regulated wastewater pollutants. The ACP arising from the HTL processing of eight selected organic waste feedstocks contain very high concentrations of traditional wastewater pollutants: i.e., 100-3,300 mg/L TN, 45-3,600 mg/L TP, and 16,000-234,000 mg/L COD. pH was 4.4-8.8. These characteristics render ACP more noxious than relevant benchmark wastewater; however, the potency of ACP has not been overtly emphasized in previous literature. Adjustment of published energy ratio metrics to account for ACP treatment reveals that energy yield is moderately decreased and energy consumption for COD, TN, and TP removal is of the same order of magnitude as liquefaction. Recovery of valuable nutrients (i.e., N and P) from ACP via chemical precipitation could reduce the energy intensity of ACP management and mitigate its impact on the EROI. In particular, precipitation-based nutrient recovery could enhance the appeal of HTL as a means of valorizing waste into renewable energy and producing valuable scarce nutrient-based materials.

### 3.5 References

- Akhtar, J. and Amin, N. A. S. (2011). A review on process conditions for optimum bio-oil yield in hydrothermal liquefaction of biomass. *Renewable and Sustainable Energy Reviews*, 15 (3), 1615–1624.
- APHA (2013). Standard methods for the examination of water and waste water, 22nd ed. *American Public Health Association*, Washington, D.C., Retrieved from <[www.standardmethods.org/PDF/22nd\\_Ed\\_Errata\\_12\\_16\\_13.pdf](http://www.standardmethods.org/PDF/22nd_Ed_Errata_12_16_13.pdf)>.
- Bauer, S., Reynolds, C., Peng, S. and Colosi, L. (2018). Evaluating the Water Quality Impacts of Hydrothermal Liquefaction: Assessment of Carbon, Nitrogen, and Energy Recovery Impacts, *Bioresource Technology Reports*, 2, 115-120.
- Bhutto, A. W., Qureshi, K., Abro, R., Harijan, K., Zhao, Z., Bazmi, A. A., Abbas, T. and Yu, G. (2016). Progress in the production of biomass-to-liquid biofuels to decarbonize the transport sector-prospects and challenges. *Royal Society of Chemistry Advances*, 6, 32140-32170.

- Biller, P., Ross, A. B., Skill, S. C., Lea-Langton, A., Balasundaram, B., Hall, C., Riley, P. and Llewellyn, C. A. (2012). Nutrient recycling of aqueous phase for microalgae cultivation from the hydrothermal liquefaction process. *Algal Research*, 1 (1), 70–76.
- Bodík, I. and Kubaska, M. (2013). Energy and sustainability of operation of a wastewater treatment plant. *Environment Protection Engineering*, 39, 15-24.
- Caetano, N. S., Silva, V. F. M., Melo, A. C., Martins, A. A. and Mata, T. M. (2014). Spent coffee grounds for biodiesel production and other applications. *Clean Technologies and Environmental Policy*, 16 (7), 1423–1430.
- Chen, W. T., Zhang, Y., Zhang, J., Yu, G., Schideman, L. C., Zhang, P. and Minarick, M. (2014). Hydrothermal liquefaction of mixed-culture algal biomass from wastewater treatment system into bio-crude oil. *Bioresource Technology*, 152, 130–139.
- Christensen, T. H., Kjeldsen, P., Bjerg, P. L., Jensen, D. L., Christensen, J. B., Baun, A., Albrechtsen, H. J. and Heron, G. (2001). Review: Biogeochemistry of landfill leachate plumes. *Applied Geochemistry*, 16, 659-718.
- Clarens, A. F., Resurreccion, E. P., White, M. A. and Colosi, L. M. (2010). Environmental life cycle comparison of algae to other bioenergy feedstocks. *Environmental Science & Technology*, 44, 1813-1819.
- Connelly, E. B., Colosi, L. M., Clarens, A. F. and Lambert, J. H. (2015). Life Cycle Assessment of Biofuels from Algae Hydrothermal Liquefaction: The Upstream and Downstream Factors Affecting Regulatory Compliance. *Energy & Fuels*, 29, 1653-1661.
- Corbin, K. R., Hsieh, Y. S. Y., Betts, N. S., Byrt, C. S., Henderson, M., Stork, J. and Burton, R. A. (2015). Grape marc as a source of carbohydrates for bioethanol: Chemical composition, pre-treatment and saccharification. *Bioresource Technology*, 193, 76–83.
- Di Iaconi, C., Pagano, M., Ramadori, R. and Lopez, A. (2010) Nitrogen recovery from a stabilized municipal landfill leachate, *Bioresource Technology*, 101, 1732-1736.
- Dubber, D. and Gray, N. F. (2010). Replacement of chemical oxygen demand (COD) with total organic carbon (TOC) for monitoring wastewater treatment performance to minimize disposal of toxic analytical waste. *J. Environ. Sci. Health A Tox. Hazard Subst. Environ. Eng.*, 45 (12), 1595-1600.
- Dominguez-Faus, R., Powers, S. E., Burken, J. G. and Alvarez, P. J. (2009). The Water Footprint of Biofuels: A Drink or Drive Issue? *Environmental Science & Technology*, 43 (9), 3005–3010.
- Ekpo, U., Ross, A. B., Camargo-Valero, M. A. and Fletcher, L. A. (2016). Influence of pH on hydrothermal treatment of swine manure: Impact on extraction of nitrogen and phosphorus in process water. *Bioresource Technology*, 214, 637-644.
- Elliott, D. C., Biller, P., Ross, A. B., Schmidt, A. J. and Jones, S. B. (2014). Hydrothermal liquefaction of biomass: Developments from batch to continuous process. *Bioresource Technology*, 178, 147–156.

- Gai, C., Zhang, Y., Chen, W. T., Zhou, Y., Schideman, L., Zhang, P., Tommaso, G., Kuo, C. T. and Dong, Y. (2015). Characterization of aqueous phase from the hydrothermal liquefaction of *Chlorella pyrenoidosa*. *Bioresource Technology*, 184, 328–35.
- Gama, R., Van Dyk, J. S. and Pletschke, B. I. (2015). Optimization of enzymatic hydrolysis of apple pomace for production of biofuel and biorefinery chemicals using commercial enzymes. *3 Biotech.*, 5 (6), 1075–1087.
- Garcia Alba, L., Torri, C., Samorì, C., Van der Spek, J., Fabbri, D., Kersten, S. R. A. and Brilman, D. W. F. (2012). Hydrothermal treatment (HTT) of microalgae: Evaluation of the process as conversion method in an algae biorefinery concept. *Energy & Fuels*, 26 (1), 642–657.
- Gruber, N. and Galloway, J. N. (2008). An Earth-system perspective of the global nitrogen cycle, *Nature*, 45, 293-296.
- Guzman, S. and McFarland, M. (2015). Energy efficiency and recovery opportunities analysis for municipal wastewater treatment plant operations. *Water Environment Federation*, 9, 1-9.
- Huang, H. J., Yuan, X. Z., Zhu, H. N., Li, H., Liu, Y., Wang, X. L. and Zeng, G. M. (2013). Comparative studies of thermochemical liquefaction characteristics of microalgae, lignocellulosic biomass and sewage sludge. *Energy*, 56, 52–60.
- Jena, U., Vaidyanathan, N., Chinnasamy, S. and Das, K. C. (2011). Evaluation of microalgae cultivation using recovered aqueous co-product from thermochemical liquefaction of algal biomass. *Bioresource Technology*, 102 (3), 3380–7.
- Kataki, S., West, H., Clarke, M. and Baruah, D. C. (2016). Phosphorus recovery as struvite from farm, municipal and industrial waste: Feedstock suitability, methods and pre-treatment, *Waste Management*, 49, 437-454.
- Liu, X., Clarens, A. F. and Colosi, L. M. (2012). Algae biodiesel has potential despite inconclusive results to date. *Bioresource Technology*, 104, 803–806.
- Maddi, B., Panisko, E., Wietsma, T., Lemmon, T., Swita, M., Albrecht, K. and Howe, D. (2017). Quantitative characterization of aqueous byproducts from hydrothermal liquefaction of municipal wastes, food industry wastes, and biomass grown on waste. *ACS Sustainable Chemistry & Engineering*, 5, 2205-2214.
- Oman, C. B. and Junestedt, C. (2008). Chemical characterization of landfill leachates-400 parameters and compounds. *Waste Management*, 28, 1876-1891.
- Pham, M., Schideman, L., Scott, J., Rajagopalan, N. and Plewa, M. J. (2013). Chemical and biological characterization of wastewater generated from hydrothermal liquefaction of *Spirulina*. *Environmental Science & Technology*, 47, 2131-2138.
- Rajeshwari, K. V., Balakrishnan, M., Kansal, A., Lata, K. and Kishore, V. V. N. (2000). State-of-the-art of anaerobic digestion technology for industrial wastewater treatment. *Renewable and Sustainable Energy Reviews*, 4 (2), 135–156.

- Ross, A. B., Biller, P., Kubacki, M. L., Li, H., Lea-Langton, A. and Jones, J. M. (2010). Hydrothermal processing of microalgae using alkali and organic acids, *Fuel*, 89, 2234-2243.
- Sawayama, S., Minowa, T. and Yokoyama, S.-Y. (1999). Possibility of energy production and CO<sub>2</sub> mitigation by thermochemical liquefaction of microalgae. *Biomass and Bioenergy*, 17, 33-39.
- Sturm, B., Butcher, M., Wang, Y., Huang, Y. and Roskilly, T. (2012). The feasibility of the sustainable energy supply from bio wastes for a small-scale brewery – A case study. *Applied Thermal Engineering*, 39, 45–52.
- Subagyono, D. J. N., Marshall, M., Jackson, W. R. and Chaffee, A. L. (2015). Pressurized thermal and hydrothermal decomposition of algae, wood chip residue, and grape marc: A comparative study. *Biomass and Bioenergy*, 76, 141–157.
- Tao, W., Fattah, K. P. and Huchzermeier, M. P. (2016). Struvite recovery from anaerobically digested dairy manure: A review of application potential and hindrances. *Journal of Environmental Management*, 169, 46-57.
- Tchobanoglous, G., Burton, F. and Stensel, H. D. (2003). *Wastewater Engineering: Treatment and Reuse*, Fourth Ed. New York: McGraw-Hill Higher Education.
- Theegala, C. S. and Midgett, J. S. (2012). Hydrothermal liquefaction of separated dairy manure for production of bio-oils with simultaneous waste treatment. *Bioresource Technology*, 107, 456-463.
- Tommaso, G., Chen, W., Li, P., Schideman, L. and Zhang, Y. (2015). Chemical characterization and anaerobic biodegradability of hydrothermal liquefaction aqueous products from mixed-culture wastewater algae. *Bioresource Technology*, 178, 139–146.
- Toor, S. S., Rosendahl, L. and Rudolf, A. (2011). Hydrothermal liquefaction of biomass: A review of subcritical water technologies. *Energy*, 36 (5), 2328–2342.
- Valdez, P. J., Nelson, M. C., Wang, H. Y., Lin, X. N. and Savage, P. E. (2012). Hydrothermal liquefaction of *Nannochloropsis* sp.: Systematic study of process variables and analysis of the product fractions. *Biomass and Bioenergy*, 46, 317–331.
- Vardon, D. R., Sharma, B. K., Scott, J., Yu, G., Wang, Z., Schideman, L., Zhang, Y. and Strathmann, T. J. (2011). Chemical properties of biocrude oil from the hydrothermal liquefaction of *Spirulina* algae, swine manure, and digested anaerobic sludge. *Bioresource Technology*, 102 (17), 8295-8303.
- Vardon, D., Sharma, B., Blazina, G., Rajagopalan, K. and Strathmann, T. (2012). Thermochemical conversion of raw and defatted algal biomass via hydrothermal liquefaction and slow pyrolysis. *Bioresource technology*, 109, 178-87.
- Xu, C. and Etcheverry, T. (2008). Hydro-liquefaction of woody biomass in sub- and super-critical ethanol with iron-based catalysts. *Fuel*, 87 (3), 335–345.
- Xu, D., and P.E. Savage. (2014). Characterization of biocrudes recovered with and without solvent after hydrothermal liquefaction of algae. *Algal Research, Part A*, 6, 1–7.

- Yang, L., Nazari, L., Yuan, Z., Corscadden, K., Xu, C. and He, Q. (2016). Hydrothermal liquefaction of spent coffee grounds in water medium for bio-oil production. *Biomass and Bioenergy*, 86, 191–198.
- Yetilmezsoy, K., Fatih, I., Emel, K. and Havva Melda, A. (2017). Feasibility of struvite recovery process for fertilizer industry: A study of financial and economic analysis, *Journal of Cleaner Production*, 152, 88-102.
- Yetilmezsoy, K. and Sapci-Zengin, Z. (2009). Recovery of ammonium nitrogen from the effluent of UASB treating poultry manure wastewater by MAP precipitation as a slow release fertilizer. *Journal of Hazardous Materials*, 166 (1), 260–269.
- Zhang, B., von Keitz, M. and Valentas, K. (2009). Thermochemical liquefaction of high-diversity grassland perennials. *Journal of Analytical and Applied Pyrolysis*, 84 (1), 18–24.
- Zhong, C. and Wei, X. (2004). A comparative experimental study on the liquefaction of wood. *Energy*, 29 (11), 1731–1741.

## **4.0 Objective 2: Evaluating the Impacts of ACP Management via Nutrient Recovery on the Energy Performance of Hydrothermal Liquefaction**

This chapter summarizes the contents pertaining to Objective 2 of this dissertation. In this objective, experimental laboratory approaches, water chemistry modeling, and energy accounting techniques are used to evaluate the management of the aqueous co-product (ACP) (i.e., wastewater) arising from the hydrothermal liquefaction (HTL) processing of select non-food, organic waste feedstocks. From Objective 1, it was found that post-HTL ACP from organic waste feedstocks contain very high concentrations of dissolved organic compounds and nutrients, making ACP unsafe for direct discharge into the receiving waters of a wastewater treatment plant (WWTP) (Bauer et al., 2018). However, there is little information in the literature on the management of ACP prior to discharge. Therefore, this objective has two goals: (1) to characterize the ACP arising from the HTL conversion of select organic waste feedstocks and evaluate the theoretical nutrient-based precipitation of valuable materials from post-HTL ACP as a novel method of ACP management and (2) to revise existing estimates of HTL energy ratio metrics (i.e., “energy return on investment” [EROI]) to account for ACP management and recovery of scarce nutrients. This research will provide insight into the sustainability of waste-to-energy systems as a means of both producing renewable energy and recovering valuable materials.

### **4.1 Introduction**

Growing population, dwindling fossil fuels supplies, and increasing concerns about energy security worldwide have spurred research into the production of renewable energy sources. Developing techniques that produce renewable energy that does not have adverse effects on the environment or society is of particular priority. Biofuels produced from non-food

feedstocks are a promising alternative to fossil fuels as they do not compete for available food supply or land that could otherwise be used for agricultural purposes (Dominguez-Faus et al., 2009; Toor et al., 2011). Leveraging organic materials (e.g., municipal solid waste [MSW], WWTP biosolids, agricultural waste, food and beverage waste, etc.) that would otherwise constitute “waste” as feedstocks for biofuel production is of particular interest (Theegala and Midgett, 2012; Vardon et al., 2011; Huang et al., 2013; Gama et al., 2015). HTL is a suitable process for converting wet, organic feedstocks into liquid fuels that are compatible with existing petroleum refining and distribution infrastructure (Bhutto et al., 2016; Elliott et al., 2014; Toor et al., 2011). However, HTL is known to produce biofuels that have a significant water footprint due to the production of large quantities of wastewater (i.e., ACP) from small quantities of solids (Dominguez-Faus et al., 2009; Jena et al., 2011; Bauer et al., 2018). This can be a challenge, as some studies have shown that ACP contain high concentrations of dissolved organic carbon (C) and nutrients (i.e., nitrogen [N] and phosphorus [P]) and may be unsuitable for direct discharge into the receiving waters of a municipal WWTP without substantial dilution and/or ACP management (Jena et al., 2011; Tommaso et al., 2015; Elliott et al., 2014; Bauer et al., 2018).

The results from Chapter 3 of this dissertation show that the high concentrations of dissolved organic C, N, and P in post-HTL ACP render it more noxious than relevant benchmark wastewaters (Bauer et al., 2018). Adjustments of published energy ratio metrics (i.e., EROI) to account for the management of ACP via theoretical conventional wastewater treatment processes reveal that energy consumption for the removal of dissolved C, N, and P from post-HTL ACP to achieve typical WWTP limits is of the same order of magnitude as liquefaction (Bauer et al., 2018). Thus, widespread commercialization of HTL without appropriate strategies for ACP management could threaten already strained water supplies.

There are few HTL studies that have characterized ACP and evaluated the implications that ACP could have on water quantity and quality. Most of these studies have characterized ACP generated from the liquefaction of various microalgae and mixed-culture WWTP algae in order to reuse ACP as a growth media for algae cultivation (Biller et al., 2012; Garcia Alba et al., 2012; Jena et al., 2011; Gai et al., 2015). Fewer studies have characterized ACP quantity and quality arising from non-algae feedstocks (Maddi et al., 2017; Ekpo et al., 2016; Bauer et al., 2018). There are even fewer studies in which conventional wastewater treatment has been evaluated for post-HTL ACP, including: anaerobic digestion of ACP from a mixed culture of WWTP-grown algae (Tommaso et al., 2015) and adsorption onto granular activated carbon (GAC) for ACP from the HTL processing of pure-culture algae (Pham et al., 2013). Still, most studies have overlooked the production of ACP and do not account for possible ACP management required prior to discharge.

To meet the demand of the growing population and concerns about food security, agricultural productivity is expected to increase dramatically over the next decade (Kataki et al., 2016). With increased agricultural activity comes increased use of scarce nutrients and generation of agricultural runoff and animal manure, leading to the amplified production of agricultural wastewaters (Kataki et al., 2016; Tao et al., 2016). These wastewaters, which can discharge high concentrations of nutrients into water bodies, such as rivers, lakes, and seas, as well as into the soil, have adverse effects on the ecosystem and human health (Yetilmezsoy et al., 2017; Mayer et al., 2016; Capdevielle et al., 2013). With increasingly stringent nutrient discharge standards and growing concern about worldwide N and P availability, research into the recovery of nutrients from wastewaters has gained importance in recent years (Yetilmezsoy et al., 2017; Ishii and Boyer, 2015; Capdevielle et al., 2013).

Several studies have shown that chemical precipitation of nutrients can be applied to concentrated agricultural and industrial wastewaters. Among those studies, several have investigated the precipitation of struvite-based slow-release fertilizer via both laboratory-based experiments and modeling techniques (Yetilmezsoy and Sapci-Zengin, 2009; Kataki et al., 2016; Capdevielle et al., 2013; Tao et al., 2016). The recovery of N and P from wastewater via precipitation as magnesium ammonium phosphate hexahydrate ( $\text{MgNH}_4\text{PO}_4 \times 6\text{H}_2\text{O}$ ) (i.e., struvite) has been used for decades in municipal wastewater treatment. More recently, it has been applied to concentrated wastewaters (i.e., landfill leachate, slaughterhouse wastewater, anaerobic digester effluent, swine and dairy manure wastewater, etc. [Yetilmezsoy and Sapci-Zengin, 2009; Rahman et al., 2011; Çelen et al., 2007; Kataki et al., 2016]) and also source-separated urine (SSU) (Ishii and Boyer, 2015; Lahr et al., 2016). These studies have shown that the addition of magnesium ( $\text{Mg}^{2+}$ ) is essential for struvite precipitation, along with other factors, such as  $\text{Mg}^{2+}$  to orthophosphate ( $\text{PO}_4^{3-}$ ) ( $\text{Mg}:\text{PO}_4$ ) molar ratio, pH (at an optimal range of 8.5-10), and competing complexing ions (Rahman et al., 2011; Çelen et al., 2007; Kataki et al., 2016).

Several other studies have investigated the precipitation of additional nutrient-based fertilizers from concentrated wastewaters. In particular, the precipitation of MPP (i.e., magnesium potassium phosphate hexahydrate,  $[\text{MgKPO}_4 \times 6\text{H}_2\text{O}]$ ) for the removal of P and potassium ( $\text{K}^+$ ) from synthetic urine and SSU has been evaluated through chemical precipitation and thermodynamic modeling (Xu et al., 2011; Xu et al., 2015; Zhang et al., 2017). Similar to the precipitation of struvite, these studies also concluded that pH and  $\text{Mg}:\text{PO}_4$  ratio are important factors for the chemical precipitation of MPP. Additional studies have researched the precipitation of HAP (i.e., hydroxyapatite,  $[\text{Ca}_5(\text{PO}_4)_3(\text{OH})]$ ) from agricultural wastewaters and

the aqueous phase of microalgae (Tsuji and Fujii, 2014; Teymouri et al., 2018). These studies found that calcium ( $\text{Ca}^{2+}$ ) concentration and alkaline pH conditions were important factors for the formation of HAP.

With an abundance of increasingly valuable, scarce nutrients (i.e., N and P) present in the post-HTL ACP of organic waste feedstocks, nutrient-based precipitation could be a favorable means of ACP management prior to discharge into the receiving waters of a WWTP (Yu et al., 2017; Munir et al., 2017). It is hypothesized that recovery of nutrients from post-HTL ACP could offset the energy cost of ACP management (i.e., the removal of C, N, and P from the ACP) prior to discharge, while also producing valuable materials, though few studies have evaluated the energy performance of HTL (Sawayama et al., 1999; Vardon et al., 2012; Connelly et al., 2015). Thus, this research aims to evaluate the impacts of the management of post-HTL processing ACP of select non-food, organic waste feedstocks through the theoretical recovery of valuable nutrients via chemical precipitation and calculate the EROI of the management of ACP via nutrient-based precipitation.

## **4.2 Materials and Methods**

### **4.2.1 HTL Conversion and Characterization of ACP**

HTL was used to process eight non-food, organic waste feedstocks selected based on bulk characteristics (e.g. water content and organic load) and logistical considerations (e.g., yearly production, cost, seasonal variability, etc.). These feedstocks include: (1) pre-digested WWTP sludge, (2) digested WWTP sludge, (3) dairy manure, and five residues from beer and wine production, i.e. (4) brewery yeast, (5) spent grains, and (6) dry hops from craft beer production, and (7) white lees and (8) red lees from wine production. Each of the feedstocks

were collected from within central Virginia from local WWTPs, dairy farms, craft breweries, and wineries. Immediately after collection, the feedstocks were characterized and converted into liquid biofuel via HTL processing conducted in triplicate in a 300-mL Parr Hast reactor with quartz liner and external heater, as previously described in Chapter 3 of this dissertation (Bauer et al., 2018). In short, 100g of wet feedstock paste, adjusted to an optimal water content of 90% (m/m) (Jena et al., 2011), was pressurized to 100 psi with nitrogen (N<sub>2</sub>) gas, continuously stirred at 300 rpm, and heated to 300 ± 5°C at ~8-10°C/min. Once heated, the reactor was maintained at 300 ± 5°C for a residence time of 30 min (Garcia Alba et al., 2012; Pham et al., 2013; Bauer et al., 2018).

HTL product phases (i.e., biofuel, biochar, and ACP) were separated using techniques adapted from Xu and Savage (2014), as outlined in Chapter 3 of this dissertation (Bauer et al., 2018). In short, solid-phase biochar was separated from the liquid phase via filtration. Liquid phase biofuel and ACP were separated from each other via extraction into dichloromethane (DCM), by which 1-2x vol/vol DCM was added to HTL liquids. The liquids were decanted and centrifuged to facilitate phase separation, and the ACP was manually drawn off, such that the liquid biocrude was operationally defined based on solubility in DCM. The solvent was then evaporated using a gentle stream of N<sub>2</sub> gas for a 24-hr period. The resulting ACP was filtered using a 0.22-um pore-size filter to remove particulates and measured. Post-HTL ACP was characterized using procedures outlined in Chapter 3 (Bauer et al., 2018) based on traditional wastewater parameters, including pH, total nitrogen (TN), ammonium (NH<sub>4</sub>-N), total phosphorus (TP), and orthophosphate (PO<sub>4</sub>-P). These water quality constituents were measured using APHA Standard Methods and commercial HACH kits (APHA, 2013). ACP quality was further characterized using a Thermo Scientific Dionex ICS 5000 DP-5 Ion Chromatograph (IC), using

U.S. EPA Method 300.1 (EPA, 1997), with a detection limit of 0.5 mg/L. Various cations and anions were measured using the Thermo Scientific Dionex IC, including: lithium ( $\text{Li}^+$ ),  $\text{Mg}^{2+}$ ,  $\text{Ca}^{2+}$ ,  $\text{K}^+$ , sodium ( $\text{Na}^+$ ), bromide ( $\text{Br}^-$ ), fluoride ( $\text{F}^-$ ), chloride ( $\text{Cl}^-$ ), nitrate ( $\text{NO}_3^-$ ), nitrite ( $\text{NO}_2^-$ ), and sulfate ( $\text{SO}_4^{2-}$ ). Together, the quantities and composition of these parameters in the post-HTL ACP result in a comprehensive characterization of the ACP of each select organic waste feedstock for evaluation of ACP management. Additionally, titration experiments with 1 N sodium hydroxide ( $\text{NaOH}$ ) solution were performed to measure the alkalinity of each of the post-HTL ACPs.

#### **4.2.2 Recovery of Nutrients from ACP**

Visual MINTEQ Version 3.1, a chemical equilibrium modeling software originally developed by the U.S. EPA, was used to theoretically determine the recoverability of N and P from the post-HTL ACP of select organic waste feedstocks (Gustafsson, 2013). Visual MINTEQ includes a broad thermodynamic database of species allowing for various calculations in aqueous solutions (i.e., solubility, speciation, and equilibrium of solid and dissolved phases of minerals). This database was used to determine the properties of species studied during this analysis. Average ACP characterization parameters for each feedstock ACP (e.g.,  $\text{NH}_4^+$ ,  $\text{PO}_4^{3-}$ , various anions and cations, etc.) and pH were entered into the modeling software individually for each ACP to determine to what extent N and P could precipitate in solid form from each of the ACPs. The model was then run with the addition of two parameter changes: (1) increasing pH from its initial point up to 14 and (2) increasing concentration of  $\text{Mg}^{2+}$  from its initial concentration up to a pre-selected endpoint.

First, pH was artificially increased at intervals of 0.5 from the starting pH of each ACP to a pH of 14. It is of interest to increase the pH of the ACP to help facilitate nutrient-based

chemical precipitation, which is shown to be more favorable at higher pH values. Specifically, P removal increases at higher pH values, as the availability of non-complexed  $\text{PO}_4^{3-}$  increases (Figure 4-1). Second, to determine what forms of solids could theoretically precipitate from each of the ACPs, all solids containing the components of the ACPs were selected by using the “Specify Possible Solid Phases” function of the model. Based on the composition of the ACPs, to specifically determine if the ACPs could precipitate struvite,  $\text{Mg}^{2+}$  was virtually added to the ACPs through the modeling software in the form of magnesium chloride ( $\text{MgCl}_2$ ). This analysis was done using the “Multi-Problem/Sweep” function of the model, where  $\text{Mg}^{2+}$  concentration was increased at a rate of 5 mg/L for 500 steps. Model outputs include the species and concentrations of the solids precipitated from each of the ACPs, as well as the concentrations of precipitated nutrients (i.e.,  $\text{Mg}^{2+}$ ,  $\text{NH}_4^+$ ,  $\text{PO}_4^{3-}$ , and  $\text{Ca}^{2+}$ ). Model outputs also include principal dissolved complexes of relevant nutrients (i.e., N and P). Optimal solid precipitation and pH for each of the feedstock ACPs were chosen based on residual N and P concentrations, as well as the concentration of added  $\text{Mg}^{2+}$ , where the “optimal” value of  $\text{Mg}^{2+}$  addition was chosen at a point up to where  $\geq 50\%$  of the  $\text{Mg}^{2+}$  concentration added was recovered as a solid precipitate.

#### **4.2.3 Energy Ratio Formulas and Parametrization**

In order to evaluate the energy performance of the HTL processing of the select organic waste feedstocks included in this study, life-cycle energy accounting was used to assess the energy cost (i.e., EROI) of ACP management via nutrient-based precipitation. The energy performance of ACP management from each post-HTL ACP was evaluated based on the quantities of nutrients (i.e., TN and TP) recovered via precipitation and the quantities of the solids precipitated, based on the theoretical results of the Visual MINTEQ modeling software. Life-cycle energy values of both the materials consumed and materials produced via the

precipitation of nutrients from the ACPs were collected from the ecoinvent database, as accessed using SimaPro v.3, and/or adapted from Clarens et al. (2010). These values are summarized in Table 4-1.

**Table 4-1.** Summary of the life-cycle energy values of the various materials consumed and produced via the precipitation of nutrients from the post-HTL ACP of select organic waste feedstocks. Parameter values were taken from the ecoinvent database, as accessed using SimaPro v.3 and/or Clarens et al. (2010).

	<b>Material Type</b>	<b>Energy Cost (MJ/kg)</b>
Materials Consumption	NaOH	46.6
	MgSO <sub>4</sub>	6.5
	MEOH	38.0
Materials Production	FeSO <sub>4</sub>	1.95
	MAP	13.0
	TSP	15.0

Various assumptions were made about the data in Table 4-1 in order to estimate the energy performance (i.e., EROI) of ACP management and nutrient recovery of post-HTL ACP. EROI values were calculated by dividing the energy value (i.e.,  $E_{OUT}$ ) of the materials produced via HTL processing (i.e., struvite, HAP, and the avoided energy cost of TN and TP removal due to the precipitation of N and P) by the energy cost (i.e.,  $E_{IN}$ ) of the materials consumed during ACP treatment and nutrient-based precipitation (i.e., NaOH, magnesium sulfate [MgSO<sub>4</sub>], and the energy cost of the removal of the remaining TN and P in the ACP after nutrient precipitation). First, the materials consumed to precipitate nutrients from the ACP include: NaOH to raise the pH of the ACP and MgSO<sub>4</sub> to facilitate the precipitation of struvite. The materials consumed for the removal of TN and TP from the ACP by conventional wastewater treatment include: methanol (MEOH) and ferrous sulfate (FeSO<sub>4</sub>), respectively, as outlined in Chapter 3 (Bauer et al., 2018). In short, TN is removed from wastewater via nitrification,

followed by denitrification (Tchobanoglous et al., 2003). Denitrification requires methanol as a co-substrate. The energy consumption required for TN removal from each of the ACPs was determined by multiplying the concentration of TN in the ACP by ACP volume to compute the TN mass (in kg) to be denitrified during treatment. This value was then multiplied by methanol demand (3.4 kg methanol/kg N) and the energy intensity of methanol production (38 MJ/kg methanol) to compute energy consumption for TN removal (Clarens et al., 2010). This value was then adjusted based on the theoretical removal of TN from the ACPs via precipitation of N-based solids.

TP is removed from wastewater via precipitation using  $\text{FeSO}_4$  (Tchobanoglous et al., 2003). The energy consumption required to remove TP from each of the ACPs was calculated by multiplying the concentration of TP in the ACP by ACP volume to compute the TP mass (in kg) to be removed during treatment. This value was then multiplied by  $\text{FeSO}_4$  demand (1.8 kg  $\text{FeSO}_4$ /kg P) and the energy intensity of  $\text{FeSO}_4$  production (1.95 MJ/kg) to compute energy consumption for TP removal (Clarens et al., 2010). This value was then adjusted based on the theoretical removal of TP from the ACPs via precipitation of P-based solids.

Based on the results from the Visual MINTEQ modeling software, the materials produced via the nutrient-based precipitation of N and P include: (1) struvite and (2) hydroxyapatite (HAP). It was assumed that the production of struvite would replace the production of monoammonium phosphate (MAP) at a molar ratio MAP:struvite of 1:1 (based on the N and P stoichiometries of struvite and MAP). The energy value of struvite was then computed by taking the mass-equivalent energy value of avoiding the production of MAP. The energy value of HAP was computed by taking the mass-equivalent energy value of avoiding the production of triple super phosphate (TSP) at a molar ratio TSP:HAP of 2:3 (based on TSP and

HAP stoichiometries). Using the data in Table 4-1 and the results of the characterization and nutrient-based precipitation of N and P from each of the ACPs, EROI values were calculated for each ACP to account for ACP management and nutrient recovery.

## **4.3 Results and Discussion**

### **4.3.1 Characterization of ACP**

The goal of this study is to analyze the quality of ACP arising from the HTL processing of several non-food, organic waste feedstocks and evaluate the recoverability of valuable nutrients from ACP as a means of novel ACP management. It was hypothesized that since ACP contains high concentrations of nutrients (i.e., N and P), recovering nutrients from ACP via chemical precipitation could be a beneficial means of treating ACP prior to discharge to the receiving waters of a WWTP (Bauer et al., 2018). Nutrient recovery as a means of ACP management could offset the energy cost of N and P removal, while also generating valuable nutrient-based materials. Thus, Table 4-2 presents data on the quality of ACP of the eight selected waste feedstocks included in this study relevant to the recovery of nutrients, including: pH, TN,  $\text{NH}_4^+$ , TP, and  $\text{PO}_4^{3-}$ , as adapted from Chapter 3 of this dissertation (Bauer et al., 2018). It is important to observe the variations in pH and nutrients of the ACPs presented in Table 4-2. With regards to pH, most of the feedstock ACPs are in the slightly basic range ( $\geq 8$  for pre-digested sludge, digested sludge, brewing yeast, and red lees ACPs). Dairy manure and spent grains ACPs are relatively acidic (4.4 and 5.3, respectively). White lees and dry hops ACPs were the only two feedstock ACPs with pH in the circumneutral range (6-8).

**Table 4-2.** Characterization of pH and nutrient parameters of ACP produced from HTL processing of select waste feedstocks. Average values of pH,  $\text{NH}_4^+$ , and  $\text{PO}_4^{3-}$  from triplicate experiments are reported and used as inputs for Visual MINTEQ modeling. The summation of all orthophosphates (OP) is expressed as  $\text{PO}_4^{3-}$ . Adapted from Bauer et al. (2018).

Waste Feedstock	pH	TN (mg/L)	$\text{NH}_4^+$ (mg/L-N)	TP (mg/L)	$\text{PO}_4^{3-}$ (mg/L-P)	N:P <sup>a</sup>
Dairy Manure	4.4	1050	315	477	39	8:1
Pre-Digested Sludge	8.4	3250	975	800	112	9:1
Digested Sludge	8.6	2180	2100	220	31	68:1
Brewing Yeast	8.3	2450	1370	2195	753	2:1
Spent Grains	5.3	2050	700	1038	352	2:1
Dry Hops	7.0	2500	1240	2425	287	4:1
White Lees	6.4	96	31	45	53	0.6:1
Red Lees	8.8	1890	1115	3632	687	2:1

<sup>a</sup>N:P ratio expresses the relationship between  $\text{NH}_4\text{-N}$  and  $\text{PO}_4\text{-P}$ .

There are also important observations that can be made regarding the dissolved nutrient concentrations in the ACPs. From Table 4-2, all the waste feedstock ACPs exhibit high concentrations of TN (1,050-3,250 mg/L) and TP (220-3,632 mg/L), with the white lees ACP as an obvious outlier. For each of the ACPs, appreciable quantities of TN and TP exist as recoverable N and P in inorganic forms (i.e.,  $\text{NH}_4^+$  and  $\text{PO}_4^{3-}$ ). An average of 50% (31-2,100 mg/L-N) of TN in the ACPs is available as inorganic N (i.e.,  $\text{NH}_4^+$ ); an average of 26% (31-753 mg/L-P) of TP in the ACPs is available as inorganic P (i.e.,  $\text{PO}_4^{3-}$ ).

#### 4.3.2 Considerations for the Recovery of Nutrients from ACP

Based on the findings from Table 4-2, it is of interest to assess the recoverability of dissolved nutrients from the feedstock ACPs as both a way of treating the ACP prior to discharge, as well as a means of recovering valuable, scarce resources in a usable form.  $\text{NH}_4^+$  and  $\text{PO}_4^{3-}$  are common forms of recoverable N and P that can be used to produce valuable products, such as soil amendments or fertilizers (Yetilmezsoy and Sapci-Zengin, 2009; Kataki et

al., 2016; Capdevielle et al., 2013; Tao et al., 2016). In all the ACPs, the concentration of  $\text{NH}_4^+$  is greater than the concentration of  $\text{PO}_4^{3-}$ , except for the white lees ACP (N:P 0.6:1). All the ACPs other than the white lees ACP exhibit ratios of N:P ranging from 2:1 to 9:1, with the digested sludge ACP also an outlier, with a ratio N:P of 68:1. Studies have shown that the ratio of N to P is important to the formation of various fertilizers (Yetilmezsoy and Sapci-Zengin, 2009; Tao et al., 2016).

Because it is of interest to recover  $\text{NH}_4\text{-N}$  and  $\text{PO}_4\text{-P}$  via chemical precipitation from the post-HTL ACPs, it is important to understand the aquatic chemistry of these substances, most specifically the speciation of N and P as a function of pH. Figure 4-1 shows the speciation of ammonia ( $\text{NH}_3$ ) between ionized  $\text{NH}_4^+$  and free  $\text{NH}_3$ , as well as the orthophosphate species over a pH range of 0-14. As seen in Figure 4-1,  $\text{NH}_3$  and orthophosphate (OP) species (i.e.,  $\text{H}_3\text{PO}_4$ ,  $\text{H}_2\text{PO}_4^-$ ,  $\text{HPO}_4^{2-}$ , and  $\text{PO}_4^{3-}$ ) are present as different ions across a wide range of pHs, making the speciation of these compounds pH-controlled (Tao et al., 2016; Çelen et al., 2007).  $\text{NH}_3$  is mostly ionized as  $\text{NH}_4^+$  at pH values less than 8.5. At higher pHs, N is present as aqueous  $\text{NH}_3$ , which cannot be recovered via precipitation. OP is mostly present as  $\text{PO}_4^{3-}$  at pH values greater than 12, whereas at lower pHs, OP is present in other forms. The summation of all orthophosphates is expressed as  $\text{PO}_4^{3-}$  in Table 4-2.

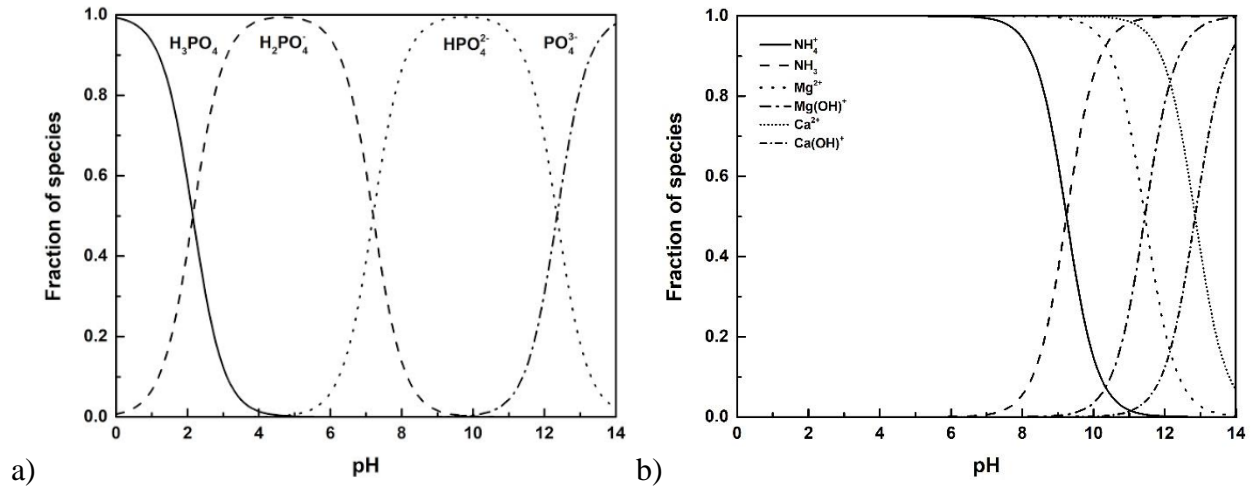


**Figure 4-1.** pH dependence of (a) orthophosphate (OP) and (b) ammonia, magnesium, and calcium speciation at 25°C. The speciation of ammonia between ionized ammonia ( $NH_4^+$ ) and free ammonia ( $NH_3$ ), as well as the orthophosphate species (i.e.,  $H_3PO_4$ ,  $H_2PO_4^-$ ,  $HPO_4^{2-}$ , and  $PO_4^{3-}$ ) is pH dependent.

Free  $NH_4^+$  and  $PO_4^{3-}$  can together form fertilizers, such as MAP and struvite, depending on species concentration and pH (Yetilmezsoy and Sapci-Zengin, 2009; Kataki et al., 2016; Çelen et al., 2007). Struvite, for example, is produced when free  $Mg^{2+}$ ,  $NH_4^+$ , and  $PO_4^{3-}$  form together at a molar ratio of 1Mg:1N:1P. These components, however, can form with other wastewater constituents (e.g.,  $Ca^{2+}$ ,  $K^+$ ,  $Na^+$ ,  $Cl^-$ ,  $SO_4^{2-}$ , etc.) depending on the concentrations of the constituent and pH (Tao et al., 2016). Table 4-3 presents additional wastewater characterization data for various anions and cations present in each of the feedstock ACPs that could have potential influence on the recovery of N and P.

**Table 4-3.** Additional characterization of post-HTL ACP to account for possible influences on the precipitation of nutrients (i.e., N and P). Average values are reported and used as inputs for Visual MINTEQ modeling. Blank values = under the detectable limit (0.5 mg/L).

Waste Feedstock	Li <sup>+</sup> (mg/L)	Mg <sup>2+</sup> (mg/L)	Ca <sup>2+</sup> (mg/L)	K <sup>+</sup> (mg/L)	Na <sup>+</sup> (mg/L)	Br <sup>-</sup> (mg/L)	Fl <sup>-</sup> (mg/L)	Cl <sup>-</sup> (mg/L)	NO <sub>3</sub> <sup>-</sup> (mg/L)	NO <sub>2</sub> <sup>-</sup> (mg/L)	SO <sub>4</sub> <sup>2-</sup> (mg/L)
Dairy Manure	-	52.5	299.1	303.3	141.0	-	-	310.9	-	-	27.1
Pre-Digested Sludge	0.9	3.2	20.4	270.9	69.3	-	-	73.3	-	-	227.2
Digested Sludge	-	4.4	32.8	298.8	99.8	-	-	100.9	-	-	344.6
Brewing Yeast	-	3.9	20.3	1324.7	38.1	-	-	95.4	-	-	299.6
Spent Grains	-	28.5	16.5	10.1	30.4	-	-	3.6	2.7	-	52.6
Dry Hops	-	3.4	23.4	1050.3	47.4	-	-	93.6	-	-	225.9
White Lees	1.2	6.0	9.3	3172.7	9.7	30.6	-	7.0	1.4	-	40.2
Red Lees	-	2.8	18.7	7116.7	14.9	688.8	-	10.1	-	-	-

From the data in Table 4-3, there is varying concentrations of the presented anions and cations in the feedstock ACPs. Li<sup>+</sup>, Br<sup>-</sup>, Fl<sup>-</sup>, NO<sub>3</sub><sup>-</sup>, and NO<sub>2</sub><sup>-</sup> are all present at low to zero concentrations in all the ACPs (with the Br<sup>-</sup> concentration of the white and red lees ACPs as an obvious outlier). There are relatively high concentrations of K<sup>+</sup>, Na<sup>+</sup>, Cl<sup>-</sup>, and SO<sub>4</sub><sup>2-</sup> in most of the ACPs, with the spent grains and white lees ACPs containing generally lower concentrations than the other ACPs. The dairy manure and spent grains ACPs contain considerably higher concentrations of Mg<sup>2+</sup> than the other feedstock ACPs. Ca<sup>2+</sup> is present in all of the ACPs at relatively low concentrations except for in the dairy manure ACP, which exhibits very high concentrations of Ca<sup>2+</sup>. It is of interest to see if/how the concentrations of the complexing ions presented in Table 4-3 effect the precipitation of N and P from the feedstock ACPs.

#### 4.3.3 Recovery of N and P from ACP via Precipitation of Solids

Visual MINTEQ modeling was used to determine the theoretical recovery of dissolved nutrients from each of the ACPs in the form of solid precipitates. Tables 4-4 through 4-11 present the model results for each ACP individually for a wide range of pH values, starting at the

initial pH of each ACP. The model was programmed separately for each ACP with water quality input data from Tables 4-2 and 4-3. The data in columns 3-8 are based on outputs from the model, whereas the values in column 2 are based on laboratory results. Column 2 quantifies the volume of NaOH required to raise the pH of the ACPs to a given value. The model was varied for each ACP based on two variables: pH and concentration of  $Mg^{2+}$ , in order to evaluate precipitation of dissolved nutrients. The value of pH was increased at a rate of 0.5 from the starting value of each ACP to pH 14.  $Mg^{2+}$  was increased from the initial concentration (Table 4-3) in each ACP by 5 mg/L for 500 steps using the “Multi Problem/Sweep” function of the model. Also presented in Tables 4-4 through 4-11 are the concentrations of recovered solids, OP, and  $NH_4^+/NH_3$ , as well as the principle dissolved complexes of theoretically recoverable nutrients after nutrient recovery for each of the ACPs.

**Table 4-4.** Theoretical recovery of nutrients via the precipitation of solids from post-HTL dairy manure ACP at pH range of 4.4 to 14. NaOH is used to raise the alkalinity of the ACP; NaOH values are based on laboratory results. Columns 3-8 are based on results from the Visual MINTEQ model. MgCl<sub>2</sub> is added to facilitate the precipitation of nutrients as solids. Optimal pH for nutrient recovery from dairy manure ACP is 8.0. Initial PO<sub>4</sub><sup>3-</sup> = 1.27 mM; Initial NH<sub>4</sub><sup>+</sup> = 22.5 mM.

pH	NaOH Consumed (mM)	MgCl <sub>2</sub> Consumed (mM)	Recovered Struvite (mM)	Recovered HAP (mM)	Recovered OP (mM)	Recovered NH <sub>4</sub> <sup>+</sup> /NH <sub>3</sub> (mM)	Principal Dissolved Complexes of Theoretically Recoverable Nutrients
4.4	-	0	0	0	0	0	NH <sub>4</sub> <sup>+</sup> (100%); H <sub>2</sub> PO <sub>4</sub> <sup>-</sup> (90%)
4.5	0.40	0	0	0	0	0	NH <sub>4</sub> <sup>+</sup> (100%); H <sub>2</sub> PO <sub>4</sub> <sup>-</sup> (90%)
5.0	0.55	0	0	0	0	0	NH <sub>4</sub> <sup>+</sup> (100%); H <sub>2</sub> PO <sub>4</sub> <sup>-</sup> (89%)
5.5	0.69	0	0	0.344	1.03	0	NH <sub>4</sub> <sup>+</sup> (100%); H <sub>2</sub> PO <sub>4</sub> <sup>-</sup> (87%)
6.0	0.83	0	0	0.416	1.25	0	NH <sub>4</sub> <sup>+</sup> (100%); H <sub>2</sub> PO <sub>4</sub> <sup>-</sup> (78%); HPO <sub>4</sub> <sup>2-</sup> (8%)
6.5	0.98	0	0	0.422	1.26	0	NH <sub>4</sub> <sup>+</sup> (100%); H <sub>2</sub> PO <sub>4</sub> <sup>-</sup> (57%); HPO <sub>4</sub> <sup>2-</sup> (20%)
7.0	1.12	0	0	0.422	1.26	0	NH <sub>4</sub> <sup>+</sup> (99%); H <sub>2</sub> PO <sub>4</sub> <sup>-</sup> (31%); HPO <sub>4</sub> <sup>2-</sup> (34%)
7.5	1.27	0	0	0.422	1.26	0	NH <sub>4</sub> <sup>+</sup> (98); H <sub>2</sub> PO <sub>4</sub> <sup>-</sup> (12%); HPO <sub>4</sub> <sup>2-</sup> (43%)
<b>8.0</b>	<b>1.41</b>	<b>0</b>	<b>0</b>	<b>0.423</b>	<b>1.27</b>	<b>0</b>	<b>NH<sub>4</sub><sup>+</sup> (95%); NH<sub>3</sub> (aq) (5%)</b>
8.5	1.55	0	0	0.423	1.27	0	NH <sub>4</sub> <sup>+</sup> (87%); NH <sub>3</sub> (aq) (13%)
9.0	1.70	0	0	0.423	1.27	0	NH <sub>4</sub> <sup>+</sup> (67%); NH <sub>3</sub> (aq) (32%)
9.5	1.84	0	0	0.423	1.27	0	NH <sub>4</sub> <sup>+</sup> (40%); NH <sub>3</sub> (aq) (60%)
10	1.99	0	0	0.423	1.27	0	NH <sub>4</sub> <sup>+</sup> (17%); NH <sub>3</sub> (aq) (82%)
10.5	2.13	0	0	0.423	1.27	0	NH <sub>4</sub> <sup>+</sup> (6%); NH <sub>3</sub> (aq) (93%)
11	2.27	0	0	0.423	1.27	0	NH <sub>3</sub> (aq) (97%)
11.5	2.42	0	0	0.423	1.27	0	NH <sub>3</sub> (aq) (99%)
12	2.56	0	0	0.423	1.27	0	NH <sub>3</sub> (aq) (99%)
12.5	2.70	0	0	0.423	1.27	0	NH <sub>3</sub> (aq) (99%)
13	2.85	0	0	0.423	1.27	0	NH <sub>3</sub> (aq) (100%)
13.5	2.99	0	0	0.423	1.03	0	NH <sub>3</sub> (aq) (100%)
14	3.14	0	0	0.423	1.25	0	NH <sub>3</sub> (aq) (100%)

**Table 4-5.** Theoretical recovery of nutrients via the precipitation of solids from post-HTL pre-digested sludge ACP at pH range of 8.4 to 14. NaOH is used to raise the alkalinity of the ACP; NaOH values are based on laboratory results. Columns 3-8 are based on results from the Visual MINTEQ model. MgCl<sub>2</sub> is added to facilitate the precipitation of nutrients as solids. Optimal pH for nutrient recovery from pre-digested sludge ACP is 10.5. Initial PO<sub>4</sub><sup>3-</sup> = 3.6 mM; Initial NH<sub>4</sub><sup>+</sup> = 69.6 mM.

pH	NaOH Consumed (mM)	MgCl <sub>2</sub> Consumed (mM)	Recovered Struvite (mM)	Recovered HAP (mM)	Recovered OP (mM)	Recovered NH <sub>4</sub> <sup>+</sup> /NH <sub>3</sub> (mM)	Principal Dissolved Complexes of Theoretically Recoverable Nutrients
8.4	-	3.29	3.12	0.101	3.43	3.12	NH <sub>4</sub> <sup>+</sup> (83%); NH <sub>3</sub> (aq) (16%); HPO <sub>4</sub> <sup>2-</sup> (89%)
8.5	0.01	3.29	3.15	0.101	3.45	3.15	NH <sub>4</sub> <sup>+</sup> (86%); NH <sub>3</sub> (aq) (13%); HPO <sub>4</sub> <sup>2-</sup> (90%)
9.0	0.10	3.29	3.23	0.101	3.53	3.23	NH <sub>4</sub> <sup>+</sup> (68%); NH <sub>3</sub> (aq) (32%); HPO <sub>4</sub> <sup>2-</sup> (92%)
9.5	0.40	3.29	3.26	0.101	3.57	3.26	NH <sub>4</sub> <sup>+</sup> (40%); NH <sub>3</sub> (aq) (60%); HPO <sub>4</sub> <sup>2-</sup> (92%)
10	0.70	3.29	3.27	0.101	3.58	3.27	NH <sub>4</sub> <sup>+</sup> (17%); NH <sub>3</sub> (aq) (83%); HPO <sub>4</sub> <sup>2-</sup> (91%)
<b>10.5</b>	<b>1.00</b>	<b>3.29</b>	<b>3.28</b>	<b>0.102</b>	<b>3.59</b>	<b>3.28</b>	<b>NH<sub>4</sub><sup>+</sup> (6%); NH<sub>3</sub> (aq) (94%); HPO<sub>4</sub><sup>2-</sup> (87%)</b>
11	1.30	3.29	3.28	0.102	3.58	3.28	NH <sub>3</sub> (aq) (98%); HPO <sub>4</sub> <sup>2-</sup> (80%); PO <sub>4</sub> <sup>3-</sup> (6%)
11.5	1.60	3.29	3.25	0.102	3.56	3.25	NH <sub>3</sub> (aq) (98%); HPO <sub>4</sub> <sup>2-</sup> (64%); PO <sub>4</sub> <sup>3-</sup> (15%)
12	1.90	3.29	2.69	0.102	2.99	2.69	NH <sub>3</sub> (aq) (99%); HPO <sub>4</sub> <sup>2-</sup> (49%); PO <sub>4</sub> <sup>3-</sup> (40%)
12.5	2.20	3.29	0	0.101	0.30	0	NH <sub>3</sub> (aq) (99%); HPO <sub>4</sub> <sup>2-</sup> (21%); PO <sub>4</sub> <sup>3-</sup> (72%)
13	2.50	3.29	0	0.101	0.30	0	NH <sub>3</sub> (aq) (100%); HPO <sub>4</sub> <sup>2-</sup> (6%); PO <sub>4</sub> <sup>3-</sup> (88%)
13.5	2.79	3.29	0	0.102	0.30	0	NH <sub>3</sub> (aq) (100%); PO <sub>4</sub> <sup>3-</sup> (95%)
14	3.09	3.29	0	0.102	0.30	0	NH <sub>3</sub> (aq) (100%); PO <sub>4</sub> <sup>3-</sup> (97%)

**Table 4-6.** Theoretical recovery of nutrients via the precipitation of solids from post-HTL digested sludge ACP at pH range of 8.6 to 14. NaOH is used to raise the alkalinity of the ACP; NaOH values are based on laboratory results. Columns 3-8 are based on results from the Visual MINTEQ model. MgCl<sub>2</sub> is added to facilitate the precipitation of nutrients as solids. Optimal pH for nutrient recovery from digested sludge ACP is 10.5. Initial PO<sub>4</sub><sup>3-</sup> = 0.99 mM; Initial NH<sub>4</sub><sup>+</sup> = 149.9 mM.

pH	NaOH Consumed (mM)	MgCl <sub>2</sub> Consumed (mM)	Recovered Struvite (mM)	Recovered HAP (mM)	Recovered OP (mM)	Recovered NH <sub>4</sub> <sup>+</sup> /NH <sub>3</sub> (mM)	Principal Dissolved Complexes of Theoretically Recoverable Nutrients
8.6	-	0.41	0.390	0.163	0.878	0.390	NH <sub>4</sub> <sup>+</sup> (87%); NH <sub>3</sub> (aq) (12%); HPO <sub>4</sub> <sup>2-</sup> (93%)
9.0	0.16	0.41	0.438	0.163	0.928	0.438	NH <sub>4</sub> <sup>+</sup> (68%); NH <sub>3</sub> (aq) (31%); HPO <sub>4</sub> <sup>2-</sup> (92%)
9.5	0.39	0.41	0.468	0.163	0.958	0.468	NH <sub>4</sub> <sup>+</sup> (40%); NH <sub>3</sub> (aq) (60%); HPO <sub>4</sub> <sup>2-</sup> (93%)
10	0.94	0.41	0.479	0.164	0.970	0.479	NH <sub>4</sub> <sup>+</sup> (17%); NH <sub>3</sub> (aq) (83%); HPO <sub>4</sub> <sup>2-</sup> (91%)
<b>10.5</b>	<b>1.50</b>	<b>0.41</b>	<b>0.482</b>	<b>0.164</b>	<b>0.973</b>	<b>0.482</b>	<b>NH<sub>4</sub><sup>+</sup> (6%); NH<sub>3</sub> (aq) (94%); HPO<sub>4</sub><sup>2-</sup> (88%)</b>
11	2.05	0.41	0.479	0.164	0.971	0.479	NH <sub>3</sub> (aq) (98%); HPO <sub>4</sub> <sup>2-</sup> (81%); PO <sub>4</sub> <sup>3-</sup> (6%)
11.5	2.60	0.41	0.467	0.164	0.958	0.467	NH <sub>3</sub> (aq) (98%); HPO <sub>4</sub> <sup>2-</sup> (66%); PO <sub>4</sub> <sup>3-</sup> (17%)
12	3.15	0.41	0.207	0.164	0.699	0.207	NH <sub>3</sub> (aq) (99%); HPO <sub>4</sub> <sup>2-</sup> (47%); PO <sub>4</sub> <sup>3-</sup> (41%)
12.5	3.70	0.41	0	0.164	0.491	0	NH <sub>3</sub> (aq) (99%); HPO <sub>4</sub> <sup>2-</sup> (22%); PO <sub>4</sub> <sup>3-</sup> (69%)
13	4.26	0.41	0	0.164	0.491	0	NH <sub>3</sub> (aq) (100%); HPO <sub>4</sub> <sup>2-</sup> (7%); PO <sub>4</sub> <sup>3-</sup> (87%)
13.5	4.81	0.41	0	0.164	0.492	0	NH <sub>3</sub> (aq) (100%); PO <sub>4</sub> <sup>3-</sup> (95%)
14	5.36	0.41	0	0.164	0.492	0	NH <sub>3</sub> (aq) (100%); PO <sub>4</sub> <sup>3-</sup> (97%)

**Table 4-7.** Theoretical recovery of nutrients via the precipitation of solids from post-HTL brewing yeast ACP at pH range of 8.3 to 14. NaOH is used to raise the alkalinity of the ACP; NaOH values are based on laboratory results. Columns 3-8 are based on results from the Visual MINTEQ model. MgCl<sub>2</sub> is added to facilitate the precipitation of nutrients as solids. Optimal pH for nutrient recovery from brewing yeast ACP is 10.5. Initial PO<sub>4</sub><sup>3-</sup> = 24.3 mM; Initial NH<sub>4</sub><sup>+</sup> = 97.8 mM.

pH	NaOH Consumed (mM)	MgCl <sub>2</sub> Consumed (mM)	Recovered Struvite (mM)	Recovered HAP (mM)	Recovered OP (mM)	Recovered NH <sub>4</sub> <sup>+</sup> /NH <sub>3</sub> (mM)	Principal Dissolved Complexes of Theoretically Recoverable Nutrients
8.3	-	23.9	23.72	0.100	24.02	23.72	NH <sub>4</sub> <sup>+</sup> (84%); NH <sub>3</sub> (aq) (15%); HPO <sub>4</sub> <sup>2-</sup> (83%)
8.5	0.06	23.9	23.78	0.101	24.08	23.78	NH <sub>4</sub> <sup>+</sup> (87%); NH <sub>3</sub> (aq) (12%); HPO <sub>4</sub> <sup>2-</sup> (84%)
9.0	0.33	23.9	23.87	0.101	24.18	23.87	NH <sub>4</sub> <sup>+</sup> (68%); NH <sub>3</sub> (aq) (31%); HPO <sub>4</sub> <sup>2-</sup> (86%)
9.5	0.60	23.9	23.92	0.101	24.22	23.92	NH <sub>4</sub> <sup>+</sup> (42%); NH <sub>3</sub> (aq) (58%); HPO <sub>4</sub> <sup>2-</sup> (86%)
10	0.87	23.9	23.93	0.101	24.23	23.93	NH <sub>4</sub> <sup>+</sup> (12%); NH <sub>3</sub> (aq) (81%); HPO <sub>4</sub> <sup>2-</sup> (85%)
<b>10.5</b>	<b>1.14</b>	<b>23.9</b>	<b>23.94</b>	<b>0.101</b>	<b>24.24</b>	<b>23.94</b>	<b>NH<sub>4</sub><sup>+</sup> (6%); NH<sub>3</sub> (aq) (94%); HPO<sub>4</sub><sup>2-</sup> (82%)</b>
11	1.41	23.9	23.93	0.101	24.23	23.93	NH <sub>3</sub> (aq) (98%); HPO <sub>4</sub> <sup>2-</sup> (75%); PO <sub>4</sub> <sup>3-</sup> (7%)
11.5	1.68	23.9	23.90	0.101	24.22	23.90	NH <sub>3</sub> (aq) (98%); HPO <sub>4</sub> <sup>2-</sup> (59%); PO <sub>4</sub> <sup>3-</sup> (17%)
12	1.95	23.9	23.21	0.101	23.51	23.21	NH <sub>3</sub> (aq) (99%); HPO <sub>4</sub> <sup>2-</sup> (39%); PO <sub>4</sub> <sup>3-</sup> (38%)
12.5	2.23	23.9	0	0.101	0.30	0	NH <sub>3</sub> (aq) (99%); HPO <sub>4</sub> <sup>2-</sup> (14%); PO <sub>4</sub> <sup>3-</sup> (72%)
13	2.50	23.9	0	0.101	0.30	0	NH <sub>3</sub> (aq) (100%); HPO <sub>4</sub> <sup>2-</sup> (5%); PO <sub>4</sub> <sup>3-</sup> (83%)
13.5	2.77	23.9	0	0.101	0.30	0	NH <sub>3</sub> (aq) (100%); PO <sub>4</sub> <sup>3-</sup> (89%)
14	3.04	23.9	0	0.101	0.30	0	NH <sub>3</sub> (aq) (100%); PO <sub>4</sub> <sup>3-</sup> (92%)

**Table 4-8.** Theoretical recovery of nutrients via the precipitation of solids from post-HTL spent grains ACP at pH range of 5.3 to 14. NaOH is used to raise the alkalinity of the ACP; NaOH values are based on laboratory results. Columns 3-8 are based on results from the Visual MINTEQ model. MgCl<sub>2</sub> is added to facilitate the precipitation of nutrients as solids. Optimal pH for nutrient recovery from spent grains ACP is 10.5. Initial PO<sub>4</sub><sup>3-</sup> = 11.4 mM; Initial NH<sub>4</sub><sup>+</sup> = 50.0 mM.

pH	NaOH Consumed (mM)	MgCl <sub>2</sub> Consumed (mM)	Recovered Struvite (mM)	Recovered HAP (mM)	Recovered OP (mM)	Recovered NH <sub>4</sub> <sup>+</sup> /NH <sub>3</sub> (mM)	Principal Dissolved Complexes of Theoretically Recoverable Nutrients
5.3	-	9.88	0	0	0	0	NH <sub>4</sub> <sup>+</sup> (100%); H <sub>2</sub> PO <sub>4</sub> <sup>-</sup> (94%)
5.5	0.03	9.88	0	0	0	0	NH <sub>4</sub> <sup>+</sup> (100%); H <sub>2</sub> PO <sub>4</sub> <sup>-</sup> (94%)
6.0	0.07	9.88	0	0	0	0	NH <sub>4</sub> <sup>+</sup> (100%); H <sub>2</sub> PO <sub>4</sub> <sup>-</sup> (80%); HPO <sub>4</sub> <sup>2-</sup> (9%)
6.5	0.09	9.88	6.09	0.072	6.30	6.09	NH <sub>4</sub> <sup>+</sup> (100%); H <sub>2</sub> PO <sub>4</sub> <sup>-</sup> (64%); HPO <sub>4</sub> <sup>2-</sup> (22%)
7.0	0.25	9.88	9.20	0.078	9.44	9.20	NH <sub>4</sub> <sup>+</sup> (99%); H <sub>2</sub> PO <sub>4</sub> <sup>-</sup> (43%); HPO <sub>4</sub> <sup>2-</sup> (44%)
7.5	0.40	9.88	10.3	0.080	10.5	10.3	NH <sub>4</sub> <sup>+</sup> (98%); H <sub>2</sub> PO <sub>4</sub> <sup>-</sup> (22%); HPO <sub>4</sub> <sup>2-</sup> (68%)
8.0	0.56	9.88	10.6	0.081	11.0	10.6	NH <sub>4</sub> <sup>+</sup> (96%); H <sub>2</sub> PO <sub>4</sub> <sup>-</sup> (9%); HPO <sub>4</sub> <sup>2-</sup> (85%)
8.5	0.72	9.88	10.7	0.082	11.1	10.7	NH <sub>4</sub> <sup>+</sup> (87%); NH <sub>3</sub> (aq) (13%); HPO <sub>4</sub> <sup>2-</sup> (93%)
9.0	0.88	9.88	10.8	0.082	11.2	10.9	NH <sub>4</sub> <sup>+</sup> (68%); NH <sub>3</sub> (aq) (32%); HPO <sub>4</sub> <sup>2-</sup> (98%)
9.5	1.03	9.88	10.9	0.082	11.2	10.9	NH <sub>4</sub> <sup>+</sup> (40%); NH <sub>3</sub> (aq) (60%); HPO <sub>4</sub> <sup>2-</sup> (99%)
10	1.19	9.88	11.0	0.082	11.2	11.0	NH <sub>4</sub> <sup>+</sup> (17%); NH <sub>3</sub> (aq) (83%); HPO <sub>4</sub> <sup>2-</sup> (96%)
<b>10.5</b>	<b>1.35</b>	<b>9.88</b>	<b>11.1</b>	<b>0.082</b>	<b>11.3</b>	<b>11.1</b>	<b>NH<sub>4</sub><sup>+</sup> (6%); NH<sub>3</sub> (aq) (94%); HPO<sub>4</sub><sup>2-</sup> (95%)</b>
11	1.50	9.88	11.0	0.082	11.2	11.0	NH <sub>3</sub> (aq) (98%); HPO <sub>4</sub> <sup>2-</sup> (89%); PO <sub>4</sub> <sup>3-</sup> (5%)
11.5	1.66	9.88	10.9	0.082	11.2	10.9	NH <sub>3</sub> (aq) (99%); HPO <sub>4</sub> <sup>2-</sup> (75%); PO <sub>4</sub> <sup>3-</sup> (14%)
12	1.82	9.88	10.3	0.082	10.5	10.3	NH <sub>3</sub> (aq) (99%); HPO <sub>4</sub> <sup>2-</sup> (55%); PO <sub>4</sub> <sup>3-</sup> (39%)
12.5	1.98	9.88	0	0.082	0.25	0	NH <sub>3</sub> (aq) (99%); HPO <sub>4</sub> <sup>2-</sup> (20%); PO <sub>4</sub> <sup>3-</sup> (79%)
13	2.13	9.88	0	0.082	0.25	0	NH <sub>3</sub> (aq) (100%); HPO <sub>4</sub> <sup>2-</sup> (6%); PO <sub>4</sub> <sup>3-</sup> (93%)
13.5	2.29	9.88	0	0.082	0.25	0	NH <sub>3</sub> (aq) (100%); PO <sub>4</sub> <sup>3-</sup> (98%)
14	2.45	9.88	0	0.082	0.25	0	NH <sub>3</sub> (aq) (100%); PO <sub>4</sub> <sup>3-</sup> (99%)

**Table 4-9.** Theoretical recovery of nutrients via the precipitation of solids from post-HTL dry hops ACP at pH range of 7.0 to 14. NaOH is used to raise the alkalinity of the ACP; NaOH values are based on laboratory results. Columns 3-8 are based on results from the Visual MINTEQ model. MgCl<sub>2</sub> is added to facilitate the precipitation of nutrients as solids. Optimal pH for nutrient recovery from dry hops ACP is 10.5. Initial PO<sub>4</sub><sup>3-</sup> = 9.3 mM; Initial NH<sub>4</sub><sup>+</sup> = 88.5 mM.

pH	NaOH Consumed (mM)	MgCl <sub>2</sub> Consumed (mM)	Recovered Struvite (mM)	Recovered HAP (mM)	Recovered OP (mM)	Recovered NH <sub>4</sub> <sup>+</sup> /NH <sub>3</sub> (mM)	Principal Dissolved Complexes of Theoretically Recoverable Nutrients
7.0	-	8.85	7.27	0.111	7.61	7.27	NH <sub>4</sub> <sup>+</sup> (99%); H <sub>2</sub> PO <sub>4</sub> <sup>-</sup> (39%); HPO <sub>4</sub> <sup>2-</sup> (47%)
7.5	0.24	8.85	8.18	0.114	8.52	8.18	NH <sub>4</sub> <sup>+</sup> (98%); H <sub>2</sub> PO <sub>4</sub> <sup>-</sup> (17%); HPO <sub>4</sub> <sup>2-</sup> (65%)
8.0	0.35	8.85	8.55	0.115	8.90	8.55	NH <sub>4</sub> <sup>+</sup> (98%); H <sub>2</sub> PO <sub>4</sub> <sup>-</sup> (7%); HPO <sub>4</sub> <sup>2-</sup> (81%)
8.5	0.46	8.85	8.73	0.116	9.07	8.73	NH <sub>4</sub> <sup>+</sup> (86%); NH <sub>3</sub> (aq) (13%); HPO <sub>4</sub> <sup>2-</sup> (86%)
9.0	0.57	8.85	8.81	0.116	9.16	8.81	NH <sub>4</sub> <sup>+</sup> (68%); NH <sub>3</sub> (aq) (31%); HPO <sub>4</sub> <sup>2-</sup> (88%)
9.5	0.67	8.85	8.85	0.117	9.20	8.85	NH <sub>4</sub> <sup>+</sup> (41%); NH <sub>3</sub> (aq) (59%); HPO <sub>4</sub> <sup>2-</sup> (88%)
10	0.71	8.85	8.86	0.117	9.21	8.86	NH <sub>4</sub> <sup>+</sup> (18%); NH <sub>3</sub> (aq) (82%); HPO <sub>4</sub> <sup>2-</sup> (86%)
<b>10.5</b>	<b>0.86</b>	<b>8.85</b>	<b>8.87</b>	<b>0.117</b>	<b>9.22</b>	<b>8.87</b>	<b>NH<sub>4</sub><sup>+</sup> (6%); NH<sub>3</sub> (aq) (94%); HPO<sub>4</sub><sup>2-</sup> (83%)</b>
11	1.00	8.85	8.86	0.117	9.21	8.86	NH <sub>3</sub> (aq) (98%); HPO <sub>4</sub> <sup>2-</sup> (76%); PO <sub>4</sub> <sup>3-</sup> (7%)
11.5	1.15	8.85	8.84	0.117	9.19	8.84	NH <sub>3</sub> (aq) (99%); HPO <sub>4</sub> <sup>2-</sup> (60%); PO <sub>4</sub> <sup>3-</sup> (17%)
12	1.30	8.85	8.22	0.117	8.57	8.22	NH <sub>3</sub> (aq) (99%); HPO <sub>4</sub> <sup>2-</sup> (41%); PO <sub>4</sub> <sup>3-</sup> (40%)
12.5	1.45	8.85	0	0.117	0.35	0	NH <sub>3</sub> (aq) (99%); HPO <sub>4</sub> <sup>2-</sup> (17%); PO <sub>4</sub> <sup>3-</sup> (68%)
13	1.60	8.85	0	0.117	0.35	0	NH <sub>3</sub> (aq) (100%); HPO <sub>4</sub> <sup>2-</sup> (5%); PO <sub>4</sub> <sup>3-</sup> (82%)
13.5	1.75	8.85	0	0.117	0.35	0	NH <sub>3</sub> (aq) (100%); PO <sub>4</sub> <sup>3-</sup> (90%)
14	1.90	8.85	0	0.117	0.35	0	NH <sub>3</sub> (aq) (100%); PO <sub>4</sub> <sup>3-</sup> (93%)

**Table 4-10.** Theoretical recovery of nutrients via the precipitation of solids from post-HTL white lees ACP at pH range of 6.4 to 14. NaOH is used to raise the alkalinity of the ACP; NaOH values are based on laboratory results. Columns 3-8 are based on results from the Visual MINTEQ model. MgCl<sub>2</sub> is added to facilitate the precipitation of nutrients as solids. Optimal pH for nutrient recovery from white lees ACP is 9.0. Initial PO<sub>4</sub><sup>3-</sup> = 1.1 mM; Initial NH<sub>4</sub><sup>+</sup> = 2.2 mM.

pH	NaOH Consumed (mM)	MgCl <sub>2</sub> Consumed (mM)	Recovered Struvite (mM)	Recovered HAP (mM)	Recovered OP (mM)	Recovered NH <sub>4</sub> <sup>+</sup> /NH <sub>3</sub> (mM)	Principal Dissolved Complexes of Theoretically Recoverable Nutrients
6.4	-	0	0	0.014	0.041	0	NH <sub>4</sub> <sup>+</sup> (100%); H <sub>2</sub> PO <sub>4</sub> <sup>-</sup> (67%); HPO <sub>4</sub> <sup>2-</sup> (19%)
6.5	0.002	0	0	0.021	0.064	0	NH <sub>4</sub> <sup>+</sup> (100%); H <sub>2</sub> PO <sub>4</sub> <sup>-</sup> (63%); HPO <sub>4</sub> <sup>2-</sup> (22%)
7.0	0.006	0	0	0.039	0.118	0	NH <sub>4</sub> <sup>+</sup> (99%); H <sub>2</sub> PO <sub>4</sub> <sup>-</sup> (38%); HPO <sub>4</sub> <sup>2-</sup> (43%)
7.5	0.024	0	0	0.044	0.132	0	NH <sub>4</sub> <sup>+</sup> (98%); H <sub>2</sub> PO <sub>4</sub> <sup>-</sup> (17%); HPO <sub>4</sub> <sup>2-</sup> (60%)
8.0	0.046	0	0	0.045	0.136	0	NH <sub>4</sub> <sup>+</sup> (95%); H <sub>2</sub> PO <sub>4</sub> <sup>-</sup> (6%); HPO <sub>4</sub> <sup>2-</sup> (70%)
8.5	0.068	5.55	0.34	0.046	0.472	0.34	NH <sub>4</sub> <sup>+</sup> (87%); NH <sub>3</sub> (aq) (13%); HPO <sub>4</sub> <sup>2-</sup> (51%)
<b>9.0</b>	<b>0.091</b>	<b>3.70</b>	<b>0.56</b>	<b>0.046</b>	<b>0.699</b>	<b>0.56</b>	<b>NH<sub>4</sub><sup>+</sup> (68%); NH<sub>3</sub> (aq) (32%); HPO<sub>4</sub><sup>2-</sup> (57%)</b>
9.5	0.113	0.41	0.13	0.046	0.271	0.13	NH <sub>4</sub> <sup>+</sup> (40%); NH <sub>3</sub> (aq) (60%); HPO <sub>4</sub> <sup>2-</sup> (71%)
10	0.135	0.21	0.09	0.046	0.227	0.09	NH <sub>4</sub> <sup>+</sup> (18%); NH <sub>3</sub> (aq) (82%); HPO <sub>4</sub> <sup>2-</sup> (71%)
10.5	0.157	0	0	0.046	0.139	0	NH <sub>4</sub> <sup>+</sup> (7%); NH <sub>3</sub> (aq) (93%); HPO <sub>4</sub> <sup>2-</sup> (70%)
11	0.179	0	0	0.046	0.139	0	NH <sub>3</sub> (aq) (98%); HPO <sub>4</sub> <sup>2-</sup> (64%); PO <sub>4</sub> <sup>3-</sup> (7%)
11.5	0.020	0	0	0.046	0.139	0	NH <sub>3</sub> (aq) (99%); HPO <sub>4</sub> <sup>2-</sup> (49%); PO <sub>4</sub> <sup>3-</sup> (17%)
12	0.224	0	0	0.046	0.139	0	NH <sub>3</sub> (aq) (99%); HPO <sub>4</sub> <sup>2-</sup> (29%); PO <sub>4</sub> <sup>3-</sup> (33%)
12.5	0.246	0	0	0.046	0.139	0	NH <sub>3</sub> (aq) (99%); HPO <sub>4</sub> <sup>2-</sup> (13%); PO <sub>4</sub> <sup>3-</sup> (49%)
13	0.268	0	0	0.046	0.139	0	NH <sub>3</sub> (aq) (100%); PO <sub>4</sub> <sup>3-</sup> (63%)
13.5	0.291	0	0	0.046	0.139	0	NH <sub>3</sub> (aq) (100%); PO <sub>4</sub> <sup>3-</sup> (77%)
14	0.313	0	0	0.046	0.139	0	NH <sub>3</sub> (aq) (100%); PO <sub>4</sub> <sup>3-</sup> (83%)

**Table 4-11.** Theoretical recovery of nutrients via the precipitation of solids from post-HTL red lees ACP at pH range of 8.8 to 14. NaOH is used to raise the alkalinity of the ACP; NaOH values are based on laboratory results. Columns 3-8 are based on results from the Visual MINTEQ model. MgCl<sub>2</sub> is added to facilitate the precipitation of nutrients as solids. Optimal pH for nutrient recovery from red lees ACP is 10.5. Initial PO<sub>4</sub><sup>3-</sup> = 22.2 mM; Initial NH<sub>4</sub><sup>+</sup> = 79.6 mM.

pH	NaOH Consumed (mM)	MgCl <sub>2</sub> Consumed (mM)	Recovered Struvite (mM)	Recovered HAP (mM)	Recovered OP (mM)	Recovered NH <sub>4</sub> <sup>+</sup> /NH <sub>3</sub> (mM)	Principal Dissolved Complexes of Theoretically Recoverable Nutrients
8.8	-	21.8	21.63	0.093	21.9	21.63	NH <sub>4</sub> <sup>+</sup> (86%); NH <sub>3</sub> (aq) (14%); HPO <sub>4</sub> <sup>2-</sup> (61%)
9.0	0.16	21.8	21.68	0.093	22.0	21.68	NH <sub>4</sub> <sup>+</sup> (70%); NH <sub>3</sub> (aq) (30%); HPO <sub>4</sub> <sup>2-</sup> (62%)
9.5	0.20	21.8	21.74	0.093	22.0	21.74	NH <sub>4</sub> <sup>+</sup> (42%); NH <sub>3</sub> (aq) (58%); HPO <sub>4</sub> <sup>2-</sup> (61%)
10	0.66	21.8	21.76	0.093	22.0	21.76	NH <sub>4</sub> <sup>+</sup> (19%); NH <sub>3</sub> (aq) (81%); HPO <sub>4</sub> <sup>2-</sup> (60%)
<b>10.5</b>	<b>1.12</b>	<b>21.8</b>	<b>21.77</b>	<b>0.093</b>	<b>22.1</b>	<b>21.77</b>	<b>NH<sub>4</sub><sup>+</sup> (7%); NH<sub>3</sub> (aq) (93%); HPO<sub>4</sub><sup>2-</sup> (57%)</b>
11	1.58	21.8	21.76	0.094	22.0	21.76	NH <sub>3</sub> (aq) (98%); HPO <sub>4</sub> <sup>2-</sup> (49%); PO <sub>4</sub> <sup>3-</sup> (7%)
11.5	2.04	21.8	21.70	0.094	22.0	21.70	NH <sub>3</sub> (aq) (99%); HPO <sub>4</sub> <sup>2-</sup> (34%); PO <sub>4</sub> <sup>3-</sup> (15%)
12	2.50	21.8	19.08	0.093	19.4	19.08	NH <sub>3</sub> (aq) (99%); HPO <sub>4</sub> <sup>2-</sup> (19%); PO <sub>4</sub> <sup>3-</sup> (28%)
12.5	2.96	21.8	0	0.093	0.28	0	NH <sub>3</sub> (aq) (99%); HPO <sub>4</sub> <sup>2-</sup> (8%); PO <sub>4</sub> <sup>3-</sup> (43%)
13	3.42	21.8	0	0.093	0.28	0	NH <sub>3</sub> (aq) (100%); PO <sub>4</sub> <sup>3-</sup> (51%)
13.5	3.88	21.8	0	0.093	0.28	0	NH <sub>3</sub> (aq) (100%); PO <sub>4</sub> <sup>3-</sup> (60%)
14	4.34	21.8	0	0.093	0.28	0	NH <sub>3</sub> (aq) (100%); PO <sub>4</sub> <sup>3-</sup> (66%)

From Tables 4-4 through 4-11, there are a number of important findings. First, pertaining to the formation of solids, the model showed that the recovery of N and P in solid form is theoretically possible for all of the feedstock ACPs. Based on the results of the model, the solids that could theoretically be precipitated include: struvite and HAP. HAP contains both  $\text{Ca}^{2+}$  and  $\text{PO}_4^{3-}$  and can be used as a source of slow-release fertilizer, like struvite (Yelten-Yilmaz et al., 2018; Teymouri et al., 2018). Model results show that struvite and HAP could be produced from all of the feedstock ACPs except the dairy manure ACP, which only produced HAP. For each pH value in the tables, the “optimal” recovery of solids was chosen based in part on the recovery of the theoretical  $\text{Mg}^{2+}$  concentration added to each of the ACPs.  $\text{Mg}^{2+}$  concentration addition versus the formation of struvite was monitored as a ratio of mol  $\text{Mg}^{2+}$  added to mol struvite recovered. The chosen concentration of  $\text{Mg}^{2+}$  to add corresponded to values for which at least 50% of the  $\text{Mg}^{2+}$  added was precipitated in solid form as struvite (i.e., product yield  $\geq 50\%$  unit input). The “optimal” pH for each feedstock was chosen based on the maximum recovery of the limiting nutrient (i.e., P in most of the feedstock ACPs) across the pH range studied. This was done by computing the recovery of P (in mmol) as struvite and/or HAP based on the molar ratio of P in struvite (1 mol  $\text{PO}_4^{3-}$ ) and HAP (3 mol  $\text{PO}_4^{3-}$ ), since P was generally the limiting nutrient.

Second, pertaining to the quantities of solids formed, several of the feedstock ACPs precipitated varying quantities of solids at the optimal pH of the ACP. For all of the ACPs except dairy manure, 0.1-5.9 g/L of struvite was precipitable. This is similar to the findings of Çelen et al. (2007) that evaluated the theoretical precipitation of struvite from liquid swine manure via chemical equilibrium modeling. For all of the ACPs, a range of 20-210 mg/L of HAP was precipitated. When adding the masses of struvite and HAP produced, the brewing yeast and red lees ACP produced the greatest quantity of solids, which is expected based on the

higher concentrations of available OP in these ACPs compared to the other feedstock ACPs (Table 4-2). The pre-digested sludge, digested sludge, brewing yeast, spent grains, dry hops, and red lees ACPs performed similarly, as these feedstock ACPs could all precipitate both struvite and HAP at the same optimal pH value of 10.5. At pH 10.5, there is sufficient available  $\text{NH}_4^+$  to form struvite, whereas at higher pHs, more  $\text{NH}_4^+$  is available as  $\text{NH}_3$ , and larger quantities of struvite cannot be formed, as seen by an excess of free dissolved  $\text{PO}_4^{3-}$  at pH values higher than the optimal pH (e.g., Table 4-5, column 8). The dairy manure (Table 4-4) and white lees (Table 4-10) ACPs performed differently than the other feedstock ACPs, as these ACPs produced lower optimal pH values (8.0 and 9.0 for dairy manure and white lees ACPs, respectively).

The dairy manure ACP has the theoretical potential to precipitate HAP, but not struvite (Table 4-4). This is due to two main variables:  $\text{Ca}^{2+}$  concentration and pH. Due to the high concentration of  $\text{Ca}^{2+}$  in the dairy manure ACP (Table 4-3) and the acidic pH outside the range of optimal precipitation of struvite (~8.5-11), struvite is not precipitated from the dairy manure ACP (Yetilmezsoy and Sapci-Zengin, 2009; Tao et al., 2016; Çelen et al., 2007). The high concentrations of  $\text{Ca}^{2+}$  instead facilitate the formation of HAP at lower pH values. As the pH is increased, more HAP is formed. Once the pH is at a value within the optimal range of struvite precipitation, the OP is fully recovered via the formation of HAP. The white lees ACP also performed differently than the other ACPs. Because the white lees ACP is N-limited, the optimal pH for solids precipitation of the white lees ACP is lower than the other ACPs, which are all P-limited. This is because N is available as  $\text{NH}_4^+$  at lower pH values, which is required for struvite precipitation. At higher pH values,  $\text{NH}_4^+$  is converted to  $\text{NH}_3$ , which is unavailable for precipitation in solid form. The formation of struvite in the ACPs that are P-limited is optimal at higher pH values, where P is more available as  $\text{PO}_4^{3-}$ . N is in excess, so once the

majority of the N becomes available as  $\text{NH}_3$  at higher pHs, there is a small portion of N available as  $\text{NH}_4^+$  to precipitate N and P as struvite.

To reiterate, the goal of this study is to assess to what extent valuable, scarce nutrients can be recovered from ACP as a means of managing post-HTL ACP and producing valuable nutrient-based materials. Table 4-12 helps to meet this goal by presenting the percent residual  $\text{NH}_4^+/\text{NH}_3$  and OP in each of the ACPs after precipitation of solids (i.e., struvite and/or HAP) at optimal pH values. The precipitation of solids from all of the ACPs, except the white lees ACP, resulted in the recovery of 98-100% of the original OP. These results are comparable to published studies that reported similar percentages of OP recovery via the precipitation of struvite (Çelen et al., 2007; Kataki et al., 2016).

**Table 4-12.** Optimum theoretical recovery of N and P via precipitation of solids from post-HTL ACP at optimal pH values of select waste feedstocks based on Visual MINTEQ model outputs.

Waste Feedstock	Optimal pH	Residual $\text{NH}_4^+/\text{NH}_3$ (mM)	Residual $\text{NH}_4^+/\text{NH}_3$ (%)	Residual TN (%)	Residual OP (mM)	Residual OP (%)	Residual TP (%)
Dairy Manure	8.0	22.5	100	100	0	0	75
Pre-Digested Sludge	10.5	66.3	95	98	0.03	>1	57
Digested Sludge	10.5	149.5	100	100	0.02	2	58
Brewing Yeast	10.5	73.9	76	82	0.07	>1	5
Spent Grains	10.5	39.0	78	90	0.11	1	3
Dry Hops	10.5	79.7	90	94	0.05	>1	64
White Lees	9.0	1.7	75	90	0.37	34	36
Red Lees	10.5	57.8	73	79	0.13	>1	42

From Table 4-2, it is shown that the available  $\text{NH}_4^+$  and  $\text{PO}_4^{3-}$  in each of the ACPs account for only an average of 50% and 26% of ACP TN and TP, respectively. Therefore, even with an OP removal rate of  $\geq 97\%$ , there is still appreciable quantities of TP (3-75%) in most of the ACPs that would need to be treated prior to discharge into a natural receiving water. It is

important to note that the ACPs arising from the HTL processing of wastes from beer and wine production (with the exception of the N-limited white lees ACP) show 100% theoretical removal of OP via nutrient-based precipitation. This is of particular interest, as smaller breweries and wineries typically do not have optimal means of waste disposal in place at their facilities, in contrast to the dairy farming and WWTP industries. Since N is in excess in most of the feedstock ACPs, large quantities of TN (79-100%) are present in the ACPs after nutrient precipitation. Residual TN would have to be treated prior to discharge into a natural receiving water.

#### **4.3.4 Energy Recovery Impacts**

With high energy costs for the removal of N and P from wastewater, ACP management could have huge implications on the energy performance of the hydrothermal processing of organic waste feedstocks (Bauer et al., 2018). Therefore, it is of interest to determine the EROI (i.e.,  $E_{OUT}/E_{IN}$ ) of ACP management via nutrient-based precipitation for each of the post-HTL ACPs evaluated in this study. Experimental ACP quality characterization data, along with theoretical nutrient recovery data from the MINTEQ model, were used to determine the EROIs of HTL processing to account for ACP management and nutrient recovery for each of the feedstock ACPs. Table 4-13 presents energy cost data and EROI calculations for the removal of N and P from post-HTL ACP via nutrient-based precipitation.

**Table 4-13.** Estimates of EROI to account for the management of the ACP arising from the HTL processing of select waste feedstocks via nutrient-based precipitation. EROI values >1 are indicative of favorable energy yield, whereas EROI values <1 are indicative of unfavorable energy yields.

Waste Feedstock	E <sub>IN</sub>		E <sub>OUT</sub>				EROI
	NaOH Energy Cost (kJ/L)	MgSO <sub>4</sub> Energy Cost (kJ/L)	Struvite Energy Value (as MAP) (kJ/L)	HAP Energy Value (as TSP) (kJ/L)	Avoided Energy Cost for TN Removal (kJ/L)	Avoided Energy Cost for TP Removal (kJ/L)	
Dairy Manure	2.6	0	0	2.5	0	0.4	<b>1.1</b>
Pre-Digested Sludge	1.9	2.6	5.1	0.6	7.6	1.2	<b>3.2</b>
Digested Sludge	2.8	0.3	0.7	1.0	0.8	0.3	0.9
Brewing Yeast	2.1	18.8	37.0	0.6	55.7	7.3	<b>4.8</b>
Spent Grains	2.5	7.8	17.2	0.5	25.7	3.5	<b>4.6</b>
Dry Hops	1.6	6.9	13.7	0.7	21.0	3.1	<b>4.5</b>
White Lees	0.2	2.9	0.9	0.3	1.3	0.1	0.8
Red Lees	2.1	17.1	33.7	0.5	50.5	7.4	<b>4.8</b>

EROI values that are greater than 1 are indicative of favorable energy yield, as the energy generated from the system is greater than the energy cost of the system. In contrast, EROI values that are less than 1 indicate that the system consumes more energy than it produces, which is unfavorable from an energy performance perspective. Based on the EROI estimates for the recovery of nutrients from the ACPs presented in Table 4-13, it is energetically valuable to recover N and P from most of the ACPs evaluated in this study. The HTL processing of pre-digested sludge, brewing yeast, spent grains, dry hops, and red lees feedstocks with ACP management via nutrient-based precipitation all produced EROI values >3 (3.2-4.8). The dairy manure feedstock has a lower, but still energetically favorable, EROI value of 1.1. Due to high concentrations of TN and TP and low precipitation yields of struvite in the digested sludge and white lees ACPs, it is not unexpected that these feedstock ACPs produce EROI values <1, as the cost for removing TN and TP is still substantial for these feedstock ACPs, despite high percentages of P and N removal, respectively, via chemical precipitation.

Overall, the results from Table 4-13 are promising, as the energy performance of the management of post-HTL processing ACP via nutrient-based precipitation for most of the ACPs evaluated in this study is favorable. From an environmental and energy perspective, it is imperative that the ACP arising from HTL processing is managed. Through the novel ACP management technique of nutrient-based precipitation, HTL not only serves as a platform for producing renewable energy, but also producing valuable, scarce materials. In order to fully investigate the precipitation of nutrients from ACP, future work should include experimentally validating the theoretical results reported in this study.

#### **4.4 Conclusions**

HTL processing of organic waste feedstocks produces potent wastewater in the form of ACP that is likely to require management before discharge into the receiving waters of a WWTP. Due to high concentrations of N and P in the ACP, the recoverability of nutrients via adjustment of pH was evaluated as a means of novel ACP management. Theoretical model results indicate that inorganic N and P can be theoretically recovered from the post-HTL ACP via nutrient-based precipitation in the form of soil amendments, such as struvite and HAP. Most of the ACPs exhibited precipitation of solids at an optimal pH of 10.5 (excluding the dairy manure and white lees ACPs, which had lower optimal pHs). Struvite and HAP precipitation accounted for more than 97% recovery of OP from the ACPs, with the exception of the white lees ACP. Recovery of  $\text{NH}_4^+/\text{NH}_3$  averaged 14% for all the ACPs, except the dairy manure and digested sludge ACPs, which exhibited <1% removal of  $\text{NH}_4^+/\text{NH}_3$ . For most of the feedstock ACPs evaluated in this study, nutrient-based precipitation offsets the energy cost of ACP management. Experimental analysis is needed to confirm theoretical recovery results in order to fully evaluate the suitability

of HTL as a means of valorizing waste into renewable energy and producing valuable scarce materials.

#### 4.5 References

- APHA (2013). Standard methods for the examination of water and waste water, 22nd ed. *American Public Health Association*, Washington, D.C., Retrieved from <[www.standardmethods.org/PDF/22nd\\_Ed\\_Errata\\_12\\_16\\_13.pdf](http://www.standardmethods.org/PDF/22nd_Ed_Errata_12_16_13.pdf)>.
- Bauer, S., Reynolds, C., Peng, S. and Colosi, L. (2018). Evaluating the Water Quality Impacts of Hydrothermal Liquefaction: Assessment of Carbon, Nitrogen, and Energy Recovery Impacts, *Bioresource Technology Reports*, 2, 115-120.
- Bhutto, A. W., Qureshi, K., Abro, R., Harijan, K., Zhao, Z., Bazmi, A. A., Abbas, T. and Yu, G. (2016). Progress in the production of biomass-to-liquid biofuels to decarbonize the transport sector-prospects and challenges. *Royal Society of Chemistry Advances*, 6, 32140-32170.
- Biller, P., Ross, A. B., Skill, S. C., Lea-Langton, A., Balasundaram, B., Hall, C., Riley, P. and Llewellyn, C. A. (2012). Nutrient recycling of aqueous phase for microalgae cultivation from the hydrothermal liquefaction process. *Algal Research*, 1 (1), 70–76.
- Capdevielle, A., Sýkorová, E., Biscans, B., Béline, F. and Daumer, M. (2013). Optimization of struvite precipitation in synthetic biologically treated swine wastewater–Determination of the optimal process parameters. *Journal of Hazardous Materials*, 244-245, 357-369.
- Çelen, I., Buchanan, J. R., Burns, R. T., Robinson, R. B. and Raman, D. R. (2007). Using chemical equilibrium model to predict amendments required to precipitate phosphorus as struvite in liquid swine manure. *Water Research*, 41, 1689-1696.
- Christensen, T. H., Kjeldsen, P., Bjerg, P. L., Jensen, D. L., Christensen, J. B., Baun, A., Albrechtsen, H. J. and Heron, G. (2001). Review: Biogeochemistry of landfill leachate plumes. *Applied Geochemistry*, 16, 659-718.
- Clarens, A. F., Resurreccion, E. P., White, M. A. and Colosi, L. M. (2010). Environmental life cycle comparison of algae to other bioenergy feedstocks. *Environmental Science & Technology*, 44, 1813-1819.
- Connelly, E. B., Colosi, L. M., Clarens, A. F. and Lambert, J. H. (2015). Life Cycle Assessment of Biofuels from Algae Hydrothermal Liquefaction: The Upstream and Downstream Factors Affecting Regulatory Compliance. *Energy & Fuels*, 29, 1653-1661.

- Dominguez-Faus, R., Powers, S. E., Burken, J. G. and Alvarez, P. J. (2009). The Water Footprint of Biofuels: A Drink or Drive Issue? *Environmental Science & Technology*, 43 (9), 3005–3010.
- Ekpo, U., Ross, A. B., Camargo-Valero, M. A. and Fletcher, L. A. (2016). Influence of pH on hydrothermal treatment of swine manure: Impact on extraction of nitrogen and phosphorus in process water. *Bioresource Technology*, 214, 637-644.
- Elliott, D. C., Biller, P., Ross, A. B., Schmidt, A. J. and Jones, S. B. (2014). Hydrothermal liquefaction of biomass: Developments from batch to continuous process. *Bioresource Technology*, 178, 147–156.
- Environmental Protection Agency (EPA) (1997). Method 300.1: Determination of inorganic anions in drinking water by ion chromatography, *USEPA*, Office of Water.
- Gai, C., Zhang, Y., Chen, W. T., Zhou, Y., Schideman, L., Zhang, P., Tommaso, G., Kuo, C. T. and Dong, Y. (2015). Characterization of aqueous phase from the hydrothermal liquefaction of *Chlorella pyrenoidosa*. *Bioresource Technology*, 184, 328–35.
- Gama, R., Van Dyk, J. S. and Pletschke, B. I. (2015). Optimization of enzymatic hydrolysis of apple pomace for production of biofuel and biorefinery chemicals using commercial enzymes. *3 Biotech.*, 5 (6), 1075–1087.
- Garcia Alba, L., Torri, C., Samorì, C., Van der Spek, J., Fabbri, D., Kersten, S. R. A. and Brilman, D. W. F. (2012). Hydrothermal treatment (HTT) of microalgae: Evaluation of the process as conversion method in an algae biorefinery concept. *Energy & Fuels*, 26 (1), 642–657.
- Gustafsson, J. P. (2013). Visual MINTEQ Ver. 3.1. KTH, Sweden. Downloaded from <vminteq.lwr.kth.se/>.
- Huang, H. J., Yuan, X. Z., Zhu, H. N., Li, H., Liu, Y., Wang, X. L. and Zeng, G. M. (2013). Comparative studies of thermochemical liquefaction characteristics of microalgae, lignocellulosic biomass and sewage sludge. *Energy*, 56, 52–60.
- Ishii, S. K. L. and Boyer, T. H. (2015). Life cycle comparison of centralized wastewater treatment and urine source separation with struvite precipitation: Focus on urine nutrient management. *Water Research*, 79, 88–103.
- Jena, U., Vaidyanathan, N., Chinnasamy, S. and Das, K. C. (2011). Evaluation of microalgae cultivation using recovered aqueous co-product from thermochemical liquefaction of algal biomass. *Bioresource Technology*, 102 (3), 3380–7.

- Kataki, S., West, H., Clarke, M. and Baruah, D. C. (2016). Phosphorus recovery as struvite from farm, municipal and industrial waste: Feedstock suitability, methods and pre-treatment, *Waste Management*, 49, 437-454.
- Lahr, R., Goetsch, H., Haig, S., Noe-Hays, A., Love, N., Aga, D., Bott, C., Foxman, B., Jimenez, J., Luo, T., Nace, K. (2016). Urine bacterial community convergence through fertilizer production: Storage, pasteurization, and struvite precipitation. *Environ. Sci. Technol.*, 50, 11619-11626.
- Maddi, B., Panisko, E., Wietsma, T., Lemmon, T., Swita, M., Albrecht, K. and Howe, D. (2017). Quantitative characterization of aqueous byproducts from hydrothermal liquefaction of municipal wastes, food industry wastes, and biomass grown on waste. *ACS Sustainable Chemistry & Engineering*, 5, 2205-2214.
- Mayer, B., Baker, L., Boyer, T., Drechsel, P., Gifford, M., Hanjra, M., Parameswaran, P., Stoltzfus, J., Westrehoff, P. and Rittman, B. (2016). Total value of phosphorus recovery. *Environ. Sci. Technol.*, 50, 6606-6620.
- Munir, M. T., Liu, B., Boiarkina, I., Baroutian, S., Yu, W. and Young, B. R. (2017). Phosphate recovery from hydrothermally treated sewage sludge using struvite precipitation. *Bioresource Technology*, 239, 171-179.
- Oman, C. B. and Junestedt, C. (2008). Chemical characterization of landfill leachates-400 parameters and compounds. *Waste Management*, 28, 1876-1891.
- Pham, M., Schideman, L., Scott, J., Rajagopalan, N. and Plewa, M. J. (2013). Chemical and biological characterization of wastewater generated from hydrothermal liquefaction of *Spirulina*. *Environmental Science & Technology*, 47, 2131-2138.
- Rahman, M. M., Liu, Y., Kwag, J. H. and Ra, C. (2011). Recovery of struvite from animal wastewater and its nutrient leaching loss in soil. *J. Hazard. Mater.*, 186, 2026-2030.
- Rajeshwari, K. V., Balakrishnan, M., Kansal, A., Lata, K. and Kishore, V. V. N. (2000). State-of-the-art of anaerobic digestion technology for industrial wastewater treatment. *Renewable and Sustainable Energy Reviews*, 4 (2), 135-156.
- Sawayama, S., Minowa, T. and Yokoyama, S.-Y. (1999). Possibility of energy production and CO<sub>2</sub> mitigation by thermochemical liquefaction of microalgae. *Biomass and Bioenergy*, 17, 33-39.
- Tao, W., Fattah, K. P. and Huchzermeier, M. P. (2016). Struvite recovery from anaerobically digested dairy manure: A review of application potential and hindrances. *Journal of Environmental Management*, 169, 46-57.

- Tchobanoglous, G., Burton, F. and Stensel, H. D. (2003). *Wastewater Engineering: Treatment and Reuse*, Fourth Ed. New York: McGraw-Hill Higher Education.
- Teymouri, A., Stuart, B. and Kumar, S. (2018). Hydroxyapatite and dittmarite precipitation from algae hydrolysate. *Algal Research*, 29, 202-211.
- Theegala, C. S. and Midgett, J. S. (2012). Hydrothermal liquefaction of separated dairy manure for production of bio-oils with simultaneous waste treatment. *Bioresource Technology*, 107, 456-463.
- Tommaso, G., Chen, W., Li, P., Schideman, L. and Zhang, Y. (2015). Chemical characterization and anaerobic biodegradability of hydrothermal liquefaction aqueous products from mixed-culture wastewater algae. *Bioresource Technology*, 178, 139–146.
- Toor, S. S., Rosendahl, L. and Rudolf, A. (2011). Hydrothermal liquefaction of biomass: A review of subcritical water technologies. *Energy*, 36 (5), 2328–2342.
- Tsuji, H. and Fujii, S. (2014). Phosphate recovery by generating hydroxyapatite via reaction of calcium eluted from layered double hydroxides. *Applied Clay Science*, 99, 261-265.
- Vardon, D. R., Sharma, B. K., Scott, J., Yu, G., Wang, Z., Schideman, L., Zhang, Y. and Strathmann, T. J. (2011). Chemical properties of biocrude oil from the hydrothermal liquefaction of Spirulina algae, swine manure, and digested anaerobic sludge. *Bioresource Technology*, 102 (17), 8295-8303.
- Vardon, D., Sharma, B., Blazina, G., Rajagopalan, K. and Strathmann, T. (2012). Thermochemical conversion of raw and defatted algal biomass via hydrothermal liquefaction and slow pyrolysis. *Bioresource technology*, 109, 178-87.
- Xu, D., and P.E. Savage. (2014). Characterization of biocrudes recovered with and without solvent after hydrothermal liquefaction of algae. *Algal Research, Part A*, 6, 1–7.
- Xu, K., Wang, C., Liu, H. and Qian, Y. (2011). Simultaneous removal of phosphorus and potassium from synthetic urine through the precipitation of magnesium potassium phosphate hexahydrate. *Chemosphere*, 84, 207-212.
- Xu, K., Li, J., Zheng, M., Zhang, C., Xie, T. and Wang, C. (2015). The precipitation of magnesium potassium phosphate hexahydrate for P and K recovery from synthetic urine. *Water Research*, 80, 71-79.
- Yetilmezsoy, K., Fatih, I., Emel, K. and Havva Melda, A. (2017). Feasibility of struvite recovery process for fertilizer industry: A study of financial and economic analysis, *Journal of Cleaner Production*, 152, 88-102.

- Yetilmezsoy, K. and Sapci-Zengin, Z. (2009). Recovery of ammonium nitrogen from the effluent of UASB treating poultry manure wastewater by MAP precipitation as a slow release fertilizer. *Journal of Hazardous Materials*, 166 (1), 260–269.
- Yu, Y., Lei, Z., Yuan, T., Jiang, Y., Chen, N., Feng, C., Shimizu, K. and Zhang, Z. (2017). Simultaneous phosphorus and nitrogen recovery from anaerobically digested sludge using a hybrid system coupling hydrothermal pretreatment with MAP precipitation. *Bioresource Technology*, 243, 634-640.
- Zhang, C., Xu, K., Li, J., Wang, C. and Zheng, M. (2017). Recovery of phosphorus and potassium from source-separated urine using a fluidized bed reactor: Optimization operation and mechanism modeling. *Ind. Eng. Chem. Res.*, 56, 3033-3039.

## 5.0 Conclusions and Future Work

In this dissertation, experimental, modeling, and energy accounting approaches are utilized to evaluate the water quality impacts of the hydrothermal liquefaction (HTL) processing of select non-food, organic waste feedstocks, with specific emphasis on the production and management of so-called aqueous co-product (ACP). Through this work, it has been demonstrated that HTL processing generates considerable quantities of potent wastewater (i.e., ACP) that must be substantially diluted and/or managed prior to discharge into the receiving waters of a wastewater treatment plant (WWTP). ACP management could be both energy and cost intensive due to the removal of wastewater constituents (i.e., dissolved organic carbon [C] and dissolved nitrogen [N] and phosphorus [P]) to achieve typical WWTP limits. Before waste HTL can be implemented at commercial scale, strategies need to be evaluated for managing ACP. From this work, it is also shown that HTL can serve as a means of decoupling C and N, as well as separating organic and inorganic N and P during HTL processing. Therefore, novel ACP management through the nutrient-based precipitation of N and P into usable materials is evaluated as a means of both offsetting the energy cost of the removal of N and P from the ACP and producing valuable materials. These conclusions are supported by the findings of Chapters 3 and 4 of this dissertation.

In order to fully understand the extent to which the HTL processing of organic waste feedstocks impacts water quality and by which ACP can be managed via the precipitation of valuable nutrients, future work should focus on the following areas:

- 1) Elucidating the impacts of various HTL processing conditions (e.g., temperature, heating rate, residence time, etc.) on the yields and composition of HTL products, with special emphasis on ACP production and quality, rather than the uniform HTL conditions used in

this dissertation. This analysis will help determine the extent that HTL parameter selection effects the decoupling of C and N, as well as the conversion of N and P into inorganic, potentially recoverable forms. HTL conversion studies thus far have primarily focused on optimizing reaction conditions to maximize biocrude quantity and quality (Akhtar and Amin, 2011; Zhang et al., 2009). However, due to the impacts of ACP management on the energy performance of HTL systems (Bauer et al., 2018), it is of interest to also optimize HTL conditions, with the goal of enhancing ACP quality for improved recovery of inorganic N and P into usable materials as a means of ACP management, which could ultimately improve the energy performance of waste-to-energy systems.

- 2) Characterizing possible toxicity impacts of ACP arising from the HTL conversion of organic waste feedstocks. Since the ACP arising from HTL processing is likely unsuitable for direct discharge into the receiving waters of a WWTP without substantial dilution and/or ACP management approaches, it is of interest to evaluate ACP toxicity and suitability for subsequent conventional wastewater treatment, such as anaerobic digestion (to produce methane-derived bioelectricity) (Tommaso et al., 2015). High levels of toxicity in wastewater can inhibit nitrification and the biological treatment processes of WWTPs. Therefore, it is of interest to assess the suitability of ACP for conventional wastewater treatment. It is also of interest to assess the suitability of post-HTL ACP from the conversion of organic waste feedstocks as a medium for microalgae cultivation (through the recycling of ACP N and P), which has been previously evaluated for algae feedstocks by several studies (Pham et al., 2013; Biller et al., 2012; Jena et al., 2011).

3) Validating water chemistry modeling results of the theoretical recovery of nutrients via chemical precipitation (Chapter 4) through the use of experimental laboratory techniques. There are several studies that have experimentally evaluated the recovery of nutrients from various wastewaters (e.g., slaughterhouse, swine, and dairy manure wastewaters, as well as landfill leachate) (Yetilmezsoy and Sapci-Zengin, 2009; Rahman et al., 2011; Tao et al., 2016). By adapting methods used in these studies, it is of interest to assess the experimental recovery of nutrients via chemical precipitation of solids, such as struvite-based fertilizers, from the ACP produced from the HTL processing of organic waste feedstocks. It is also of interest to determine the relationship between  $\text{PO}_4^{3-}$  availability and the availability of other complexing ions and the precipitation of solids, such as struvite and HAP (as precipitated according to the Visual MINTEQ model), from post-HTL ACP. This will validate model results presented in this dissertation in order to further evaluate the impacts of ACP management and nutrient recovery on the energy performance of waste HTL processing.

The proposed future work, together with the results of this dissertation, will provide valuable information about the water quality impacts of the HTL processing of organic waste feedstocks, which can be further used for optimizing waste-to-energy systems to achieve environmental and energy sustainability.

## 5.1 References

Akhtar, J. and Amin, N. A. S. (2011). A review on process conditions for optimum bio-oil yield in hydrothermal liquefaction of biomass. *Renewable and Sustainable Energy Reviews*, 15 (3), 1615–1624.

- Bauer, S., Reynolds, C., Peng, S. and Colosi, L. (2018). Evaluating the Water Quality Impacts of Hydrothermal Liquefaction: Assessment of Carbon, Nitrogen, and Energy Recovery Impacts, *Bioresource Technology Reports*, 2, 115-120.
- Biller, P., Ross, A. B., Skill, S. C., Lea-Langton, A., Balasundaram, B., Hall, C., Riley, P. and Llewellyn, C. A. (2012). Nutrient recycling of aqueous phase for microalgae cultivation from the hydrothermal liquefaction process. *Algal Research*, 1 (1), 70–76.
- Jena, U., Vaidyanathan, N., Chinnasamy, S. and Das, K. C. (2011). Evaluation of microalgae cultivation using recovered aqueous co-product from thermochemical liquefaction of algal biomass. *Bioresource Technology*, 102 (3), 3380–7.
- Pham, M., Schideman, L., Scott, J., Rajagopalan, N. and Plewa, M. J. (2013). Chemical and biological characterization of wastewater generated from hydrothermal liquefaction of *Spirulina*. *Environmental Science & Technology*, 47, 2131-2138.
- Rahman, M. M., Liu, Y., Kwag, J. H. and Ra, C. (2011). Recovery of struvite from animal wastewater and its nutrient leaching loss in soil. *J. Hazard. Mater.*, 186, 2026–2030.
- Tao, W., Fattah, K. P. and Huchzermeier, M. P. (2016). Struvite recovery from anaerobically digested dairy manure: A review of application potential and hindrances. *Journal of Environmental Management*, 169, 46-57.
- Tommaso, G., Chen, W., Li, P., Schideman, L. and Zhang, Y. (2015). Chemical characterization and anaerobic biodegradability of hydrothermal liquefaction aqueous products from mixed-culture wastewater algae. *Bioresource Technology*, 178, 139–146.
- Yetilmezsoy, K. and Sapci-Zengin, Z. (2009). Recovery of ammonium nitrogen from the effluent of UASB treating poultry manure wastewater by MAP precipitation as a slow release fertilizer. *Journal of Hazardous Materials*, 166 (1), 260–269.
- Zhang, B., von Keitz, M. and Valentas, K. (2009). Thermochemical liquefaction of high-diversity grassland perennials. *Journal of Analytical and Applied Pyrolysis*, 84 (1), 18–24.